University of Strathclyde
Renewable Energy Marine Structures - Centre for Doctoral Training
Department of Naval Architecture, Ocean, and Marine Engineering

Defining the offshore wind monopile structural design envelope

Kingsley Sunday-Uko

A thesis submitted in partial fulfilment of the requirements for the degree of Doctor of Engineering (EngD)

2023

Supervisor: Professor Feargal Brennan

DECLARATION OF AUTHENTICITY AND AUTHOR'S RIGHTS

This thesis is the result of the author's original research. It has been composed by the author and has not been previously submitted for examination which has led to the award of a degree.

Kingsley Sunday-Uko

September 2022

STATEMENT OF PREVIOUSLY PUBLISHED WORK

During this research study, several papers were published in scientific journals or are still under review at the time of writing, as listed in Section 1.2. The author of this thesis was and is the creator of all these publications even if the paper is co-authored. The author's contributions to the publications comprise: conceiving the works, administering the studies, realising the works, performing literature studies, developing the methodologies, performing the research, developing and applying the approaches, working with and extending the software, curating the data, verifying and validating the methods and results, analysing and investigating the data and results, post-processing and visualizing the results and findings, writing the papers and preparing the original drafts, interacting with journal editors and reviewers, as well as reviewing and editing the papers for the final publications.

Kingsley Sunday

September 2022

ACKNOWLEDGEMENTS

First and foremost, I would like to thank my supervisor, Professor Feargal Brennan, for the support, resources, and opportunities he has provided to me over the years. I also like to thank Professor Athanasios Kolios and all my lecturers for their support.

My thanks go to my mum and sisters and their respective families, for their love and support.

I would like to thank my friends and colleagues, Ayodele Fajuyigbe and Anuj Singh for their support and encouragement.

Big thanks to Sarah Wakefield for patiently proofreading my journal articles and thesis and for her support throughout this research journey.

I would like to thank everyone on the Renewable Energy Marine Structures centre for doctoral training.

I would like to thank my colleagues and friends at KA Engineering Group Ltd and the Institution of Civil Engineering and Structural Engineering.

I would like to thank the countless individuals I met along the way, whether they became my friend, colleague or only a brief acquaintance, for the knowledge and thoughts shared.

. . . in the end, I would humbly like to give at least a little pat on the back for a job well executed. Well done, me!

My profound gratitude to God for the wisdom and knowledge to complete this research. This thesis is dedicated as a steppingstone to my lovely daughter Eva Uko as she begins her own journey in seeking wisdom and knowledge.

ABSTRACT

Important and compelling questions presently facing the renewable energy industry require an understanding of the upper bound capacity limit of offshore wind turbine (OWT) monopile structures. The areas of interest include, but are not limited to, the following: understanding the influence of modelling techniques on current and future OWT monopile concepts, application of appropriate modelling methods in defining the design envelope, identifying current and future factors limiting how deep offshore wind monopiles structures can be installed and the limit of the installation water depth, the size and weight of the structures according to capacity demand, and installation and operational considerations such as acceptable and excessive pile inclination that may arise from driving larger diameter piles. This research investigated these areas with respect to 5-MW, 10-MW, 15-MW, and 20-MW OWT monopile structures. These were modelled using the application of a 3D finite element to capture the interaction and response of the foundation and structure correctly. The objective was to provide a design tool in the form of an OWT structural design envelope that will serve as an indicative guide for engineering feasibility design and feed into detailed design. This envelope indicated a narrowing of the allowable structural design window because of the complex structural response and behaviour of the new larger and heavier OWT monopiles under operational and 50-year return loading conditions. It clarified the direction of the dynamic response for 5-MW to 20-MW OWT monopiles, considering non-linear soil-structure interactions. The OWT design envelope was defined according to salient design criteria such as the permissible deflection (tilt and rotation), natural frequency/stiffness, buckling, and stresses. The governing design criterion and possible design improvement solutions can be identified from the design envelope. Harmonic response analysis was performed to provide an in-depth understanding of the natural frequency and amplitude response. This was achieved by defining the relative position of the external loads and regions to be avoided with respect to resonance initiation.

This research consists of a portfolio of four research areas which have been published in peer-reviewed journal articles. The research areas covered include: 1) A comprehensive literature review and gap analysis considering previous and on-going studies, with particular focus on offshore wind turbine monopiles. 2) The influence of the soil-structure modelling techniques on the offshore wind monopile structural response where different soil-structure modelling techniques and methodologies are assessed, and the outcome provides direction for improving the engineering design of offshore wind monopile structures and a roadmap for future research developments. 3) Investigating the response of the offshore wind monopile structures under 50-year return loading environmental and operational conditions. 10-MW OWT monopile structure is used as a case study to test the findings and recommendations, from this research on how soil-structure modelling techniques influence the structural response of offshore wind turbine monopiles. 4) The creation and definition of offshore wind monopile structural design envelope for existing 5-MW and 10-MW offshore wind monopile structures and future

generation concepts of 15-MW and 20-MW offshore wind monopile structures. Furthermore, the larger and heavier future generation concepts of 15-MW and 20-MW OWT monopile structures are assessed for modelling approaches and understanding of the structural response when subjected to environmental and operational loads.

CONTENTS

LIST OF FIGURES

LIST OF TABLES

1 INTRODUCTION

1.1 Research Background and Motivation

The transferred knowledge of offshore structural design and analytical techniques from the offshore oil and gas industry form the fundamental basis for the assessment of offshore wind turbines. These transferred engineering techniques are not fit-for-purpose considering the larger and heavier offshore wind turbine sections, in addition to the unique operational loads from the rotor-nacelle-assembly. It is crucial to understand and quantify the current gaps in knowledge and understanding of the structural modelling techniques and responses to different loading conditions. This would lead to improvements in the engineering of offshore wind turbine structures and competitiveness with other matured energy industries such as oil and gas. Efficient and effective engineering of the offshore wind monopile structures is vital in improving the technical and commercial value of these large and heavy structures.

Land-based (Onshore) wind turbine initially demonstrated the usefulness of wind energy as a viable form of energy for large scale generation of electricity [1]. Furthermore, technological improvements have yielded promising results which show that the offshore wind turbine (OWT) industry can significantly contribute to electricity generation. The efficiency of offshore winds is enhanced by the relatively low surface roughness and reduced turbulence of the ocean, leading to greater availability of wind speeds. Hence, OWT can generate increased wind power compared with land-based wind turbine systems. There are engineering design and installation challenges that are associated with the increased wind power capacity generated by OWT. Other challenges faced by OWT structures in addition to the land-based installation loads, include wave action, currents, accidental scenarios, 50-year return loading and operational conditions.

Despite previous and on-going research in identifying design gaps, more work is still required in the modelling techniques of larger and heavier offshore wind turbine monopiles and understanding of their responses. As more offshore wind structures are being designed and commissioned into operation, a significant number of the structures are now in the final phase of their design life. With the potential for life extension, design improvements and understanding, interpretation of system responses are urgently required. The future of OWT and investments is heavily dependent on improved and efficient designs and the engineering cost of the new generation larger and heavier monopile structures.

Most offshore wind turbines in operation are supported on monopiles and jacket-type fixed foundations. These comprise more than 80% of offshore wind turbine foundations (Wind Europe 2018) [2]. The increasing demand for clean renewable energy brings about a corresponding increase in the size and capacity of the offshore wind turbine structures and diameter of their foundation systems. There is a relationship between the capacity and efficiency of offshore wind turbines and the size of the structure and the foundation system.

This research aims to provide understanding and improvement in the structural design techniques of present and future generations of larger and heavier offshore wind turbine monopiles through identification and assessments of uncertainties. The scope of this research also includes identification of the governing structural design criteria, the structure's dynamic response subjected to different loading conditions, and the generation of allowable structural design envelope that will be useful for feasibility stage engineering design for OWT monopile up to 20-MW capacity.

1.2 Publications and Previous Studies

The following peer review journal submissions and publications have been made as part of this research. These journal articles are incorporated and forms part of this thesis.

1. Sunday K, Brennan F. A review of offshore wind monopiles structural design achievements and challenges. Journal of Ocean Engineering, 2021.

2. Sunday K, Brennan F. Influence of soil–structure modelling techniques on offshore wind turbine monopile structural response. Wind Energy, 2022.

3. Sunday K, Brennan F. OWT monopile structural response under 50-year return condition. Renewable and Sustainable Energy Reviews, 2022. (Submitted for peer review).

4. Sunday K, Brennan F. Offshore wind monopile structural design envelope. Royal Society Publishing, 2022. (Submitted for peer review).

The main industry recommended design codes and guidelines for offshore wind turbine support structures includes IEC 61400-3, DNVGL-SE-0263, DNVGL-ST-0262, DNVGL-ST-0126 Design of Support Structure, DNV-OS-J103, API RP-2A WSD, ISO-19902, and NORSOK N-004 [3] [4] [5] [6] [7]. Some representative previous research/Joint Industry Projects (JIPs) contributions include:

- The BOEMRE (Bureau of Ocean Energy Management, Regulation, and Enforcement) of US DOI delegated ABS (American Bureau of Shipping) to study the support structure of NREL 5MW reference wind turbine under hurricane conditions. This study covered the fitness of IEC and API standards for the potential offshore wind farm locations under hurricane conditions [1].

- IEA has commissioned series of projects for code comparison since 2010 to conduct OWT simulation code comparison based on 5MW OWT published by NREL [1].

- Offshore wind turbine monopile supported structure is one of the main focuses in the OC3 project and OC4 dealt with reference turbine with jacket support structures and semi-submersible support structures.

- PISA Project through European joint industry academic research project [8] [9, 10].

1.3 Selected Offshore Wind Turbine Support Structures

Offshore wind turbine support structures are primarily grouped into two:

1. Fixed foundation supported offshore wind turbine structures:
   a. Monopile foundation supported structures are offshore wind turbine structures that are installed in shallow waters [11]. The classification of water depth is subject to individual/corporate experience, industry/sector, and work history.
   b. Jacket foundation supported configurations and gravity base-type foundations.

2. Floating foundation supported offshore wind turbine structures:
   a. Catenary mooring configuration and tensioned mooring configuration.
   b. Semi-submersible and spar floating wind turbine structures.

Currently, the fixed foundation offshore wind turbine configuration has been deployed more than other types of OWT due to the overall costs of engineering, manufacturing, installation, and the operating costs compared with other configurations. This research is focused primarily on investigating and improving current design techniques of fixed foundation offshore wind monopiles.

1.4 Research Scope and Objectives

The research scope and the objectives of this study are as follows:

- Perform a comprehensive literature review and gap analysis considering previous and on-going studies, with particular focus on offshore wind turbine monopiles. The review includes the important history and evolution of the offshore wind monopile structure configurations and capacities, modelling approaches, current methodology and identification of important areas of interest requiring detailed research investigation and improvements. This activity is completed and presented in Section 2 of this report, outlining the milestone achievements and challenges in the offshore wind turbine industry with a focus on monopile supported structures. Part of the work from this stage of the research was peer reviewed and published in the Ocean Engineering Journal, titled "A review of offshore wind monopiles structural design achievements and challenges" [12].

- Following on from the findings of the comprehensive literature review and gap analysis, the influence of the soil-structure modelling techniques on the offshore wind monopile structural response is identified to be one of the areas of significant research interest requiring further investigation, understanding, and improvement. This part of the research is completed and presented in Section 3. Different soil-structure modelling techniques and methodologies are assessed, and the outcome provides direction for improving the engineering design of offshore wind monopile structures and a roadmap for future research

developments. This stage of the research is published in a peer reviewed Wind Energy open source journal, titled "Influence of soil-structure modelling techniques on offshore wind turbine monopile structural response" [13].

- The next stage of the research journey is investigating the response of the offshore wind monopile structural response under 50-year return loading environmental and operational conditions. 10-MW OWT monopile structure is used as the case study to test the findings and recommendations from the work on the influence of the soil-structure modelling techniques on the offshore wind turbine monopile structural response. This stage of the research brief, findings and conclusions are presented in Section 4. The investigation of the response of the offshore wind monopile is submitted and under peer review in the journal for Renewable and Sustainable Energy Reviews, titled "Offshore wind monopile structural response under 50-year return condition".

- Section 5 of this report presents the study and findings on the creation and definition of offshore wind monopile structural design envelope for existing 5-MW and 10-MW offshore wind monopile structures and future generation concepts of 15-MW and 20-MW offshore wind monopile structures. Furthermore, larger, and heavier future generation concepts of 15-MW and 20-MW OWT monopile structures are assessed for modelling approaches and understanding of the structural response when subjected to environmental and operational loads. The findings from this stage of the research are used to define and generate global allowable structural design envelopes for the different turbine capacities, water depths, and configurations. This study is submitted and under peer review in the journal for Philosophical Transactions of the Royal Society, titled "The offshore wind monopile structural design envelope".

- The overall research conclusions and contributions to the offshore wind turbine industry and academic progress are presented in Section 6. Flow-chat of the scope and integration of the different stages of research, salient structural assessments, and overall objective as outlined in this section is presented in Figure 1.1. This research is primarily focused on the structural design improvement of offshore wind monopile and a limited geotechnical design checks regarding SLS permanent rotation and ULS overturning capacity are covered in this thesis. However, detailed geotechnical design and associated geotechnical design improvements of offshore wind monopile are not covered in this research.

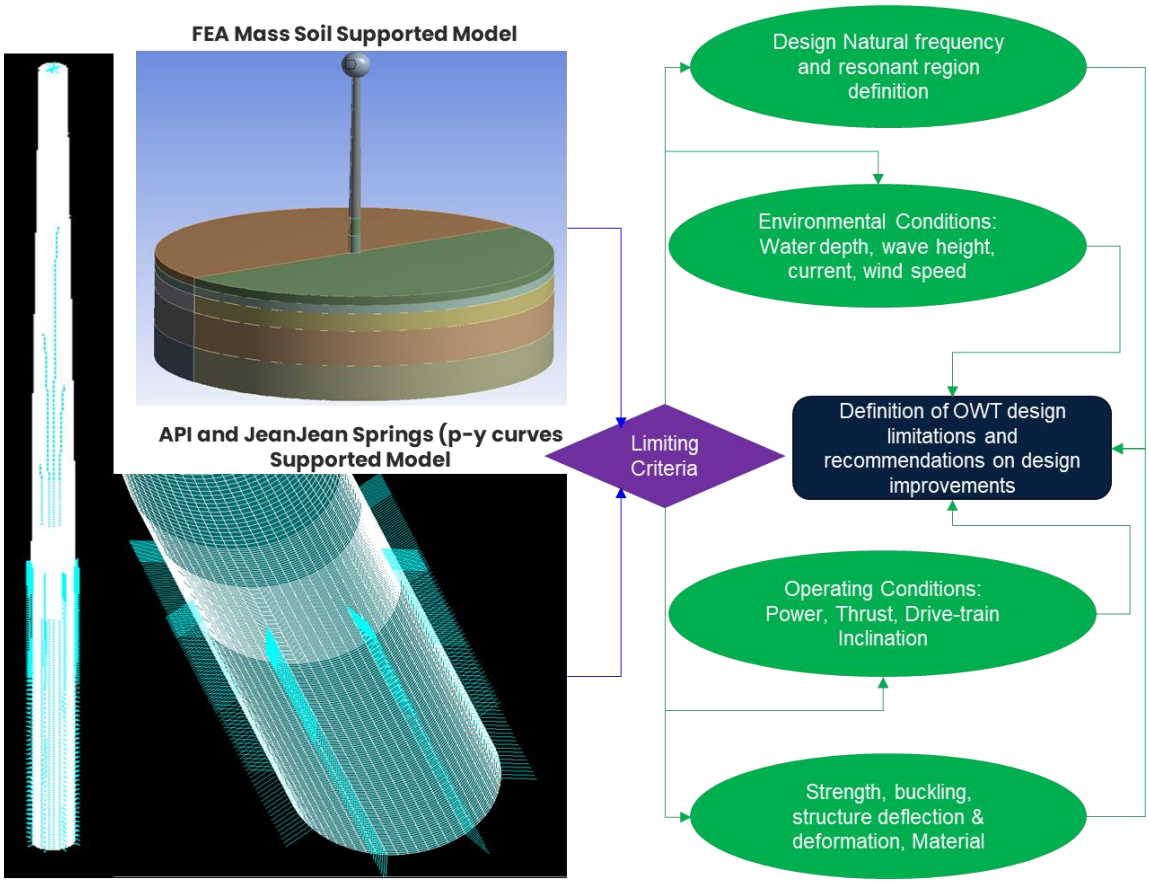

Figure 1.1 – Flow-chat of Research Scope

2 COMPREHENSIVE LITERATURE REVIEW AND GAP ANALYSIS

The published peer reviewed journal article: Sunday K, Brennan F. A review of offshore wind monopiles structural design achievements and challenges. Ocean Engineering, 2021 was authored by myself as part of my research completed under the direction and consultation of my supervisor, Professor Feargal Brennan. The published article is incorporated, and forms part of the comprehensive literature review and gap analysis presented in this section.

2.1 Evolution and Improvements of Design to Codes and Standards

Much of the guidance on offshore wind turbine structures is currently being provided in DNVGL-ST-0126: Support structures for wind turbines and BS EN 61400-3: Design requirements for offshore wind turbines [14] [3]. This research is based primarily on DNVGL guidance, and references are made to other industry recommended codes and standards as necessary. Due to the relatively young but growing nature of offshore wind turbines and the gaps in knowledge and understanding of structural modelling and dynamic behaviour, the recommended guidance by DNVGL for the design of offshore wind turbine structure has undergone several updates. These updates, minor and major, are essential to keeping up with improvements in technology and in understanding of structural modelling, interpretation, and response of the systems.

Since the first release of DNVGL guidance on offshore wind turbine structures in 2004 [15], then DNV, updated revisions were released in 2007 [16], 2009 [17], 2010 [18], 2011 [19], 2013 [20], 2014 [21], 2016 [22], and in most recently in 2018 [14]. After the merger of Det Norske Veritas (DNV) and Germanischer Lloyd (GL) in 2013, all standards are in the process of harmonisation and alignment [23]. The journey of support structures for wind turbines is best presented in Figure 2.1.

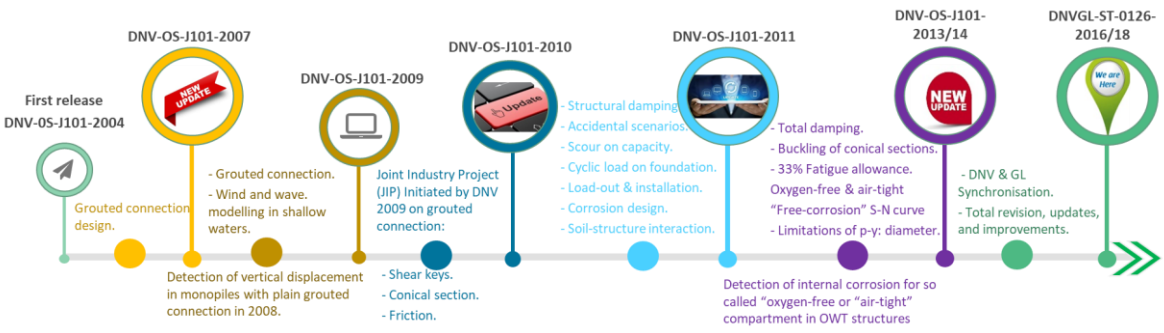

Figure 2.1 – The Journey of Support Structures for Wind Turbines to DNVGL

Offshore wind turbine structures guidance is based on the experiences of the oil and gas industry. However, the design, manufacturing, transportation, installation of offshore wind farms brings new challenges. This is mainly due to the larger and heavier section properties, configuration, and the number of structures per site to install, operate and maintain throughout the intended design life.

The guidance on offshore wind turbine structures by DNV is titled DNV-OS-J101 from its first release in 2004 to the 2014 revision; thereafter, the title is updated to DNVGL-ST-0126 in 2016 and 2018 releases. The standard provides the fundamental principles, technical requirements and guidance for design, construction, and in-service inspection of offshore wind turbine structures. This standard is primarily for the design of offshore wind turbine structures, including the support structures and foundation systems. Items such as construction, installations and inspection are also covered in the design standard. However, the standard does not cover the design of wind turbine components such as the nacelle, rotor, generators, gear boxes, support structures and foundations for transformer stations [16].

This section-2, aims to review and outline the salient updates in order to understand the previous and current challenges in the design and analysis of offshore wind turbine structures.

1. The first release of the offshore standard DNV-OS-J101: 2004 was revised and updated in 2007 and amended in 2009, and identified that the established industry practice for calculating the axial capacity of the grouted connections does not fully represent their physical behaviour [15] [16] [17]. It was understood that in some cases, this may result in an overestimation of the calculated axial capacity of the grouted connections. This initiated the need for further research, led by DNV, together with other industry and research institutions. The objective was to further understand the long-term behaviour and response of grouted connections and to establish a reliable framework and method for estimation of the axial load capacity for offshore wind turbine structures. In this revision, the guidance expanded wind and wave modelling in shallow waters.

2. In October 2010, a new revision of the design standard DNV-OS-J101 was released in keeping with improvements in technology, knowledge and understanding of offshore wind turbine structures [18]. The primary technical update related to gaps in the calculation of the axial load capacity of grouted connections, including their physical behaviour. The following guidance updates for the design of grouted connections were presented:

    a. Grouted connections with plane sections (without shear keys) with a constant radius over the height of the connection (pile and transition piece) should be designed with low utilisation ratio, with respect to axial capacity. Clarification is presented for the definition of a low utilisation ratio. The idea was to mitigate the risks in the design method and practices. This led to an overestimation of the axial capacity.

    b. Grouted connections with conical tower geometry and the transition piece should be designed with a utilisation ratio ≤ 1.0. Conical connections are defined as cones with angles in the order of $\geq 1^{o}$. It was understood that the

overestimation of the axial capacity for grouted connections was moderate in conical connections compared with straight connections.

c. Friction coefficient between the steel and the grout used in design should not exceed 0.4, unless verified and documented otherwise. Limiting friction coefficient was aimed at ensuring that the axial capacity, which is directly related to the friction between the interface of the steel or primary material, and the grouted connection, are maintained within a conservative allowable limit.

These recommendations offered notable progress with the aim of improving the design by reducing the overestimation of the axial capacity of grouted connections; however, the problem remained unresolved at this stage.

3. Updates and a new revision for the design of offshore wind turbines DNV-OS-J101 was released in July 2011 [19]. The following important updates and attempts to understand and address the design challenges of OWT are presented:

a. For temporary design conditions, the characteristic loads and load effects in design checks shall be based either on specified environmental design conditions or on specified design criteria. It is recommended that selecting the design criteria for all temporary phases should depend on measures taken to achieve the required safety level. Design criteria shall be specified with due attention to the actual location, the season of the year, the weather forecast and the consequences of failure.

b. Ship impacts and collisions: boat landings, ladders, and other secondary structures in and near the water line shall be designed against operational ship impact in the ultimate limit state (ULS). However, the primary structure in and near the water line shall be designed against accidental ship impact in accidental limit state (ALS). The requirement for design against accidental ship impact in the ALS are merely robustness requirements, not necessarily a requirement for full ALS as specified for maximum authorised service vessels.

c. Consideration and application of appropriate structural damping for ice loading scenario. The method for analysis of dynamic ice loading, when the structural damping is not too small, must be used with caution for structures with small total damping as this may lead to an underestimation of the dynamic amplifications and ultimately incorrect design. As a guide, for assessing whether the structural damping is too small, structures with natural frequencies in the range of 0.4 to 10 Hz have experienced lock-in vibrations when the total structural damping is lower than 3% of the critical damping.

d. Consideration of scour on the capacity of the foundation and its influence on the structural response must be accounted for. This should include ultimate

and fatigue design criteria on structural components due to erosion of soil particles at and near the foundation caused by waves and currents.

e. Loads and their influence on offshore wind turbine structures and their foundations during load-out, transportation, installation and dismantling shall be considered in defining the design criteria for acceptable environmental conditions. Effects of tides, where appropriate, shall be considered. Ice may be an issue for maintenance and repair operations in harsher climates.

f. For material thicknesses greater than 50mm, post weld heat treatment (PWHT) is recommended to be applied to joints in C-Mn steels in special areas. However, this can be waived if a satisfactory performance in the as-welded condition can be demonstrated by a fitness-for-purpose assessment based on fracture mechanics testing or based on a fracture mechanics and fatigue crack growth analysis. BS 7910 recommends two principal methods to determine the stress intensity factors for tubular joints: numerical (e.g. finite element or boundary element) analysis of tubular joints; standard and analytical (e.g. weight function) solutions for semi-elliptical cracks [24] [25]. Research by Stutzmann et al. (2017) considers the use of detection results from underwater inspection to update simulated crack size distributions of offshore wind monopile structures and to determine whether crack inspections reduce the uncertainties in remaining useful life predictions for offshore wind turbine structures [26].

g. It is recommended that the ULS structural design for steel wall thickness be equal to the nominal thickness reduced by the corrosion allowance over the full-service life of the structure. Special consideration should be given to primary steel structures in the splash zone when calculating the corrosion allowance. Presently, the 2mm corrosion allowance often applied, for replaceable secondary structures in the splash zone, is usually not sufficient for a 20-year service life.

h. Corrosion allowance shall be considered by decreasing the nominal wall thickness in fatigue limit state analyses. Presently, it is recommended to reduce the nominal wall thickness by half the corrosion allowance for fatigue calculations. Special consideration and calculations are required for steel structures in the splash zone.

i. The application of stress reduction factors on welds prior to fatigue analysis, depending on whether the mean stress is a tensile or a compressive stress, accounts for effects of partial or full fatigue crack closure when the material is in compression.

j. Vibration in secondary structures such as internal and external J-tubes are undesirable. An assessment of vibrations in J-tubes should be performed, either based on experience from similar structures or by calculations.

k. The effects of cyclic loading on soil properties shall be considered in foundation design for offshore wind turbine structures. Effects of wave- and wind-induced forces on soil properties for a single storm shall be investigated and for normal operating conditions followed by a storm or an emergency shutdown.

l. For dynamic analysis of the offshore wind turbine system, the support structure and foundation shall be assessed by applying appropriate soil stiffness. The p-y curves representing the pile-soil interaction are used in modelling and analysis. However, there have been improvements in capturing the realistic pile-soil interaction and behaviour.

4. The July 2011 release was amended, and the updated version presented as DNV-OS-J101 in January 2013 [20]. The 2013 release has fewer amendments than the updates captured in the 2011 release which may have been due to a progressive understanding of offshore wind turbine structural modelling and response interpretation or a slowdown in research and technological improvements or a combination of both. The primary update in the 2013 version is to the design material factors for concrete, grout, and reinforcement for the different limit state designs.

5. An improved version of the DNV-OS-J101 (2013) was released in May 2014 [21]. The 2014 version contains more updates and amendments than the 2013 version (and an increased number when compared with the timeframe of the 2011-2013 updates). This confirms there are still significant challenges and gaps in the design and analysis of offshore wind turbine structures. The important structural updates are presented and discussed below:

   a. Further amendments on some of the salient updates of earlier versions of the recommended standard. The continuous improvements on already amended methodologies demonstrates a notable understanding and technological advancements in the offshore wind turbine industry. The understanding and advancements in technology are underpinned by increased in-service data which helps when interpreting the modelling and responses of the structure to loads.

   b. In determining the wind turbine loads, appropriate damping should be considered which is a combination of structural damping, soil damping, hydrodynamic damping, and aerodynamic damping. Structural damping depends on the blade material and the material in other components such as the tower. The aerodynamic damping can be determined by the outcome of an aeroelastic calculation using the correct properties.

   c. Ultimate limit states design for tubular members, joints, and conical transitions for buckling requirements of towers and monopiles may account for the bias included in the parametric formulas for shell buckling in EN 1993-1-6. Based on the membrane theory, applicable to tubular steel towers

with D/t < 250, this bias may be accounted for in the global buckling design by reducing and using a material factor of 1.1 [27] [28].

d. In accordance with DNV-OS-C502, the cumulative fatigue damage of structures or components that are not planned to be inspected should be limited to 33%. While this recommendation is conservative, this criterion can be expensive in terms of materials, manufacturing, and fabrication to achieve a maximum of 33% allowable damage over the design life of the structure. This negates the need for conducting optimisation as part of holistic and sustainable engineering designs.

e. The effects of permanent buckling and plastic hinges in monopile foundations needs to be analysed if relevant. Otherwise, permanent deformations in the monopile structure are not allowed.

f. Corrosion control by exclusion of oxygen is primarily an option for structural compartments which are only externally exposed to seawater, e.g., the annulus of jacket structures legs and bracings that are completed and flooded at installation. Any compartments potentially exposed to air will need to be kept permanently sealed by welding or by constant overpressure by nitrogen to prevent any air ingress. Some compartments such as the interiors of monopiles are periodically accessed for inspection and repair and can therefore not be completely sealed. Effects of large tidal variations on the internal water level should be considered. In addition, even in the virtual absence of oxygen in the seawater, corrosion by anaerobic bacteria can occur. It is recognised that an air-tight compartment in monopile structures is not feasible, hence, it is recommended that these issues are taken into consideration when evaluating options for corrosion control for internal compartments [29].

g. Fatigue calculation will be affected by the corrosion allowance applied to the structural component. The corrosion allowance corresponds and is determined by the corrosion rate and conforms to the assumed corrosion conditions which dictate the S-N curve used for the fatigue calculation. It is recommended that if substantial metal loss is expected, free corrosion conditions must in general be assumed, and the "free-corrosion" S-N curve is then required. This aspect of design requires further research to understand the extent and envelope definition of "substantial metal loss" and if the "free-corrosion" S-N curve is appropriate or whether other S-N curves suitable for the condition along with engineering quantifiable justification should be applied. Further guidance states that the "free-corrosion" S-N curves can be applied for the internal surfaces of monopiles below the waterline.

h. The non-linear p-y curves are primarily used in the analyses of piles to determine and evaluate the pile lateral capacity in the ULS. These p-y curves have been calibrated for long slender jacket piles with diameters of up to 1.0m. They have not been calibrated for monopiles with larger

diameters and are in general not valid for such monopiles. P-y curves to be used for monopile design should be validated for such use, e.g., by FE analysis or using measured monitoring data.

6. Latest releases in the offshore wind turbine structure's design standard are the April 2016 and July 2018 versions: DNVGL-ST-0126 Support Structures for Wind Turbine [22] [14]. The new title reflects the DNV and GL merger. The document was totally revised, including further improvements on amendments to previous revisions.

2.2 Environmental and Operational Loads

The site conditions relevant for calculating and generating the loads on wind turbines and other design parameters are discussed in this section. The different sources of loading, calculation of loads, safety factors, load case definitions and evaluation of loads are also presented.

As exposed structures, the offshore wind turbines are subjected to various external forces and effects. Effective operation of the offshore wind turbines is dependent on wind speeds as a functional requirement, along with meteorological conditions such as turbulence. Oceanographic and other marine climate conditions are the second main category of external conditions which primarily contribute to the loading of the offshore wind turbine structures. The meteorological and oceanographic conditions are the primary offshore wind turbine loading conditions, also referred to as metocean data.

These secondary loading conditions include ambient temperature, seismic activity, geotechnical conditions, scour, icing, electrical grid conditions, corrosion and erosion, altitude, lightning, solar radiation, abrasive particles in air or water. For site-specific load case conditions, the relevant meteorological and oceanographic data shall apply. Where the actual environmental conditions are not sufficiently known, the wind turbine may be designed according to one of the wind turbine classes described in this section along with relevant assumptions regarding the parameters not defined by the classes.

The offshore wind turbine structures are categorised into four main classes: I, II, III, and special class "S". The class is primarily defined based on the reference wind speed, average annual wind speed, high-medium-low turbulence intensity, and the significant wave height. The wind turbine is designed to one of the following safety classes:

- The normal safety class applies when failure results in a risk of personal injury and/or economic, environmental, or social consequences.
- The special safety class which applies when safety requirements are determined by local regulations and/or the safety requirements are agreed between the designer and the customer.

Wind conditions are the primary external conditions for the structural integrity of the RNA structure, although marine conditions, including wave conditions, also have an influence in some cases, depending on the dynamic properties of the support structure. Hence the marine conditions should be accounted for in the design of the RNA. In general, dynamic analysis of the wind turbine structure, in respect of the dynamic response for the external and operating conditional, is required including the primary support structure. The primary loads for structural design of offshore wind turbines are discussed below.

1. Operational loads: result from the operation and control of the offshore wind turbine such as the control of the rotor speed, torque control by pitching of the blades or other aerodynamic devices. Other operational loads are the mechanical braking and transient loads during start-up and shutdown of the rotor, connection and disconnection of the generator, and yaw movements.

2. Inertia and gravitation loads: result from vibration, rotation, gravity, and seismic activity. The following items are to be considered: elasticity of the blades, drive train dynamics (drive train and generator), support structure elasticity, soil-structure interaction, global dynamics, and motions. The non-linear axial and lateral behaviour of soil-structure interaction should be modelled explicitly to check and ensure load deflection compatibility between the structure and the pile-soil system. The effects of increased member thickness, due to marine growth, and the water in enclosed submerged members and their influence on the hydrodynamic masses should be accounted for in modelling and design.

3. Aerodynamic loads: divided into quasi-static and dynamic loads generated by the airflow and its interaction with the stationary and moving parts of the wind turbines. The aerodynamic loads (lift, drag and torsion, if applicable) on structural members depends on, amongst other factors, the average wind speed across the rotor plane, wind shear, wind direction, density of air, rotational speed of the rotor, three-dimensional turbulence intensity, aerodynamic shapes of the wind turbine components and their interactive effects, including aeroelastic effects.

4. Hydrodynamic loads: comprise of the stationary and non-stationary loads which are caused by the flow of water and interaction between this and the offshore wind turbine support structure. This load depends on the water flow kinematics and density, water depth, shape of the wind turbine support structure and their interactive effects, including hydro-elastic effects. Hydrodynamic loads on the wind turbine support structure, including vortex-induced vibration consideration for slender structures, are best modelled and analysed by non-linear dynamic analysis. Previous research has shown that non-linear loads can have a negative impact by reducing the structure design lifetime [30] [31].

a. Selection of wave theory for the representation of the wave kinematics and the method for wave load prediction shall account for the water depth, size, shape, and type of structure. BIncludingus effects and potential flow (including wave diffraction and radiation) effects may be important in determining the wave-induced loads on the wind turbine support structure.

b. For the evaluation of load effects from wave loads, possible ringing effects should be considered. When a high wave encounters the monopile, high frequency nonlinear wave load components may coincide with the natural frequencies of the structure causing resonant transient responses in the global bending models of the pile. Ringing effects become significant in combination with extreme first order wave frequency effects, evaluated in time domain with due consideration of higher order wave load effects. The magnitude of the first ringing cycles is governed by the magnitude of the wave impact load and its duration is related to the structural response period. Ringing may occur if the lowest natural frequencies of the structure do not exceed three to four times the typical wave frequency. If the natural frequency of the structure exceeds about five to six times the wave peak frequency, then ringing may be ruled out.

5. Others loads which are to be considered are as follows:

a. Hydrostatic loads may occur if a member or compartment is wet only from one side. The hydrostatic force typically acts on the surface and can have considerable influence on large structures with empty spaces.

b. Sea-ice loads which can be either static or dynamic loads acting on the offshore wind turbines, caused by the current- and wind-induced motion of ice flows and their failure when in contact with the support structure. The relevance of sea-ice loads depends on the specific location and characteristics of the site at which the offshore wind turbine is to be installed. Ice loads shall be evaluated for a range of interactions (determined by the ice environment) between the ice and the structure. Three modes of interaction are known: intermittent ice crushing which involves loading and unloading phase; frequency lock-in which may occur at intermediate ice speeds, typically 0.04m/s to 0.1m/s; and continuous brittle crushing at higher ice speeds, typically above 0.1m/s.

c. Seismic loads using recognised procedures such as response spectrum and time history dynamic response analysis methods.

d. Boat impact loads on the primary structures such as boat landings, ladders, and other secondary structures in and near the water line are to be considered as a normal event. The primary structure shall in addition be designed for supply vessel impacts as an abnormal event.

6. Combination of external conditions
   Scatter diagrams (long-term statistics) including wave height, wave period and wind speeds should be used to generate the wind/wave combinations to be considered for the load analysis of offshore wind turbines. The combination of 50-year return external conditions (wind, wave, current, sea ice, and water level) is shown to result in a global extreme environmental action on structures with a specified 50-year or 1-year return period.

7. Variation of support structure natural frequency and operations within the resonance range: the mass and stiffness of the structure and soil may change considerably during the wind turbine design life. In load analysis, the change in the support structural natural frequencies and influence on responses due to scour, corrosion, marine growth, soil settlement, and sand movement are to be considered by applying the most adverse conditions. Mean values may be applied for fatigue analysis if no resonant operational modes appear.

8. Design situations and load cases.
   The offshore wind turbine and associated components structural integrity shall be verified through consideration of several design load cases. As a minimum, the design load case given in Table 4.3 DNVGL-ST-0437 shall be considered [32]. The primary design situations for the design of offshore wind turbine structures are presented. The design load cases (DLC) are defined in DNVGL-ST-0437.

   a. Power production (DLC 1.1 to 1.7):
      Power production design situation is when the offshore wind turbine is operational and connected to the electric grid, no fault situation occurs, and the control systems are active. The offshore wind turbine design configuration shall account for any rotor imbalance, maximum mass, and aerodynamic imbalances (e.g., blade pitch and twist deviations) specified for the rotor manufacturing. Deviations from theoretical optimum operating conditions such as yaw misalignment and control system delay shall be accounted for in the analyses of the operational loads.

   b. Power production plus occurrence of fault (DLC 2.1 to 2.5):
      In addition to power production design situation, any fault in the control or safety systems or any internal faults in the electrical system that are significant for wind turbine loading (such as generator short circuits) shall be assumed to occur. The assessment of the faults should be based on the failure mode and effect analysis (FMEA or similar) and mean time between failures (MTBF) provided by control and safety system assessments.

   c. Start-up (DLC 3.1 to 3.3):
      The offshore wind turbine start-up design scenario includes all the events resulting in loads on the wind turbine structure during the transitions from any standstill or idling condition to operational power production condition. Start-up design situation shall include the different possible combinations of

start-up procedures associated with the start-up wind speeds per year and site-specific start-up requirements.

d. Normal shut-down (DLC 4.1 to 4.2):
This design scenario includes all the events resulting in loads on the offshore wind turbine during normal transitions from power production to stand-by condition which includes standstill and idling.

e. Emergency shutdown (DLC 5.1):
This design scenario covers the manual activation of the emergency stop pushbutton to bring the rotor to a standstill condition.

f. Parked (DLC 6.1 to 6.5):
At parked condition, the offshore wind turbine rotor is in stand-by (standstill or idling) condition.

g. Parked plus fault conditions (DLC 7.1 to 7.2):
This design situation considers a non-standby (standstill or idling) scenario resulting from the occurrence of a fault. This deviation in the offshore wind turbine from normal behaviour of a parked wind turbine, resulting from faults in the electrical network or within the wind turbine is analysed.

h. Transport, installation, maintenance, and repair (DLC 8.1 to 8.5)
The wind and marine conditions and design situations are specified by the manufacturer. The relevant situations include transport, installation, maintenance, and repair of the offshore wind turbine. The wind turbine may be erected in wind conditions of up a maximum average speed of 10-min mean, in which significant wave height and oblique inflow are maintained and are assessed.

2.3 Fabrication and Transportation and Installation Design Considerations

Offshore structure installations are limited by weather conditions, especially in rougher seas which narrows the window for safe installation. This is further exacerbated for offshore wind turbine structures due to the larger and heavier structural members and components. The North Sea, for example, has an installation window of approximately 120 days a year [33]. Lifting processes for transportation and installation of offshore wind turbine structures are restricted to certain specified permissible wind and wave windows [34]. DNVGL-OS-C401 provides guidance for the fabrication and testing of offshore Structures [35]. Denis et al. (2017) outlined some key fabrication challenges and installation steps for current infrastructure design [36]. It is important to optimise the design phase for transportation and installation by considering available weather windows and logistics. This is at a cost of approximately 15% - 20% of the total cost of delivery the structure [33]. The installation phase is divided into two broad stages:

1. Foundation and transition piece installation phase.
2. Wind turbine tower and nacelle assembly (one or more sections of the tower, nacelle, hub, and three blades) installation phase.

Assembling and transport methods and their influence on the structural members are important factors in achieving a cost-effective and optimised engineering design with respect to fabrication, transportation, and installation conditions [37]. Three main assembling and transportation methods are applied in the offshore wind turbine industry [33]:

1. The Bunny Ear: where the nacelle, hub, and two of the blades are pre-assembled at port, achieving a shape like a rabbit's head. The tower is carried in two or three pieces along with the third blade and the bunny ear assembly, Figure 2.2.

2. Full rotor star: assembling of the hub and all three blades are completed onshore as single unit and transported along with the nacelle and tower sections separately but on the same vessel, Figure 2.3.

3. Separate Parts: involves assembling the nacelle and hub onshore and transporting along with the tower sections and blades as separate parts. The blades are arranged and held in the blade stacker, Figure 2.4.

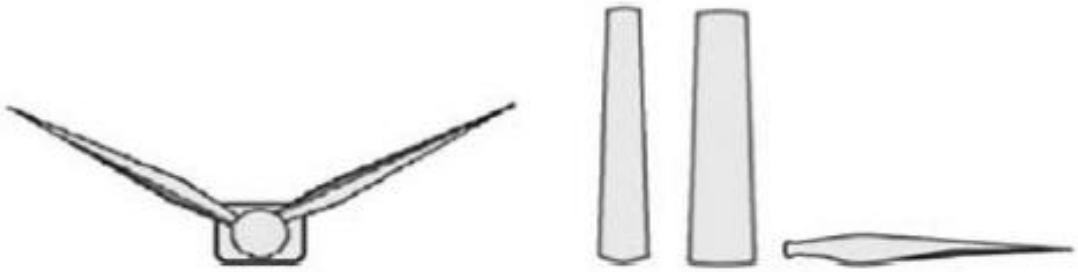

Figure 2.2 – "Bunny Ear" Assembling and Transportation Method [33]

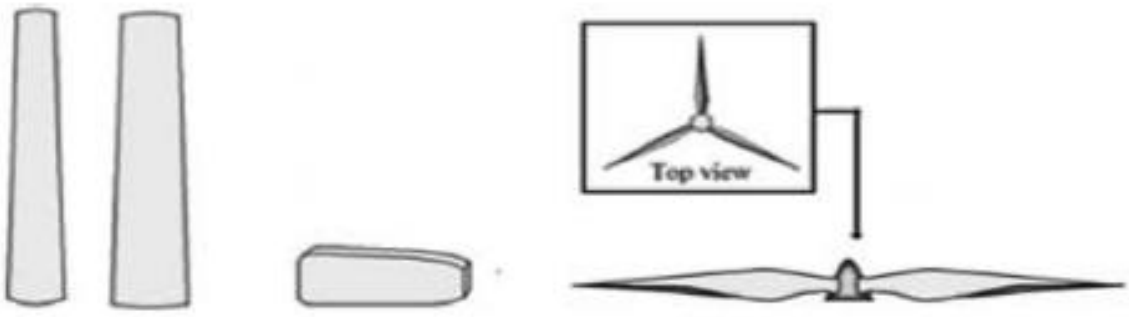

Figure 2.3 – "Full Rotor Star" Assembling and Transportation Method [33]

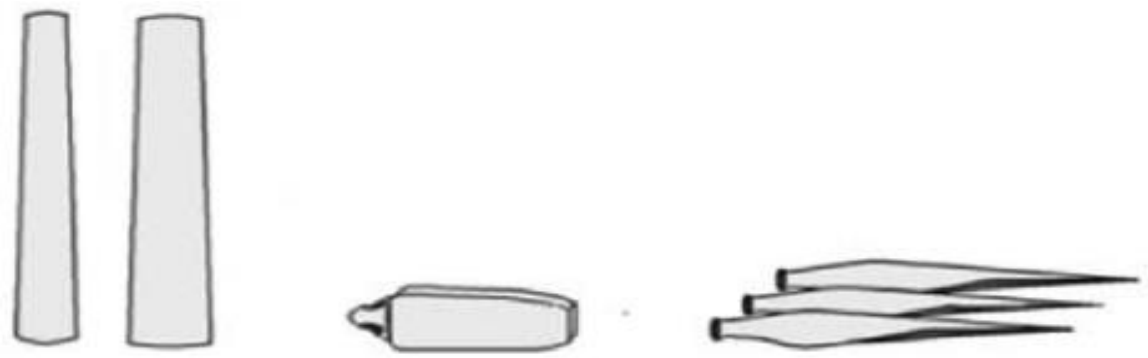

Figure 2.4 – "Separate Parts" Assembling and Transportation Method [33]

The design for transport and installation is dependent on the selected processes and steps undertaken from fabrication to installation and commissioning. The weather window, selected vessel, and lifting techniques are important design inputs in completing the modelling and analysis of the structure.

During operation and maintenance conditions, the most unfavourable rotor positions are at maximum intervals of 30° for a three bladed wind turbine and the most unfavourable breaking torque is to be applied for the assessment of the structure in a mechanical break scenario (situation after the actuation of the emergency stop pushbutton). All situations, which may persist for longer than one week, shall be modelled and analysed during transport, installation, maintenance, and repair, including:

1. Partially completed tower.
2. Tower standing without nacelle.
3. Tower with nacelle but without one or more blades attached.

The design scenarios assume that the electrical network is not connected in any of these cases. Fatigue and ultimate load analysis for periods not less than 3 months of the wind turbine design life shall be assessed for a configuration that is partially erected or assembled, and without grid connection. Yaw error of up to ±180° for the most unfavourable response shall be applied during the operations. The modal response and natural frequency of the structure at different stages during transport and installation shall be analysed and investigated, including possible vortex shedding conditions due to wind, waves and current but as separate non-correlated events.

Operational and accidental boat impacts shall be considered in conjunction with the environmental conditions that correspond to the most severe conditions under which the maintenance boat is permitted to approach the offshore wind turbine structure. The application of appropriate methodology and input parameters are required for the safe installation design and the selection of wind turbine installation vessel as described in DNV design standards and previous research [38].

2.4 Governing Design Criteria for Bottom-Fixed Structures

Offshore wind turbine structural design and analysis in accordance with DNVGL-ST-0126 is based on limit state design requirements, a condition beyond which the primary structure and the associated components no longer satisfy the specified minimum design requirements [14]. The design of offshore wind turbines is governed by the following limit states:

1. Ultimate limit states (ULS) which correspond to the maximum load-carrying capability or resistance. The ultimate limit states include:
   a. Loss of structure resistance: excessive yielding and buckling.
   b. Structural failure due to brittle fracture.
   c. Loss of static equilibrium of the structure or parts in overturning or sliding.
   d. Transformation of the structure into a mechanism: collapse due to excessive deformation.
   e. Failure caused by exceeding the ultimate resistance or the ultimate deformation of the structure or associated components.

2. Fatigue limit states (FLS) which correspond to the failure from the effects of dynamic loads. The structural failure is due to cumulative damage from repeated or cyclic loads. The design of fatigue life shall account for accumulated fatigue during stages of transportation, installation, and pre-operation.

3. Serviceability limit states (SLS) correspond to tolerance criteria applicable to normal use, these include:
   a. Deformations or motions that exceed the permissible limit of equipment.
   b. Deflections that may alter the effect of forces.
   c. Excessive vibrations leading to discomfort or affecting non-structural components, turbine operations and production.
   d. Durability and temperature-induced deformations.

Where the limiting vertical deflection is not specified in the design basis, the deflection criteria in Table 2.1 and Figure 2.5 may be applied.

Structural component	Limit for δ_{max}	Limit for δ_2
Deck beams	L/200	L/300

Table 2.1 – Deflection Criteria: Vertical Deflections

Where:
L: designates the nominal span.
δ_{max} designates the resulting sagging of the member = $\delta_1 + \delta_2 - \delta_0$
δ_0 is the pre-camber.
δ_1 the deflection of the beam due to permanent loads immediately after applicable.
δ_2 the sum of the deflection of the beam due to variable loading and time-dependent deflections due to permanent load.

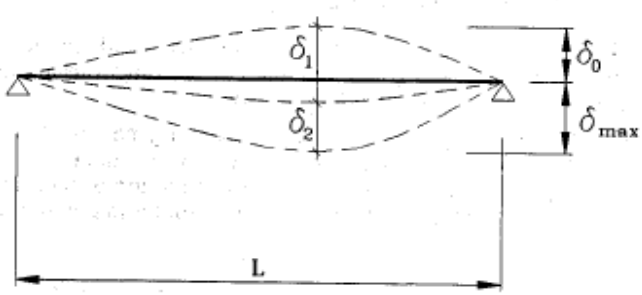

Figure 2.5 – Definition of Vertical Deflections [14]

In addition to vertical deflections, horizontal displacements and/or rotational limits should be defined. In lieu of defined limits, the foundation structure and tower should be erected with a total tolerance of axial tilt of 0.25°. The total and permanent tilt rotation should be limited to 0.50°, accounting for a permanent deformation in the soil that may develop and generate an additional nominal tower axis tilt rotation of 0.25°.

4. Accidental limit states (ALS) correspond to:
   a. Maximum load-carrying capacity for (rare) accidental loads which deals with any structural damage caused by accidental loads.

   b. Post-accidental integrity for damaged structures: ultimate resistance of damaged structures or loss of structural integrity after local damage.

2.5 Important Industry and Research Contributions and Challenges

In this section certain significant updates, design achievements and challenges to offshore wind turbine structures and foundation systems are discussed following critical a review of the design codes and standards, research, and industry contributions.

2.5.1 Soil-Structure Interaction

Geotechnical designs of the foundations are completed for both strength and deformation of the soil-foundation structure in the ultimate limit state (ULS). Geotechnical design check, regarding the soil carrying capacity to resist moment and lateral loads, is subsequently covered in Section 5.4 of this thesis. Cyclic loading is likely to reduce the ultimate bearing capacity of the soil in the ultimate limit state (ULS), hence, the effects of cyclic loading with respect to soil strength and stiffness should be addressed for both ULS and SLS design conditions in different loading situations. The soil-structure modelling technique and its analysis and interpretation is crucial in the overall offshore wind turbine structure design. The natural frequency as well as the fatigue loading, and response are significantly affected by the soil-structure interaction understanding and modelling technique.

The renowned p-y curves, in accordance with API-RP 2014 and as described in DNV-ST-0126, are limited to smaller pile diameters, hence it is recommended to

validate the use of p-y curve generated soil springs for pile diameters greater than 1.0m by using finite element analysis methods or other suitable means [39] [40] [14] [40]. The API-RP 2014 is read in conjunction with the API-RP 2GEO 2011 – Geotechnical and Foundation Design Consideration [41] [42]. The p-y curves for sand were developed by O'Neill and Murchinson [43], while Dunnavant and O'Neil [44] proposed the p-y method for clay (2000) which were adopted by the API-RP (2000) and still serve as basis for many offshore wind turbine designs [45]. The p-y curve model is used to represent the soil resistance to the displacement by the non-linear transfer curve, and the t-z curves are used to model the axial loading to structure displacement [39]. The pile tip load to displacement (Q-z) curve is used to calculate the end bearing resistance. Previous research and experiments indicate that full end bearing resistance is mobilised when the pile tip displacement is up to 10% of the pile diameter [39]. Schematic description of soil resistance to structure is presented in Figure 2.6. The force to deflection interaction is generally constructed using stress-strain data interpreted from soil samples.

The monopile support structures, including diameters exceeding 7.5m are designed according to the soft-stiff approach. Based on several research and industry applications, the response of the conventional p-y curve method without calibration is limited in performance due to their weak non-linear behaviour under operational loading. PISA research work indicated that, as well as the lateral soil reaction of the standard p-y modelling approach, three additional soil reaction components are relevant and require calibration to improve the p-y method for offshore wind monopile foundations, these include a distributed moment, a base horizontal force, and a base moment [10]. Furthermore, the PISA research identified that even a calibrated 1D p-y curve method may be less accurate compared with a 3D finite element model for sites where layers of soil occur with highly contrasting strengths and stiffness, and, as such, a model detailed analysis is recommended [10]. The conventional p-y curve generated soil springs demonstrate an overall underestimation of the soil-structure stiffness [46]. Although research into soil-structure interaction continues to be one of the focuses of research, there is yet to be an updated and industry design code and standard recommended modelling technique. The finite element modelling method is another technique that is adopted for representing and analysing soil-structure interaction.

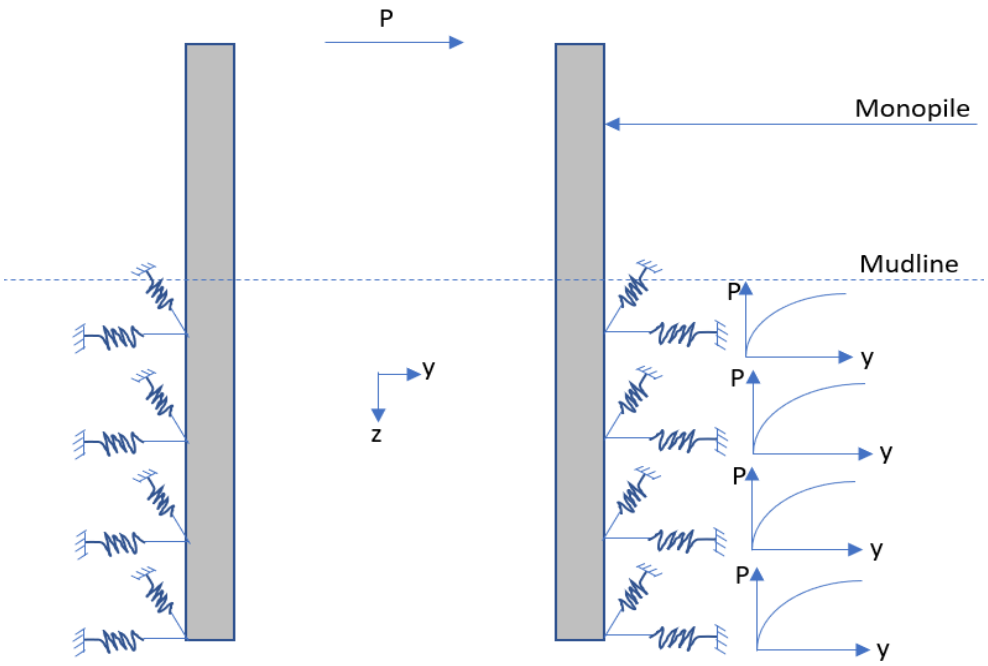

Figure 2.6 – Schematic of P-Y Curve Method

In order to avoid resonance, the first frequency of the OWT system must be isolated from the frequencies of external excitations of wind, wave, and current, including the rotational frequency of rotor (1P) and the blade passing frequency (3P for three bladed turbine) [47, 48]. The effect of cyclic loading on the p-y curve method and on the soil response is not covered in this research, but the following research was considered in this thesis regarding cyclic loading on soil [47] [49] [50] [51].

Other soil modelling techniques used for offshore structure foundations are the Matlock [52], Reece and Cox [53], and Jeanjean [54-57] p-y models. The API-RP p-y curves are originally generated from the Matlock model, although research shows that the stiffness of API-RP p-y curves is significantly lower than that of the Matlock p-y curves for very small displacements. The Jeanjean p-y model is suitable for assessing the fatigue life of offshore well conductors and is applied in designing offshore wind turbines for serviceability limit state [58] [59]. Jeanjean et al (2017), presented a framework for the calculation of monotonic backbone p-y curves in cohesive materials which provides an improvement in the calculation of pile response in very soft to stiff clays [57]. The Jeanjean curves are stiffer than the API-RP p-y curves at all lateral displacements and stiffer than the Matlock curves at all but very small displacements, Figure 2.7. Stiff clay was used for the Jeanjean and API-RP p-y stiffness comparison; details of the soil properties for subsequent modelling and analysis are presented in Section 3.2. Several researchers recommend improvements to the Matlock p-y curves; however, these modifications are known to be only suitable for the cases studied and not for wider applications. Therefore, the modifications to the Matlock p-y formulation are yet to be implemented, awaiting a comprehensive review to develop an alternative design method for monopiles that is robust, and provides efficient and effective design for

different soil conditions [60]. Refined design models and predictions using FEA techniques and measured data to establish the most appropriate soil-structure models is acceptable practice.

The scaling method is a new approach for developing soil p-y curves from stress-strain curves. This method involves scaling the stress-strain into compatible soil reaction p and pile deflection y, respectively. This method incorporates some important simplification and approximation such that a single stress and a single strain are selected to represent the response of the entire soil formation under any given loading condition. Hence, this method is not expected to accurately capture the detailed response of the soil [61]. However, Osman and Bolton (2005, [62]), demonstrated that the method is a simplified approach that can provide a reasonable engineering estimate of load-deformation. Known soil stress-strain relationship can be converted to an equivalent load-displacement relationship for any given loading condition.

Recent work completed through a major European joint-industry academic research project, known as the PISA project, was designed to develop soil modelling approaches for laterally loaded offshore wind turbine monopiles. The PISA project focused on large diameter, relatively rigid piles, with a low length to diameter (L/D) ratio. The PISA project introduced new procedures for site specific calibration of soil reaction curves that can be applied within a one-dimensional (1D), Winkler-type computational model. The 1D model incorporates the standard p-y lateral soil reaction, denoted as p-v in the PISA design model, but is extended to allow for a distribution of the bending moment along the pile length, as well as a horizontal and a moment soil reaction at the pile base. The 1D model is verified against data from 3D FE analysis of layered soil profiles, calibrated using inputs from field tests. The PISA project identified that, for piles under lateral loading with a low L/D ratio (buried pile length/diameter), the failure mode is more complex than assumed with the traditional p-y method [8-10] .

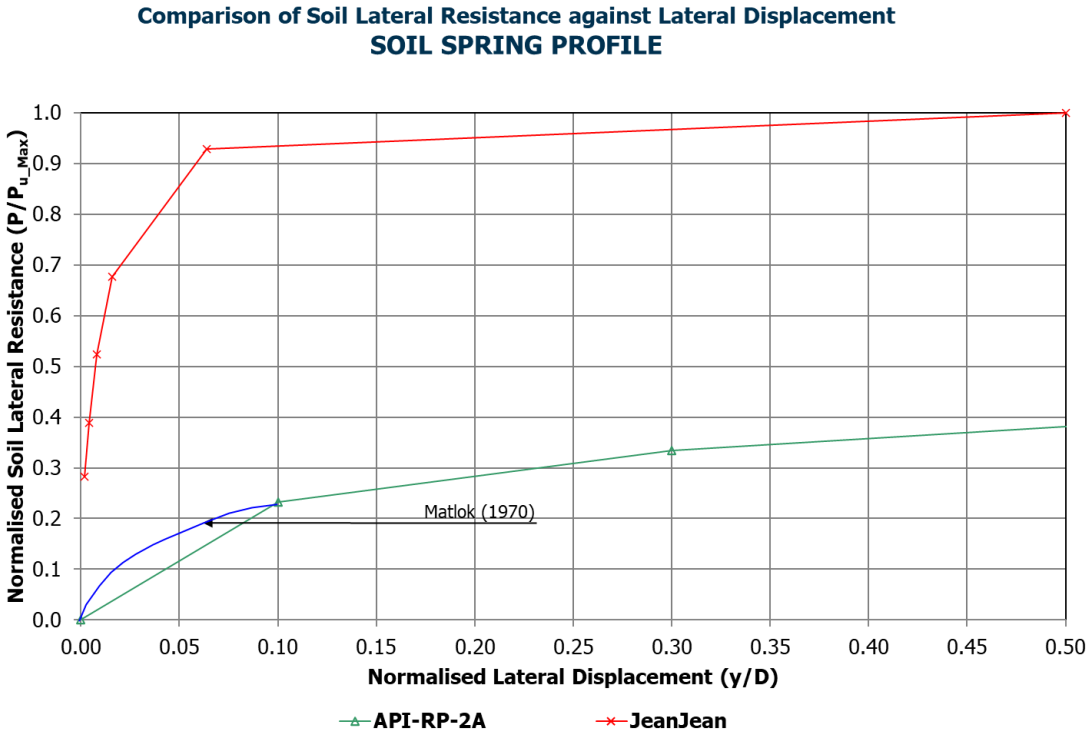

Figure 2.7 – Comparison of Matlock (1970), AP-RP 2GEO (2011), and Jeanjean Curves for Normally Consolidated Clay.

2.5.2 Soil Scour and Cyclic Loading on Capacity of Foundation and Influence on Structural Response

The effects of scour and cyclic loading on soil properties must be considered in foundation design for offshore wind turbine structures. The effects of wave- and wind-induced forces on soil properties for a single storm must be investigated, for normal operating conditions followed by a storm or an emergency shutdown. Geotechnical design of foundation is completed for both strength and the deformations of the foundation structure and of the soil as presented in subsequent sections of this thesis. Cyclic loading may reduce the ultimate bearing capacity of the soil in the ultimate limit state (ULS), hence, the effects of cyclic loading on the ground strength and stiffness must be addressed for ULS and SLS design conditions for different loading situations.

In the case of steady current, the scour process is mainly caused by the presence of a horseshoe vortex combined with the effect of contraction streamlines at the edges of the pile. Measured data across different offshore wind farms indicates a significant variation in the scour hole shape which tends to be elongated with a steep upstream slope and a gentle downstream slope. In the event of waves, the horseshoe vortex and lee-wake vortex form the processes that govern scour, dictated primarily by the Keulegan-Carpenter number, KC as follows:

$$KC = \frac{u_m . T_P}{D} \tag{6}$$

Where TP is the peak wave period, D is the cylinder diameter and Um = 1.41ums. ums is the standard deviation of the velocity at the seabed.

Long-term cyclic lateral loading induced by waves and wind can lead to a change in soil stiffness during the lifetime of the offshore wind turbine structure and foundation system [49]. Although scouring is an important area of research interests and previous research work has been conducted, scour and the design around structural geometries is not well understood [63]. Therefore, it is important to understand and refine the soil-structure modelling technique and analysis in generating the response of the offshore wind turbine when subjected to cyclic lateral loading. The change in soil-structure stiffness and response due to cyclic lateral loads can lead to a risk of resonance and fatigue damage of the structure.

The stiffness of a structure is a function of the deflection and the natural frequency, fundamental to the design of an OWT monopile structure. Deflection and natural frequency using the reference 5 MW NREL OWT monopile, modelled in a 20m water depth is presented in Table 2.2 for API p-y supported springs. The model and analysis are completed using Ansys, as presented in Figure 2.8. The impact and sensitivity of global soil scour on the structure stiffness is conducted for different scour depths below the mudline: no scour, 2.5m scour, 5.0m scour, and 7.5m scour. The results show an increase of 5.0%, 12.6%, and 22.4% in global deflection at the mudline for 2.5m scour, 5m scour and 7.5m scour, respectively, compared to a model with no scour. A corresponding reduction in natural frequency of -2.4%, -6.2%, and -11.4%, respectively, is observed compared with no scour. This analysis is repeated for a new finite element model supported using stiffer p-y springs generated according to the JeanJean technique [54], this shows an average reduction (improvement) in deflection of -11.5% and a corresponding average improvement in stiffness of 5.2% compared with the p-y springs generated according to API method. It is worth noting that the scouring angle is not accounted for in this sensitivity analysis. Detailed analysis to quantify the impact of soil scour depends on the quality of the design data from field measurements that characterise the scour such as the scouring angle, depth of scour, predominate scouring direction, and radius and/or diameter of the scour. Analytical models can also be calibrated and validated using measured monitoring data to enhance the accuracy of the predictions.

A total deflection 1.01m (0.44°) was recorded at the top of the tower with the model fixed at the mudline. This was used to further benchmark and verify the analytical models. The corresponding top of tower deflections for the API and JeanJean models are 3.12m (1.35°) and 2.74m (1.19°), respectively. The mudline shear is 6.38 MN, and the bending moment is 250 MN-m.

Scour Depth (m)	Natural Frequency (Hz)		Mudline Deflection (Deg)	
	API p-y Springs	JeanJean p-y Springs	API p-y Springs	JeanJean p-y Springs
0.0	0.2028 Hz	0.2132 Hz	0.56°	0.49°
2.5	0.1979 Hz	0.2080 Hz	0.59°	0.52°
5.0	0.1902 Hz	0.1999 Hz	0.63°	0.56°
7.5	0.1796 Hz	0.1895 Hz	0.69°	0.61°

Table 2.2 – Effect of Scour on OWT Monopile Stiffness

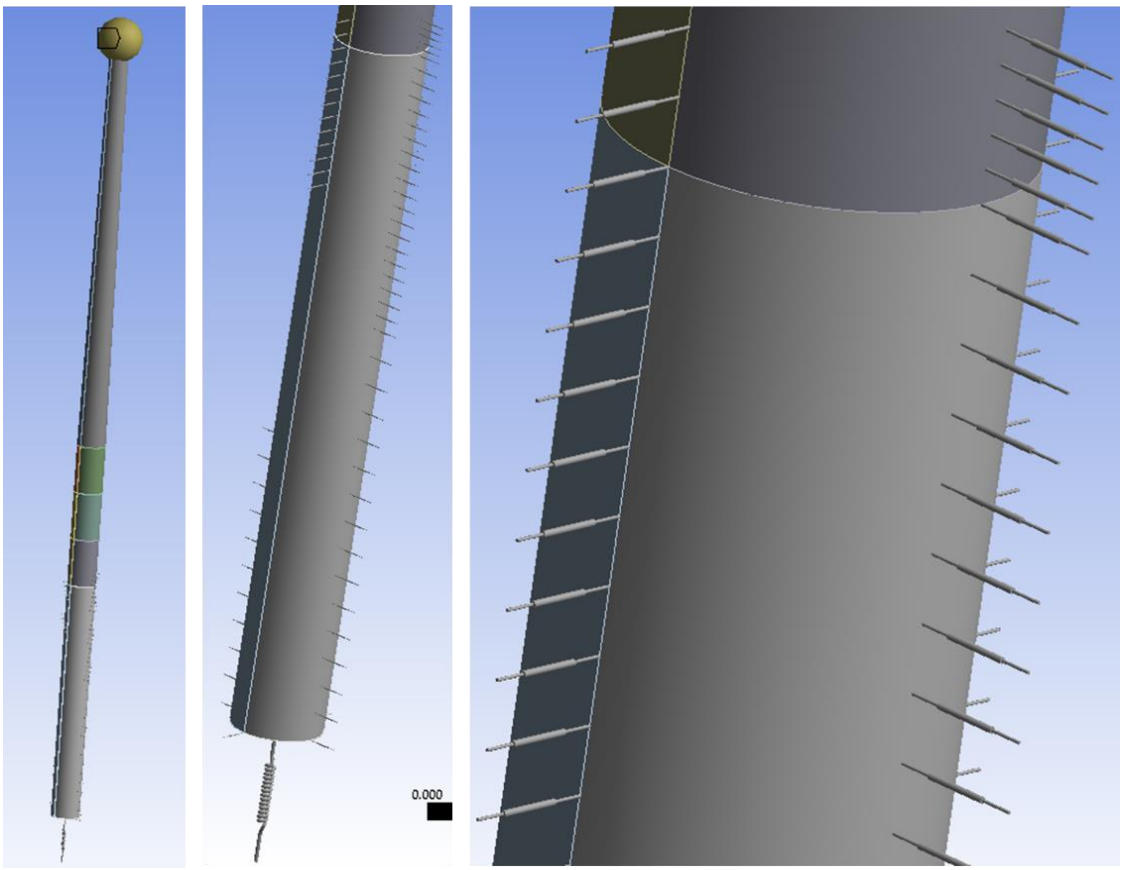

Figure 2.8 – Typical Finite Element Model: API p-y and JeanJean p-y Generated Soil Springs

2.5.3 Natural Frequency and Resonance

The design of offshore wind turbine structures is directly influenced by the natural frequency of the structure. Accurate calculation of the natural frequency is important to understanding the response of the system for efficient design and to avoid resonance effects which have an impact on the serviceability limit state criteria and ultimately compromise the fatigue life of the structure [58] [64] . The natural frequency of the structure, and hence, avoidance of resonance effects depends on several factors, including the following:

1. The stiffness of the soil and soil-structure interaction discussed in 2.5.1. Stiffer soil and foundation systems will lead to a corresponding higher frequency. The

natural frequency and response of the offshore wind turbine are sensitive to the foundation and soil properties [65, 66].

2. Degradation of the soil modulus and scour can shift the natural frequencies of the offshore wind turbine structure. The shift in natural frequency can also be caused by long term cyclic loads acting on the structure [67].

3. Damping ratio: structural, soil, hydrodynamic, and aerodynamic. The accurate estimation of the damping ratios is important in the design of offshore wind turbines as the amplitude of vibrations at resonance are inversely proportional to these ratios [68]. The total damping of the offshore wind turbine's first bending mode consists of aerodynamic damping, structural, hydrodynamic, and soil damping [69]. A research study conducted by James et al. (1996) reported on the estimation of modal damping using strain-gauge data from an operating wind turbine structure. They used the Polyreference method to extract the modal parameters from the correlation functions [70].

4. Investigations into floating offshore wind turbines have revealed that turbulent intensity effects increase the structure's motion and influence the dynamic response and natural frequency when the turbulent intensity increases to 20% [71]. The turbulent intensity effect is exacerbated within low-frequency regions below the resonant frequency, Figure 2.9. The lower and higher turbulent intensities are observed to match the frequency range of the resonant frequencies (right of the dashed line). However, the resonant response is somewhat amplified when the turbulent intensity increases. Furthermore, the increase in the turbulent intensity leads to a corresponding increase in the structural loads.

5. The size and total stiffness of the structure: optimal designs usually aim to reduce the overall weight, size and cost of the monopile foundation and the turbine structure, leading to an increase in flexibility and reduced stiffness. A small change in the total stiffness may result in a shift in the natural frequency and a significant change in the resonance response.

6. Rotor induced resonance was identified by Li and Lui et al. (2019) as an important factor in the natural frequency and response. The occurrence of fault conditions such as seized blades, was observed to influence the wind turbine structure frequency compared with parked conditions for feathered blades. A fault condition (floating OWT) with three blades seized was observed to resonant at higher motions, Figure 2.10 [72].

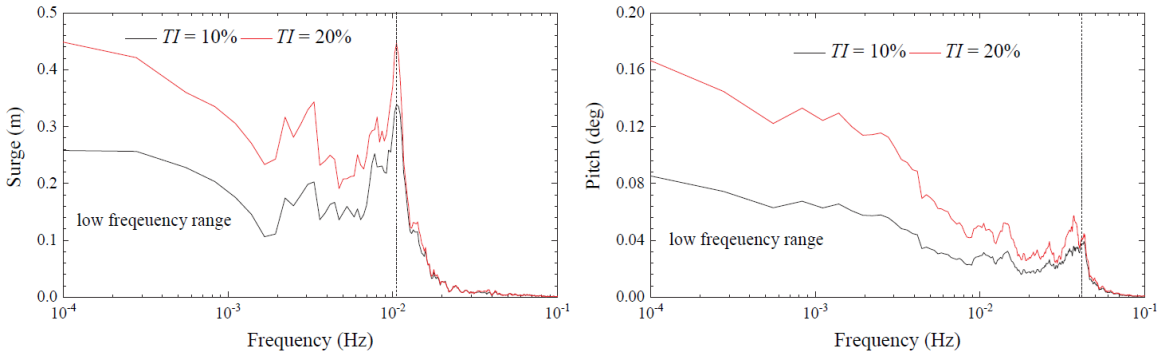

Figure 2.9 – FFT Analysis Showing Turbulent Intensity Effects [71]

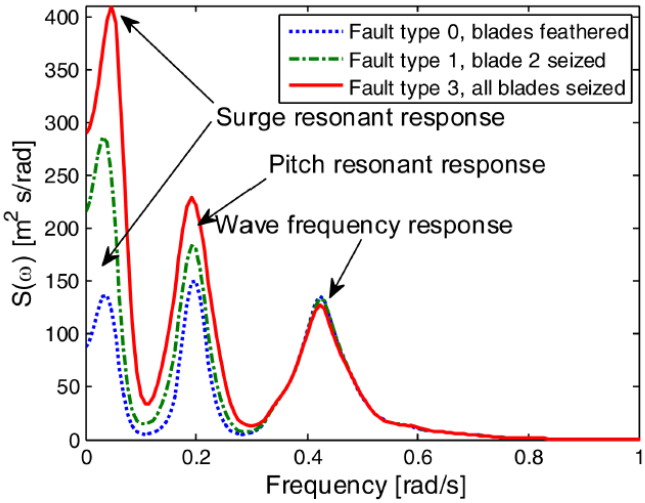

Figure 2.10 – Resonant Response: Fault Conditions [72]

2.5.4 Appropriate Structural-Soil-Hydrodynamic-Aerodynamic Damping

Total damping due to a simultaneous occurrence of different loads and structural behaviour does not always follow a linear combination of the separately determined individual loads and damping coefficient. The total damping is influenced by the character of the individual loads and the combined effects and total structural damping may be established from structural analytical investigations and sensitivity checks. The total damping depends on the wind loading and its direction relative to other loads, for example, if the wave load effect becomes dependent on the characteristics of the wind loading. The overall damping of OWTs plays an important role in the design process as it limits the amplitude of the OWT dynamic response at frequencies near resonance [73]. The aerodynamic damping depends on whether there is wind, and if the turbine is in power production or at stand-still, including if the wind is aligned or misaligned with other loads such as wave loads on the structure [74]. Aerodynamic damping is reported to be dominant damping contributor in the fore-aft direction during power production; however, the aerodynamic damping is less significant for the same direction during parked and feathered rotors, including side-to-side direction for wind-wave misalignment [75]. This is required as an input for calculating the total damping of the OWT structure. Previous research study has investigated the

influence of passive, semi-active, and active structural control and damping on fatigue life, and concluded that there was a notable improvement in the fatigue life due to reduced bending stresses [76] [77]. Soil damping is the most unquantifiable contributor to offshore wind turbine structure damping [78].

Currently, assumptions are made regarding the stiffness and damping of both soil and structural members. Although, these assumptions may be tested through sensitivity analysis and parametric studies, this allows for subjective applications which may lead to over-conservative but expensive designs or under-conservative unsafe designs. Appropriate individual damping ratios and total damping are crucial for dynamic analysis and to avoid resonance, the estimation and control of the natural frequency for the overall structure should be in isolation from the excitation frequencies [14]. Hansen et al. (2006) described two different experimental methods for estimating the aeroelastic frequencies and damping of the operational modes of wind turbines from test data [79]. Aeroelastic simulation of wind turbines was carried out by Shirzadeh et al. (2013) using aeroelastic code [80]. Information on the structure's frequencies and damping values are crucial to quantify the reliability and design life and can also provide an indication of the current state of the soil and foundation, for example, monitoring scour development [81].

Studies show that due to the complexity of modelling soil structure and interpreting the behaviour upon loading, verification of the soil stiffness and determination of soil damping ratios for offshore wind turbine structures is by full scale testing [82]. Soil damping is the highest contributor to the total damping after tower oscillation dampers. Damgaard et al. (2012, 2013) conducted "rotor stop" tests to determine the soil damping, including different wind parks to evaluate the first natural frequency and modal damping of the structures [82, 83]. Cyclic motion was observed to take place during the "rotor stop" test which resulted in material damping and geometric damping. The material damping is also known as internal damping which is the dissipation of energy within the soil mass due to friction, sliding between particles and rearrangement. Geometric damping is also known as radiation (external) damping of waves into the subsoil and can be ignored for frequencies below 1 Hz. From the "rotor stop" test, the irreversible deformations in the soil were established as a measure of the energy dissipation in the first cycle after the "rotor stop" takes place. The tower oscillation damper was determined from full scale "rotor stop" tests as 1.36%, the steel material damping and aerodynamic damping according to [84] were estimated as 0.19% and 0.062%, respectively. The hydrodynamic damping was assumed to be 0.12%, hence, the soil damping was calculated to be 0.58%, deduced from the system total damping of 2.31% following the tests.

A study by Malekjafarian et al. (2021) presented several field tests and experimental research where signals were measured using accelerometer, and strain gauges measured the structure motions and vibrations for determining the OWTs foundation damping [73]. The damping ratios were determined using the recognised logarithmic decrement method for identifying the damping ratio from

free decay response. The calculated natural bending frequency and soil damping ratio depend on the measured and calculated soil strength. Once the appropriate soil stiffness and damping ratio are determined, these can be used in the soil-foundation structure interaction model for local and global design and analysis. Carswell et al. (2015) investigated the significance of foundation damping on an offshore wind monopile structure subjected to a 50-year return storm loading using a linear elastic two-dimensional finite element model which showed that damping reduced the mudline bending moment by 7 – 9% [85].

Aerodynamic damping significantly affects the fatigue life of offshore wind turbine structures. According to Rezaei et al. (2018), normal or unforeseen shutdowns of wind turbines is likely to induce fatigue damage of up to 60%. This is primarily driven by a significant reduction in aerodynamic damping influences on the structural responses rather than a corresponding reduction in operational dynamic loads. Proper calculation of damping ratios and appropriate applications can lead to significant improvements in the structural fatigue life [86]. The fatigue life is reported to increase almost linearly with applied damping [76].

The total structural damping ratio is also influenced by the presence of marine growth on the foundation and turbine structure. The impact of marine growth is greater for the hydrodynamic damping ratio and overall structural response. The thickness and imposed weight of the marine growth as a damper are necessary for estimating the influence on the natural response of the structure. The uncertainties in estimating the damping contribution from the tower oscillation damper, structural damping, soil, aerodynamic, and hydrodynamic effects is highlighted by several researchers. Hence, why further research, including investigation into stand-still, faulty, and shut-down conditions is needed. The damping coefficient is an important dynamic parameter for modelling and conducting representative dynamic analysis of offshore wind turbine structures [82].

2.5.5 Corrosion

The inside of the offshore wind turbine tower and foundation were previously considered to be airtight, and therefore it was assumed that there would be no corrosion due to lack of oxygen in the compartment to achieve the necessary chemical reactions. However, this assumption is invalid as both seawater and oxygen access the inside of the monopile under certain conditions, including in sites where significant tidal variations exist. This can lead to active corrosion that can negatively impact the integrity and capacity of the offshore wind turbine structure. Industry recommended codes and standards have also been revised to reflect these findings as explained in Section 2.1.

Condition monitoring and assessment of offshore wind turbine foundations consists of visual inspections, corrosion measurements and evaluation of the water quality. Visual inspection is the least expensive of the Non-Destructuve-Inspection methods, but the quality and effectiveness of visual inspection may be hindered by access to offshore wind turbine structures and the capability of the inspection team

[87] [88]. Cathodic protection is one of the established methods for mitigating corrosion using sacrificial anodes. However, there is no established method to control the current output from the anodes due to the partially closed compartments (non-airtight). This was recorded in several cases which resulted in acidification and health issues which compromised the structural integrity and safety of the wind turbine monopile structures [89]. Acidification can result in a higher current requirement for steel surfaces. Steel surfaces are not adequately protected from this which leads to shorter life of anodes.

Ingress of water is possible if the airtight platform is not properly sealed. Below the waterline, corrosion is facilitated by differential aeration between the upper water layer and the active steel surfaces. For non-tidal stagnant water, highly localised corrosion can occur, and at locations where inspection and maintenance access are limited at greater foundation depths. Water-and-airtight foundation structure was observed to be compromised through slow seawater ingress and minor leaks at the J-tube seal into the foundation. This resulted in seawater with dissolved oxygen entering the foundation system, increasing the amount of corrosion inside of the monopile system [90].

Localised accelerated low water corrosion of up to 0.5 mm/year has been observed where there is failure in the J-tube seal, leading to substantial ingress of seawater and tidal variations occurring inside the foundation system. The water level changed daily and at extreme spring tides. The recorded corrosion of 0.5 mm/year exceeded the permissible design corrosion rate stipulated by DNV. The permissible design corrosion allowance by DNV is 0.10 mm/year for submerged internal surfaces, 0.15 mm/year for the splash zone in temperate climates and 0.20 mm/year in tropical/subtropical climates [90]. Study completed by Moan showed that the corrosion rate fluctuates and exhibits a large scatter of between 0.04 to 1.2mm/year depending on the location in the structure [91]. The offshore wind structures are typically designed with service life of at least 25 years which makes coating requirement against corrosion challenging without adequate maintenance and integrity plan [92]. Research work by Weinell et al. (2017) explores the possibly of improving the coating life to meet the 25 years design life of the offshore wind turbine structure and the possibility of reducing the costs for corrosion protection [93].

There is a risk of microbiologically influenced corrosion (MIC) and sulphate reducing bacteria (SRB) being present on submerged surfaces and in the buried but upper sediment parts of closed monopile foundation. Where favourable conditions exist to support growth, the results will be localised corrosion attacks on the submerged surfaces. MIC increases with the availability of organic matter in the soil, this can be exacerbated by the occurrence of scour and should be accounted for in designs. MIC is also possible in an oxygen free environment, making the concept of corrosion prevention inside the offshore wind turbine by ensuring of airtight oxygen free environment a questionable phenomenon [23].

Existing monopile structures are being retrofitted with internal corrosion protection (CP) systems with galvanic anodes. New monopile designs incorporate CP systems as part of the engineering solution for corrosion. Furthermore, these monopile structures are monitored to gather data to improve the level of understanding on internal corrosion, challenges and mitigation strategies related to internal CP systems. Previous research has identified fatigue life and the risks of hydrogen-induced stress cracking (HISC) as an issue in the presence of CP. The use of steel with a specified minimum yield greater than 550 N/mm^2 should be analysed particularly for applications where anaerobic environmental conditions such as stagnant water, active mud bacteria and hydrogen sulfide may dominate [90].

Presently, new offshore wind turbine structures are conservatively designed for internal corrosion through the application of protective coatings, corrosion allowance designs, and implementation of CP [94]. Monitoring is also used as an additional corrosion control and mitigation strategy. However, these measures are expensive and therefore, research to establish an optimised cost-effective solution is required.

Microbiologically induced corrosion is usually linked to sulfate-reducing bacteria (SRB) and the mechanism by which sulfate accelerates metal corrosion is still an area where significant research is needed to close the gap in understanding the process. SRB leads to a reduction in the pH level inside the monopile structure and prevents the sacrificial CP system from functioning as intended. In addition, at low pH levels, there can be a corresponding reduction in the current output of the galvanic anodes. Hence, combining adequate coating with cathodic protection systems is necessary to prevent/mitigate corrosion and subsequent growth [95]. The offshore wind turbine coating process is conducted near the completion stage of the structure and is often not given the same care and attention dedicated to other activities as projects may have already overrun schedule at the time of implementing corrosion protection designs and systems [23] [96]. Furthermore, due to the geometry of the offshore wind turbine structures and the generated impact energy during pile driving, galvanic anodes are attached and installed together with the transition piece (TP). The anodes are clustered to fit within the available space on the TP leading to interference issues and the likelihood of under-protection of larger areas.

Corrosion protection system (CPS) on offshore wind turbine structures around the splash zone is a challenging case to design and control due the continuous and intermittent exposure to seawater and oxygen in response to tidal and wave variations [93]. Corrosion protection systems have been found to be ineffective around the splash zone, which is considered a severe corrosive environment compared with atmospheric and submerged zones; hence, further research is required for design and control measures [97]. Furthermore, there is no established detailed method to model and analyse patch-type and pitting corrosion which is an area of active research. The localised forms of corrosion such as

pitting, and crevices can lead to local stress concentrations and a corresponding reduction in fatigue life and structure utilisation [98] [99].

Demonstration of corrosion and growth inside a monopile is presented in Figure 2.11, recorded using corrosion coupons at three different zones:

1. Atmospheric zone
2. Waterline – tidal and wave variation zone
3. Submerged zone.

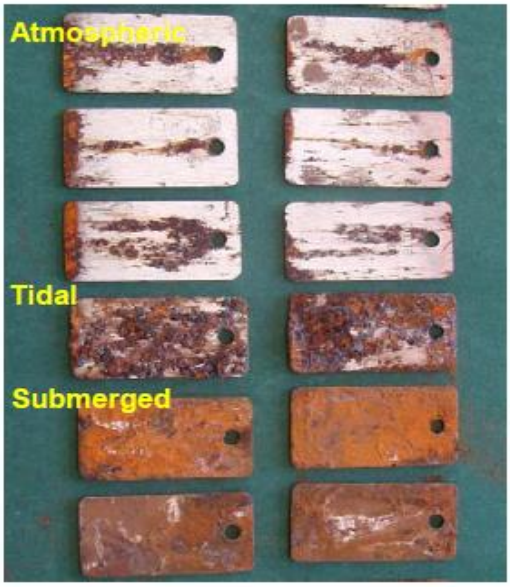

Figure 2.11 – Corrosion Coupons Inside a Monopile from Three Different Zones [100]

Studies have recommended corrosion design using a time-dependent corrosion rate model instead of corrosion design by assuming a generic allowance based on corrosion wastage thickness. The time-dependent corrosion rate model assumes deterioration of the CPS and reduced effectiveness. Corrosion growth exhibits non-linear behaviour which consists of the following stages [97]:

1. Phase one: the corrosion protection system is effective with little or no corrosion occurrence.
2. Phase two: there is a depletion of the corrosion protection system and a reduction in effectiveness, leading to a non-linear corrosion growth with time, including the presence of localised pitting corrosion.
3. Phase three: Asymptotic corrosion wastage and growth.

2.5.6 Transition Piece: Grouted with or without Shear Keys Connection

The offshore wind turbine tower is connected to the foundation system through the transition piece. The introduction of shear keys in the grouted connection is aimed at improving capacity, but this has the disadvantage of a corresponding poor fatigue strength. The shear keys introduce fatigue hotspots and currently,

designers conservatively assume poor fatigue details and design S-N curve data for engineering the joint. Hence, there is the need to refine the design and analysis of grouted joints with or without shear keys. Placing the shear keys within the centre of the connection improves the impact on the fatigue capacity of the joint. Through testing, the presence of shear keys is demonstrated to increase the stiffness of the connection and reduce local sliding distance and gaps by a factor of 2. Although it understood that the shear keys can lead to hotspots and exacerbate fatigue damage, tests shows that plain steel surface grouted joints leads to reduced fatigue and ultimate performance compared to connections with shear keys [101]. The failure modes for grouted joints include grout cracking, compression strut failure, sliding failure, and ground shear failure [102] [103]. Grouted connection failure and damage detection in the joint can be identified through the implementation of a structural health monitoring (SHM) system based on the fibre optic sensor-type Fibre Bragg Grating (FBG), including the detection of the occurrence and the global severity of the damage [104] [105]. Higher flexibility in response to bending loads has been observed to lead to gap openings and relative sliding motion between adjacent material surfaces causing abrasive wear of the grout, which can considerably reduce the service life of the connection [106] [107].

The influence of steel surfaces and shear keys on the fatigue performance of grouted connections was investigated by [106]. The research was conducted for plain grouted joints and for grouted joints with shear keys. The research concluded that local stress concentrations are distributed more evenly with an increase in the number of shear keys and that local stress plastifications occur at the outer shear keys. It was further concluded that for fatigue design, the shear keys lead to local stress concentrations in the grout layers of the connection. However, the failure modes can be reduced if shear keys beads are arranged at the centre of the joint. The introduction of shear keys is favourable regarding the durability of grouted connections.

There is a lack of detailed guidance on state-of-the-art fatigue assessments for offshore wind turbine structures with grouted joint connections, that accurately captures the occurrence of non-linear effects [108]. The non-linear effects of ovalisation and S-shaped buckle mode as the grout punches into the slender steel shell must be correctly captured as a stress riser. Where analytical methods lead to a non-favourable design solution due to simplifications and approximations, it is then recommended to complete numerical analysis by means of 3D finite element modelling and analysis [14]. However, several parameters required for assessment of capacity of grouted connections using finite element analysis are encumbered with uncertainty such as element types, element mesh in the region of the highest stresses, friction coefficient, characteristics of the grout materials, material modelling, contact formulation, and convergences criterion. Therefore, grouted connection design and analysis by finite element require calibration.

The research project "Grouted Joints for Offshore Wind Turbine Structures" (GROW) and a follow-up research project "GROWup" investigated improving the strength of hybrid connections by applying shear keys to address reported sliding damage which occurred in 2009 at several offshore wind farms which have plain cylindrical grouted joints. An important task within the GROW project was to develop detailed finite element models (FEM), calibrated against large-scale tests. The primary objective of the calibrated detailed FEM was to replace expensive experimental verifications and to undertake parametric studies and analysis to improve the designs of grouted connections. It was concluded that the calibrated detailed finite element model gave a good understanding of how the loads in the grout are transferred, mainly between the shear keys, and was a useful tool for detailed design verifications. The research made recommendations for further work to be undertaken aimed at providing guidance on geometric boundary conditions or simplified analytical verification concepts where tests data may not be available for calibration. Details of the experiments, calibration process, and the refined finite element model for the design and analysis of grouted connections are presented in [109]. This is in line with the recommendation that it is appropriate to perform grouted connection design and analysis using a finite element model; however, such finite element analysis must be calibrated and bench-marked with reliable experimental test data or well-known cases where such data exists [14].

The design of the grouted joint primarily accounts for loading due to bending, shear, axial, and torque which usually results in a complex combination and response. The bending moment is dominant over all the loading modes, hence, there is an assumption that the grouted connection capacity is improved due to an increased frictional resistance generated by the induced bending moment [110]. This assumption resulted in a simplified modelling approach separating the axial load and torque from the bending and shear. An earlier version of DNV-OS-J101 recommended demonstrating that the axial loads and bending moment do not interact, then the design conditions of two separate loadings can be justified:

1. Axial load and torque without bending and shear.
2. Bending and shear without axial load and torque.

Distribution of the contact pressure between the grout and steel is presented in Figure 2.12. There is an increased contact pressure at the near-face top and far-face bottom in the direction of the bending moment. The bending moment leads to vertical rotation of the pile and the sleeve, giving rise to two opposing areas of contact pressure at the top and bottom of the connection couple. Load transfer between the transition piece and the monopile is made possible by the resulting force couple [111] and [106].

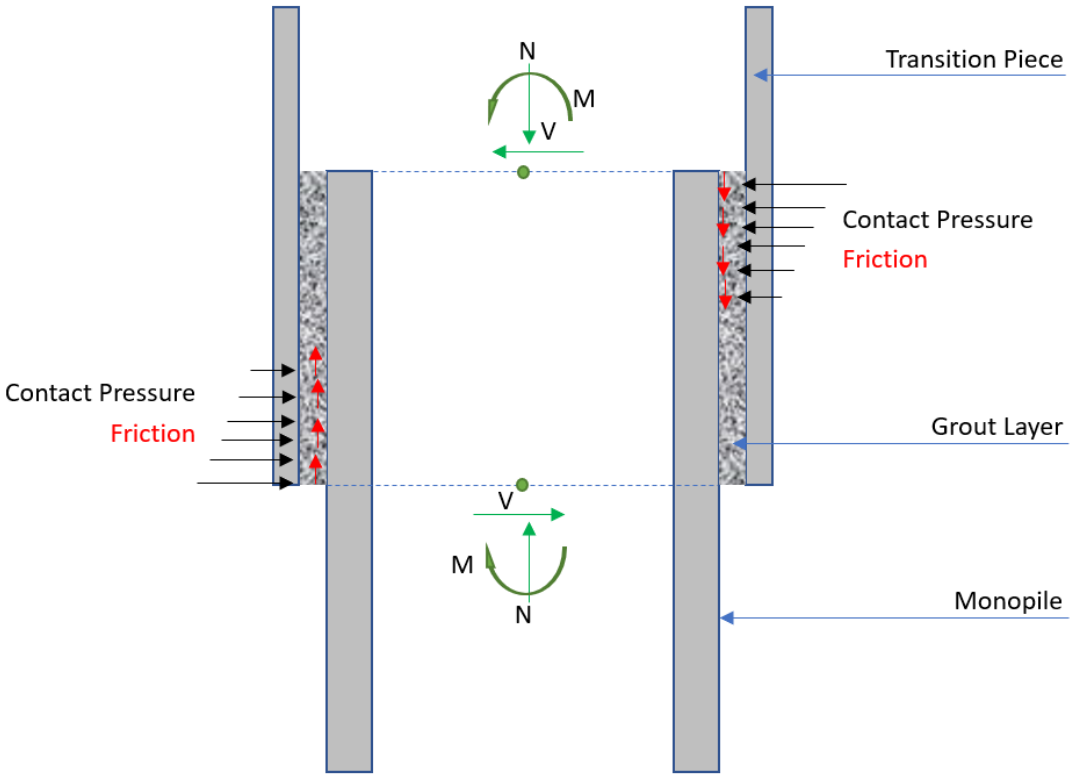

Figure 2.12 – Grouted Joint Contact Pressure Distribution

For Tubular and Conical Grouted Connection without Shear Keys

The maximum nominal contact pressure, $P_{norm,M}$ at the top and at the bottom of the grouted connection, caused by an applied bending moment M, may be calculated from the following expression:

$$P_{norm,M} = \frac{3\pi M}{R_p\, L_g^2(\pi + 3\mu) + 3\pi\mu R_p^2\, L_g} \qquad (1)$$

Where:

μ is the friction coefficient.
L_g $= L - 2.t_g$ is the effective length of the grouted section.
L is the full length of the grout thickness.
t_g is the grout thickness.
R_P is the outer radius of the innermost tube for tubular connections and the average of the outer radius of the innermost for conical connection over the effective area.

Equation (1) assumes that the dependency on a horizontal shear force on the grouted connection is insignificant. This assumption is valid for grouted connection for monopiles.

Wherever the pressure from the shear force is significant, then the effects of this shear force on the pressure, $P_{norm,Q}$ may be calculated from following expression:

$$\boldsymbol{P_{norm,Q} = \frac{Q}{2R_p \times L_g}} \quad (2)$$

The maximum nominal contact pressure due to the bending moment M and shear force Q becomes:

$$\boldsymbol{P_{norm} = P_{norm,M} + P_{norm,Q}} \quad (3)$$

The design tensile stress in the grout can be calculated using the following expression:

$$\boldsymbol{\sigma_d = 0.25 \times P_{local,d}\left(\sqrt{1 + 4\mu_{local}^2} - 1\right)} \quad (4)$$

Where:

μ_{local} is the local friction coefficient representative at the top and bottom of the grouted connection.

$P_{local,d}$ is the design value of the local contact pressure, P_{local}.

For Tubular Grouted Connection with Shear Keys

The maximum nominal radial contact pressure, $P_{norm,d}$ at the top and at the bottom of the grouted connection, caused by an applied bending moment M_d may be calculated from the following expression:

$$P_{norm,d} = \frac{3\pi M_d E L_g}{\left[\begin{array}{c} EL_g \times \{R_p L_g^2(\pi + 3\mu) + 3\pi\mu R_g^2 L_g\} \\ +18\pi^2 k_{eff} R_p^3 \left\{\frac{R_p^2}{t_p} + \frac{R_{TP}^2}{t_{TP}}\right\} \end{array}\right]} \quad (5)$$

where:

k_{eff} is the effective spring stiffness for the shear keys

μ characteristics friction coefficient, equal to 0.7

R_P outer radius of the pile

R_{TP} outer radius of transition piece

t_P wall thickness of transition piece

L_g = L - 2.t_g = effective length of grouted section

L full length of grouted section from the grout packers to the top of the pile

T_g nominal grout thickness

Following observation and detection of vertical settlements in monopiles with plain grouted connections in 2008, a Joint Industry Project (JIP) was initiated by DNV in 2009. It was realised that the industry practice used for the design of large diameter connections did not correctly represent the in-service behaviour and response of the physical structure [112]. The JIP tests revealed salient design parameters and considerations that influence the long-term behaviour of large diameter grouted connections [111] and [109]:

1. Surface irregularities and fabrication tolerances: using the correct design data can lead to an increase in capacity of grouted connections generated by friction between the irregular surface and interface of the grout and steel.

2. Slenderness ratio and connection flexibility affects the stiffness, ovality and buckling behaviour of the grouted connection. The flexibility and ovality is

increased when the structures are subjected to horizontal wind and wave action inducing a bending moment.

3. Accumulated sliding length due to cyclic loading leads to reduced frictional and joint capacity.

4. Friction coefficient at the steel-grout interface: application of the appropriate friction coefficient. Higher friction can lead to under-conservative/incorrect resistance capacity, while lower friction leads to over-conservatism and an expensive design.

5. Abrasive wear at the steel-grout-interface due to a combination of moment from sliding, bending, reduced friction and slenderness ratio, leading to ultimate reduction in surface roughness and a loss of friction and capacity.

Conical grouted joints or straight grouted joints with shear keys are favourable and identified for improved performance and capacity to resist bending, shear, axial and torsional loads [113]. The design of grouted connections requires improvement and appropriate design guidelines, outlining the acceptable design approximation for modelling the grout geometry, friction, ovality, and the contact behaviour upon bending and axial loads and the response under dynamic loads.

2.5.7 Early Age Cycling of Grouted Connection

The strength of the grouted connection is influenced by early age cyclic induced dynamic effects under offshore installation conditions and the strength gain window, coupled with the impact of temperature and other environmental conditions. The offshore wind monopile grout connection capacity at both serviceability and ultimate loads can be significantly affected by cyclic movement [114]. High performance mortar grout typically used with an ordinary Portland cement grout can be beneficial in improving the strength of grouted connections [115]. The dominant loads that induce early age cycling of grouted joints are installation loads, wind, and wave actions. During construction, the loads on the grouted joint generate relative movement between the foundation, annulus filled with new grout, and the transition piece, leading to a reduction in the load-carrying capability of the grouted joint. The presence of weld bead connections or shear keys leads to improved radial and frictional capacity against sliding [116]. Shear keys are also introduced to reduce the effective length of the grouted connection while maintaining the load transfer capability [117]. Furthermore, the range of induced movement is unknown, leading to the following negative effects on the grout strength [118]:

1. Sedimentation and segregation of the grout material, initiating progressive accumulation of the coarser particles lower in the grouted connection, while the cement paste filters to the upper section. The homogeneity of the mix is significantly altered and susceptible to cracking.

2. Structural damage of the grout matrix during strength gain, affecting the mechanical and durability properties.

3. Plastic deformation of the hardening grout which can lead to cavities around the shear keys and in the annulus between the foundation and transition piece.

Test results conducted by previous researchers have shown compressive strength variation of the grouted connection between the top part and bottom part in the range of 22% to 45% due to a combination of negative activities caused by early age cycling [118]. Although these effects of early age cycling are captured through testing of the representative grout samples, the validity of the model and response in real life projects are unknown. Hence, further investigation is required to calibrate the models, and analyse and quantify the impact on the grouted connection due to early age dynamic loads. The effect of the reconstructed grouted connection is demonstrated in the resulting air void content at the upper part, middle part, and lower part of the grouted samples for both static loads and dynamic loads, Figure 2.13.

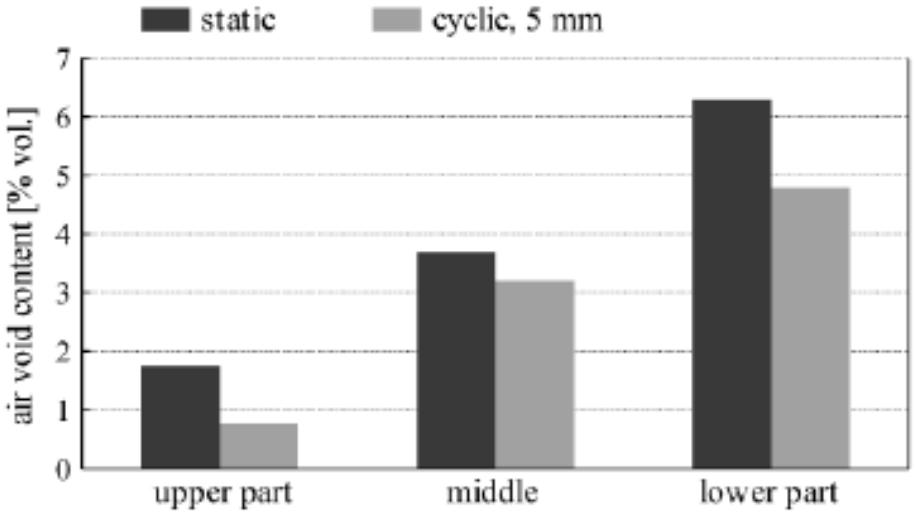

Figure 2.13 – Reconstructed Grouted Connection Due Loads [119]

The expected relative movement during grouting is limited to a maximum of 1mm, which includes the combined effect of rotation and displacement over a 24-hour installation phase. Although the restriction in relative movement is important, it is strict and difficult to achieve in design, manufacturing, and installation stages [119]. The introduction and design of the temporary grippers between the foundation and the transition piece/top structure was implemented during the installation of the Beatrice Offshore Wind Turbine Project to achieve the 1mm limit due to the early age movement of a grouted connection over a period of 24 hours of the grouted joint installation phase. This movement is deemed to be in any direction, and if exceeded may result in significant degradation of the grout connection [120].

2.5.8 Air-tight Corrosion Design and Control by Exclusion of Oxygen

Most offshore wind turbine support structures are designed and fabricated using S355 steel grade. However, the corrosion-fatigue properties and corrosion-fatigue resistant material selection are still a subject of research interest [121] [122]. The inside of the offshore wind turbine tower and foundation was in recent times considered to be airtight, there was an assumption that there was no corrosion due to lack of oxygen to complete the necessary chemical reactions. However, this assumption has been shown to be invalid as both seawater and oxygen have access to the inside of the monopile under certain conditions, including sites where significant tidal variations exists. This can lead to active corrosion and impact the integrity and capacity of the offshore wind turbine structure. Industry recommended codes and standards have been revised to reflect these findings.

Corrosion control by exclusion of oxygen is primarily an option for structural compartments which are only externally exposed to seawater, e.g., internal compartment of legs and bracings of jacket structures that are completed and free flooded at installation. Any compartments potentially exposed to air will need to be kept permanently sealed by welding or by maintenance of overpressure by nitrogen to prevent any air ingress. Some compartments such as the interiors of monopiles are periodically accessed for inspection and repair and can therefore not be considered completely sealed. Levels and zones in sea water environment schematic representation is shown in Figure 2.14. Effects of large tidal variations on internal water levels must be considered. In addition, even in the virtual absence of oxygen in the seawater, corrosion by anaerobic bacteria can occur. It is recognised that an air-tight compartment in monopile structures is not feasible, hence, it is recommended that these issues are taken into consideration when evaluating options for corrosion control for internal compartments.

Presently, new offshore wind turbine structures are conservatively designed for internal corrosion by the application of protective coatings, corrosion allowance designs and implementation of corrosion protection and monitoring as an additional corrosion control and mitigation strategy. However, these are expensive; therefore, research to establish an optimised cost-effective solution is required.

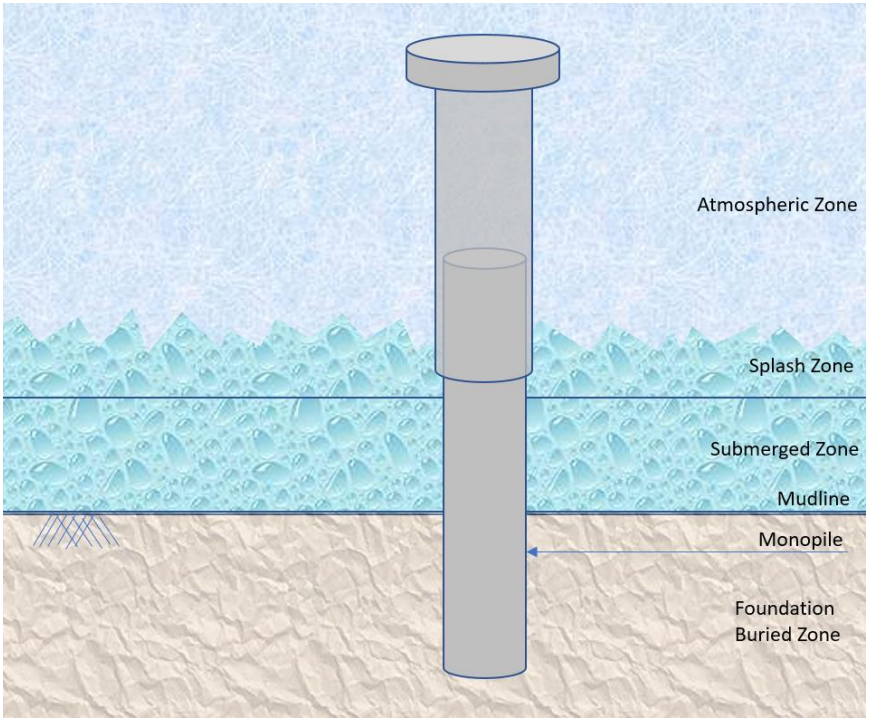

Figure 2.14 – Schematic Representation of Levels and Zones

2.5.9 Corrosion Allowance and Fatigue Design

Fatigue calculation is affected by the corrosion allowance applied to the structural component. The corrosion allowance corresponds and is determined by the corrosion rate and conforms to the assumed corrosion conditions which dictate the S-N curve used for the fatigue calculation. The fatigue damage assessment is best captured by considering the coupled effects of wind, wave loads and operation loads and conditions [123] [124]. The cumulative fatigue damage is the sum of the individual damage from all of the considered stress range intervals, referred to as the Palmgren-Miner Rule [125] [126]. However, the dynamic response of offshore wind turbine structures is likely to be influenced primarily by the wind load [127]. It is recommended that if substantial metal loss is expected, free corrosion conditions must in general be assumed, and the "free-corrosion" S-N curve is then required. Fatigue criterion may govern the design where substantial metal loss or corrosion is expected for welded connections [128]. The spatial interaction of welded tubular joints leads to a complex interference of stresses and load distribution between the welds and the tubular member [129]. This aspect of design requires further research to understand the extent and envelope definition of "substantial metal loss" and if the "free-corrosion" S-N curve is appropriate or other S-N curves are suitable for the condition along with engineering quantifiable justification. Further guidance states that "free-corrosion" S-N curves can be applied for the internal surfaces of monopiles below the waterline.

Cathodic protection is one of the established methods used to mitigate corrosion using sacrificial anodes. However, challenges exist and there are no established methods for controlling the current output from the anodes due to partially closed

compartments (non-airtight). This was recorded in several cases showing acidification and health issues which compromised the structural integrity and safety [89]. For surfaces where primary structural parts are exposed in the splash zone and for internal surfaces in the submerged zone, which are without CP, the corrosion allowance (CA) for the surface with or without coating is according to the expression:

$$CA = V_{corr}(T_D - T_C) \tag{6}$$

Where V_{corr} is the expected maximum corrosion rate, T_C is the design useful life of the coating and T_D is the design life of the structure.

The Corrosion Protection System (CPS) on offshore wind turbine structures around the splash zone is challenging to design and control due the continuous and intermittent exposure to seawater and oxygen in response to tidal and wave variations. Guidance on corrosion protection such as coating and corrosion thickness allowance are provided in [130] [29] Corrosion protection systems are ineffective around the splash zone, which are considered a severe corrosive environment compared with atmospheric and submerged zones, hence, further research is required for design and control measures [97].

Studies recommend corrosion design using time-dependent corrosion rate models instead of corrosion design by assumed generic allowance based on corrosion wastage thickness. The time-dependent corrosion rate model assumes deterioration of the CPS and reduced effectiveness. The spectral fatigue design method is commonly used in fixed offshore oil and gas structures as the method is not computationally expensive compared with other renowned methods. However, this method needs to be verified and validated to handle the non-linearity associated with the larger and heavier offshore wind monopile structures [131].

2.6 Structural Monitoring

In-service Structural Health Monitoring (SHM) or Structural Monitoring (SM) of offshore wind turbines is one of the reliable measures to substantiate/verify and investigate design uncertainties. The SHM data is used to improve and optimise existing and future structural designs through analytical calibration. It is a useful and applicable design technique that can provide early warning of structural degradation, enabling early intervention and maintenance. SHM enables condition-based monitoring and maintenance, providing condition status and real-time structural evaluation which offers input for lifetime extension and identifies any required operational change. Vibration-based damage detection is a global damage testing method that considers the difference in dynamic characteristics between the initial state (baseline) and the experimental results to detect and quantify localised damage. Manzocchi et al. (2012) reported the application of this method on a jacket structure in the North Sea [132].

SHM applications for offshore wind turbines are used to measure and quantify environmental loads, deformation/displacements, foundation scour, corrosion, structural response of tower and foundation systems (natural frequency and damping), settlement and soil stiffness, amongst other useful design data.

Integrated SHM systems have been deployed across several offshore wind turbine sites in Europe and the US. The aim of the integrated SHM systems is to reduce total costs and improve the engineering design of wind farms. The integrated SHM is an improvement on independent and specialised monitoring systems used to monitor and record structural, material, geotechnical, and metocean data. Integrated SHM instrumentations are configured to link and correlate all the recorded parameters [133]. Design and installation considerations of integrated SHM systems are as follows:

- Instrumentation design plan for the selection of required sensors and appropriate location considering accessibility for quality data.
- Type and specifications of sensors and sensor interface suitable for the type of monitoring campaign, storage, and back-up.
- Data logging and transfer interval, including filtering, threshold, appropriate and available communication lines.
- Objectives, data use and interpretation, and reporting.

Examples of integrated SHM were installed by DONG Energy Wind Power's (now Orsted) which incorporated and implemented 141 SHM sensors on a prototype Suction Bucket Jacket BKR01 installed in 2014. The integrated sensors were remotely controlled, enabling early detection of deviations from predicted analytical results. The system led to the transition from planned maintenance to condition-based maintenance.

Research and practice have demonstrated that for monopiles, tilt/displacement is critical for monitoring. The dynamic response and stiffness of the structure as a governing design criterion are of interests in SHM. Furthermore, local and site related issues such as scour, corrosion, and the response of the transition piece are also relevant [133]. Soil response, stiffness, and the corresponding foundation and tower motions offer important design information for calibrating the analytical model, fatigue life estimation, and prediction.

Conclusions from previous studies have recommended Vibration-based damage detection. This is a global testing technique based on the difference in dynamic characteristics between an initial state (baseline state) and experimental results to detect and quantify damage. Information such as mass, stiffness, and damping of the structure can be ascertained. Although this method can be traced back to mid-1970s, it is not widely favoured in the industry [134] [135]. Other promising methods are Optical Fibre technology such as the Fiber Bragg Grating (FBG) test which transmits light through glass or plastic, reflected in the form of wavelengths

based on the properties of the grating [135] [105]. Parameters such as strain and temperature can be measured using this technology.

Acoustic Emission Testing (AET) and CrackFirst are established technologies for detecting and measuring fatigue cracks and fatigue damage initiation, irrespective of the SHM method deployed. Measured monitoring data is usually processed and interpreted using Fast Fourier Transformation to transform the time domain data to frequency domain. Underwater inspection of OWT foundations with a focus on fatigue crack growth, health and safety risks, by using a probabilistic approach for inspection planning of fatigue cracks in fixed and floating offshore wind turbine structures are discussed in [136, 137].

2.7 Design Uncertainties, Reliability, and Structural Responses

The condition of an offshore wind turbine structure can be deterministically or stochastically determined through established indices of the safety margin which accounts for load and resistance uncertainties or reliability index in accordance with industry design codes and standards [138]. The reliability level of offshore wind turbine structures may be selected based on cost optimisation analysis considering the design and operational life-cycle of the turbines [139] [140]. Current design standards and industry practices are primarily based on deterministic design techniques, where partial factors are used to account for the load and resistance and modelling uncertainties. These uncertainties and a gap in understanding can lead to either over-conservative design or an unsafe catastrophic outcome [4].

Measuring structural condition using a reliability index is one of the most relevant applications for approaching challenges of high design and response uncertainties such as observed in OWT monopile structures. Examples of design and response uncertainties are soil-structure interactions and environmental data and modelling. Reliability analysis methods can be used to understand, quantify, and interpret the influence of the uncertainties of OWT structures. In addition, Structural Health Monitoring (SHM) or Condition Monitoring (CM) discussed in Section 2.6, are methods developed to verify design of OWT structures and assess the safety levels established through stochastic data and probabilistic approaches. Studies have demonstrated improved response and design outcomes through reliability-based design optimisation methods [2].

Monte Carlo simulation is one of the recognised methods for evaluating uncertainties related to structural, environmental and fatigue analysis models and parameters. The Monte Carlo method (Metropolis and Ulam 1949) provides an estimate of multi-dimensional integral problems, which are analytically complicated to solve. The uncertainties related to wind turbulence intensity are identified as having a significant influence on the fatigue loads during power production. Furthermore, the uncertainties and assumptions of Miner's Rule contribute to a larger influence on the structural reliability. The structural reliability method has been developed and progressed since the 1980s and commonly applied to assess

the safety of offshore structures as outlined by Madsen et al. (1986, [141]), Melchers (2018, [142]), and Moan (1994, [143]). Several studies have attempted to quantify design uncertainties and their influence on the structural response and reliability. For example, uncertainties in wind design parameters have been shown to contribute about 10-30% of the total uncertainties in the structural analysis. Procedures focused on inherent uncertainties in the modelling of offshore structures, environmental loads and fatigue damage phenomenon have been recommended by researchers [4].

Uncertainties are generally classified into two subgroups [5] [144] [145]:

1. Aleatoric (or statistical) uncertainties which are related to physical random processes or stochastic nature of data such as variability in soil properties, material strength, and metocean conditions [146]. These uncertainties are unavoidable due to the randomness in the nature of the data and load processes.

2. Epistemic or systematic uncertainties which are related to errors associated with modelling simplifications, measurement imperfections, and statistics such as limited number of observations. These uncertainties can be avoided or minimised by improving the data sample space and the quality of measurements.

The individual and combined effects of stochastic design are a source of uncertainty in design data and analytical assessment.

2.8 OWT Monopile Concepts Future Outlook and Other Structural Considerations

Some important and interesting questions presently being faced by the industry include understanding the upper bound capacity limit of OWT monopiles, the limiting structural criteria, how large and heavy can the structures increase in line with the capacity increase, how deep and the limit of the installation water depth for OWT monopile structures, and manufacturing and installation considerations. The impact on the dynamic response and structure modes arising from refined hydrodynamic and aerodynamic loads on the larger and heavier structures is also an area of on-going research. The findings and understanding from these topics are required to enhance and improve the structural design techniques and methodology for the future concepts of larger and heavier OWT monopiles.

The transportation and installation analysis and operations of future larger and heavier OWT require updating to industry design codes and standards in-line with new technologies. Although current industry codes and standards provide guidelines for best practice, they do not fully cover new transport and installation activities and assessments required for the future concept of OWT structure installations. Structural evaluation of new concept OWT transportation and installation can be addressed using finite element tools with the help of codes and

standards but require relevant structural experience and technical knowledge on how to manage these future OWT structures. Another challenging area of interest for future concepts is the assessment and control of construction peak noise, noise exposure level, excessive pile inclination, and plastic deformation of the thin-shell pile head associated with driving larger and heavier OWT monopiles into the designed embedment depth.

The average fixed-bottom offshore wind turbine size for European deployment in 2018 was 6.8 MW [147]. GE Renewable Energy have recently introduced the Haliade-X offshore wind turbine range which features a 14 MW, 13 MW or 12 MW capacity, 220m rotor diameter, 107m long blade, and 260m high. In a similar move, Vestas also introduced the 15 MW offshore wind turbine in 2021. A new reference 15 MW fixed-bottom offshore wind turbine was presented by the National Renewable Energy Laboratory (NREL) in a joint effort with the Technical University of Denmark (DTU) [147]. These reinforced the pressing questions of understanding the design envelops for future larger and heavier OWT monopile structures and how deep they can safely and successfully be installed, operated, and maintained.

Investigation into 5 MW OWT monopile diameter, thickness, and tower height performed by [47] gives an insight into the stiffness of the system. The investigation shows a reduction in the tower stiffness as the height increases and/or a reduction in wall thickness. The research concluded that the impact of height change has a greater impact on the stiffness of the tower in comparison with the corresponding change in wall thickness as presented in Figure 2.15. The influence of the tower diameter was also investigated which showed a decrease and increase in the bending moment of 19% and 6.3% for 5m and 7m pile diameter compared with original 6m diameter, respectively. Although the investigation did not include the extensive definition of the design envelop for the 5 MW OWT monopile and the governing factors for increasing water depth and structure size, it did highlight the impact on the structure stiffness and natural frequency which is fundamental to the design of OWT monopiles.

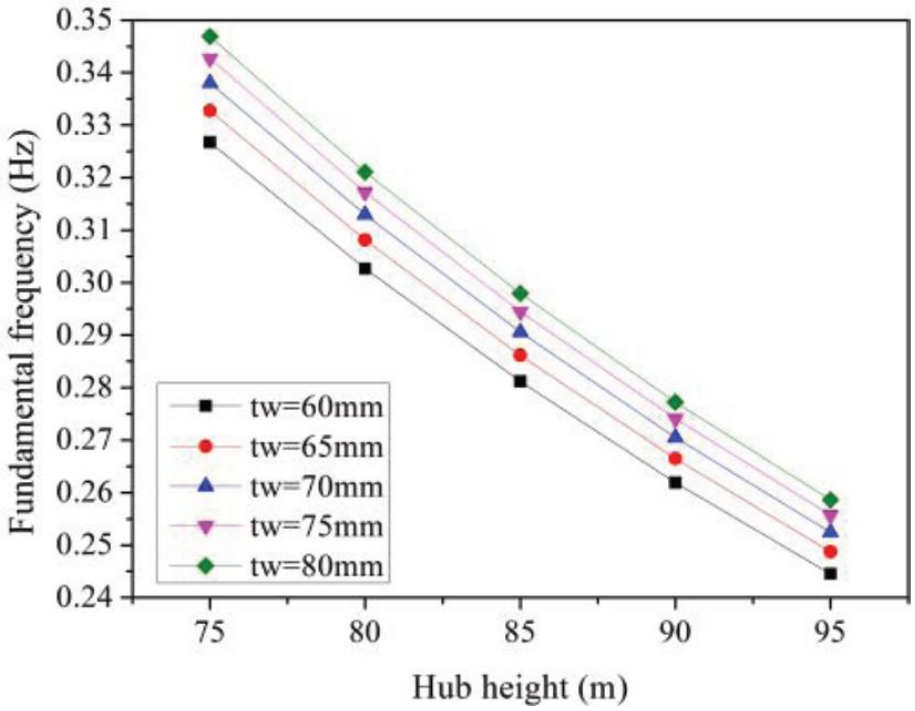

Figure 2.15 – Fundamental Frequencies for Different Tower Heights and Wall Thicknesses [47]

2.9 Conclusions and Research Contribution

A holistic review of offshore wind turbine structural design techniques and practices in accordance with industry design codes and standards is presented in this paper. The review is primarily focused on fixed-bottom OWT monopile structural design and analysis. Several academic works and existing industry techniques and technologies are reviewed, highlighting the salient design achievements, challenges, and opportunities for future research and development activities for larger and heavier OWT monopile concepts and structural design. The following conclusions can be drawn:

1. Grouted connection structural response and capacity is improved by the introduction of shear keys; however, this limits the fatigue strength through stress hotspots and should be addressed through detailed refined local analysis. There is a lack of detailed guidance on state-of-the art fatigue assessment of OWT and the use of finite element analysis is encumbered with significant uncertainties, requiring calibration with experimental test data or well-known cases where such data exists.

2. Total damping is influenced by the character of the individual loads and the combined effects may be established from structural analytical investigations and sensitivity checks. Calculation of the total damping currently suffers from assumptions and subjective applications on estimating the individual damping ratio. The damping coefficient is an important dynamic parameter for modelling and conducting representative dynamic analysis. Hence, further

research is required to address this issue and to improve the calculation of the offshore wind turbine design fatigue life. Previous research has attempted to calculate the tower oscillation and soil damping through "rotor stop" tests and the conservative assumption of unknown parameters. The steel material damping, and aerodynamic damping were estimated, and the hydrodynamic damping was assumed. There is a strong interest in improving the total (and individual) damping coefficient, including the influence on the structural dynamic behaviour and response of future larger and heavier OWT monopile concepts.

3. Modelling and analysis of cyclic loading and foundation scour remain a challenging issue. Data from different offshore wind farms indicates a significant variation in the scour hole shape (horseshoe). The horseshoe vortex and lee-wake vortex form the processes that govern scour, dictated primarily by the Keulegan-Carpenter number. Results from sensitivity demonstrate the influence of scour on the global stiffness and modes of the OWT monopile structures, including the impact of soil-structure foundation modelling techniques. However, more work is required to fully capture the influence of scour on larger diameters, thicknesses, and turbine capacity loads.

4. The natural frequency as well as the fatigue loading, and response are significantly affected by the soil-structure interaction understanding and modelling. The renowned p-y curves method is limited to smaller pile diameters. Although strides in research are being made in the offshore wind turbine industry such as the PISA project for soil-structure interaction, there is the need for future research and calibrated modelling techniques, including the understanding on future OWT monopile structure concepts.

5. It is recommended that if substantial metal loss is expected, "free-corrosion" conditions and S-N curve must be assumed and applied. This aspect of design requires further research and justification to understand the extent and definition of "substantial metal loss" and the appropriateness of "free-corrosion" S-N curve. In addition, there is no established method of managing corrosion in offshore wind monopile structures and there is a need for future research into modelling and analysis of patch-type and pitting corrosion.

6. Extensive research and industry studies are required on the low technology readiness levels of future larger and heavier OWT monopile structure concepts. Some areas of interests include but are not limited to: defining the design envelope and limits of future concepts up to and including 20 MW OWT monopiles, and possibly higher, the limiting structural criteria, installation depth, and installation considerations such as acceptable noise exposure levels and excessive pile inclination that may arise from driving larger diameter piles. Although, financial models and economic analysis are not reviewed in this paper, the cost impact on structural design techniques and methodology may be worth investigating for future OWT monopile concepts.

This comprehensive literature review and gap analysis research contributes to knowledge, specifically offshore wind turbine engineering knowledge, is scientifically sound, provides value to stakeholders, and direction for new future research and industry development. This literature review has been successfully published as a peer reviewed journal paper. The unique knowledge contribution is presented in Table 2.3.

Section	Unique Contribution	Contribution to Knowledge
Comprehensive literature review and gap analysis	Identified the important structural design gaps and improvements made from the release of the first DNV design guideline to latest revision.	Provides a useful overview and holistic information and understanding of the evolution of the offshore wind turbine. This provides useful fundamental and applicable structural engineering design knowledge required for problem solving.
	Outlined the influence of the gaps and their impact on structural design and systems response.	Provides understanding and quantitative information on design conservatism, how to avoid and improve the design techniques and methodology. Provides direction for future research and industry developments.
	Identified new design methods and contributions to improve on existing design approach and methods.	The new design methods can lead to safe, efficiency, and cost-effective engineering solutions.
	Quantified the influence of scour on 5-MW offshore wind monopiles.	Provides information and understanding on the importance of scour and natural frequency in designing offshore wind monopile structures, along with recommendations for detailed assessment for new generation turbines.

Table 2.3 – Unique Knowledge Contribution

3 INFLUENCE OF SOIL-STRUCTURE MODELLING TECHNIQUES ON OFFSHORE WIND MONOPILE STRUCTURAL RESPONSE

The published peer reviewed journal article: Sunday K, Brennan F. Influence of soil–structure modelling techniques on offshore wind turbine monopile structural response. Wind Energy, 2022, was authored by myself as part of my research completed under the direction and consultation of my supervisor, Professor Feargal Brennan. The published article is incorporated and forms a significant part of the research on the influence of soil-structure modelling techniques on offshore wind monopile structural response presented in this section.

3.1 Introduction

Serviceability limit state design is generally considered the strictest governing design criterion for offshore wind turbines to ensure efficient operational functionality throughout the design life of the structure [11]. Offshore wind turbines are a dynamic-sensitive structure, subjected to complex external dynamic environmental and operational loads such as wind, waves, rotational frequency of the rotor (1P), and blade passing frequency (3P for 3 bladed turbine) [14] [148]. The operating envelope of the wind turbine is defined by the allowable deflection (tilt and rotation) of the rotor-nacelle-assembly (RNA) specified by the manufacturer and the general structural deflection limit according to industry design standards. Modal analysis and harmonic response analyses are performed to establish the natural frequency and response amplitude of the structure which forms an important and fundamental aspect of the serviceability limit state check. The aim is to avoid resonance effects that will ultimately lead to large amplitude stresses and subsequent accelerated structural fatigue damage. One of the primary design aims is to ensure that the natural frequency of the structure does not coincide with the fundamental frequencies of the external loads. The accuracy in estimating the natural frequency of the offshore wind turbine primarily depends on the modelling technique, analytical model verification, and model calibration where data exists. The importance of the natural frequency and structural response cannot be overstated, as this can mean the difference between an accurate and cost-effective design or an overconservative and expensive design [58].

The structural modelling technique is crucial in capturing the soil-monopile relationship and interaction. Inaccurate modelling can result in soft soil-structure or on the other hand, stiffer soil-structure than is accurate which directly affects the natural frequency and response of the offshore wind turbine. The problem is exacerbated by the coupled and non-linear nature of the structure foundation and the variability of the soil properties along the buried monopile length. Typically, the soil-structure modelling can be completed using amongst others, the following approaches:

a. 3D finite element modelling with mass soil.
b. API p-y curve non-linear soil springs.
c. JeanJean non-linear soil springs.

This paper investigates the influence of modelling techniques on offshore wind turbine structural response and the impact on achieving an efficient and cost-effective engineering design. Section 3.2 of this article presents and discusses the three modelling techniques considered. Fundamental frequencies and generation of the safe design and operational zones of the offshore wind turbine is covered in Section 3.4. Wind and wave spectra calculation and generation are presented in Sections 3.5 and Sections 3.6, respectively. The results and discussions from the investigation are presented in Section 3.7. Important highlights and conclusions are discussed in Section 3.8.

3.2 Design Data and Modelling Techniques

The model is based on a validated NREL 5 MW offshore wind turbine embedded 60m below ground level and in a water depth of 20m. The pile penetration depth of 60m is selected to fix this variable, suitable for a workable design, considering the range of pile diameters, thicknesses, and water depths of up to 70m. The pile embedment depth is checked according Randolph [149] to determine the required minimum pile length for the pile to be considered as "infinitely long" according to the following equations:

$$L_P \geq D_p \left(\frac{E_e}{G^*}\right)^{\frac{2}{7}} \qquad E_e = \frac{E_P I_P}{D^4 \pi / 64} \qquad G^* = G_S \left(1 + \frac{3}{4}\vartheta_s\right) \tag{1}$$

Where L_P is the pile embedded length, E_e is the pile equivalent Young's modulus, G* is the soil equivalent shear modulus, $E_P I_P$ is the pile bending stiffness, G_S is the soil shear modulus, and υ_s is the soil Poisson's ratio. The required minimum embedded pile length is calculated to be in the range of 25m to 50m considering pile diameter of 6m to 11m, and minimum required wall thickness of driven piles according to the API [150]. The required minimum embedded pile length is less than the 60m embedded pile length considered in this research.

$$t_P(mm) \geq 6.35mm + \frac{D_p(mm)}{100} \tag{2}$$

Furthermore, 60m embedment depth is selected to match the verification model and reference study conducted by Senanayake et al. (2017, [58]). Three modelling techniques are considered in this study, as described in this section. The basic structural design properties are outlined in Table 3.1, and the soil properties are presented in Table 3.2 for clay soil. The soil friction angle of 20 degrees for clay soil is applied at the interface of the sensitivity models for completely, but the soil friction angle does not influence the behaviour clay soil. Sensitivity was conducted for zero- and 20-degree friction angles to verify that the soil friction angle does not influence the structural response considering the Mohr-Coulomb constitutive model. The zero- and 20-degree friction angles showed good agreement, with <1% difference between the soil friction angles for stress utilisation and deflection at mudline, and below 2% difference for the structure's natural frequency.

Description	Value	Units
Rating	5	MW
Rotor Diameter	126	m
Hub Height	87.6	m
Hub Mass	56780	Kg
Nacelle Mass	240000	Kg
Tower Mass	347460	Kg
Rotor Mass	110000	Kg
Cut-in, Rated Wind	3, 11.4	m/s
Cut-in, Rated Rotor Speed	6.9, 12.1	rpm
Tower base Diameter and Thickness	6, 0.05	m
Tower Top Diameter and Thickness	3.87, 0.025	m

Table 3.1 – Properties of NREL 5 MW Reference Wind Turbine Model [1]

Description	Value	Units
Tower/Steel Structure Material Properties		
Density (Effective to account for paint, bolts, welds, flanges*)	7850 (8500*)	kg/m^3
Young's Modulus	210	GPa
Shear Modulus	80.8	GPa
Steel Grade	355	MPa
Soil/Foundation Properties		
Installation Depth Below Mudline	60	m
Soil Density	1800 – 2000	kg/m^3
Undrained Young's Modulus	40 – 70	MPa
Poisson's Ratio	0.45	-
Soil Angle of Internal Friction	20	Deg
Undrained Shear Strength (S_U) (Cohesion)	150 – 250	kPa

Table 3.2 – Turbine Tower and Soil-Foundation Design Data [1][11, 58, 151]

The soil angle of internal friction of 20° is used to calculate the friction coefficient of 0.35 between the soil and monopile steel structure.

Mohr-Coulomb soil constitutive model is used for the soil modelling in Ansys Structural. The Mohr-Coulomb model is an elastic-perfectly plastic model which captures the soil complicated non-linear behaviour. The Mohr-Coulomb is applicable to three-dimensional stress space model where the plastic behaviour is described by two strength parameters. The Mohr-Coulomb model stress-strain behaves linearly in the elastic range, governed by the Young's Modulus, E, and Poisson's ration, υ, according to Hooke's law. The failure criteria are defined by the friction angle, φ and cohesion, c; and the flow rule is governed by the dilatancy angle, ψ, for realistic irreversible change in volume due to shearing. The flow rule also used as the evolution law for plastic strain rates. Other practical soil constitutive models include the Drucker-Prager, Duncan-Chang or Hyperbolic model, Modified Cam Clay, Plaxis Soft Soil and Plaxis Hardening Soil Model.

However, the benefits and limitations of each models are not covered in this research and some information can be found in the research work by Huat [152].

Using NREL 5-MW reference model data, a 5-MW offshore wind monopile model was developed for verification purposes. The model was verified against the research completed by Senanayake et al. (2017, [58]) and according to the field-scale wind turbine model by Jonkman et al. (2009, [153]). The verification process includes sensitivities of the generated model and compares the natural frequency and displacements to the NREL 5-MW reference model. The soil properties, including the Young's Modulus, are generated considering the research work by Arany et al. (2015, [11]) and Sahasakkul et al. (2016, [151]). The soil model profile is presented in Figure 3.1.

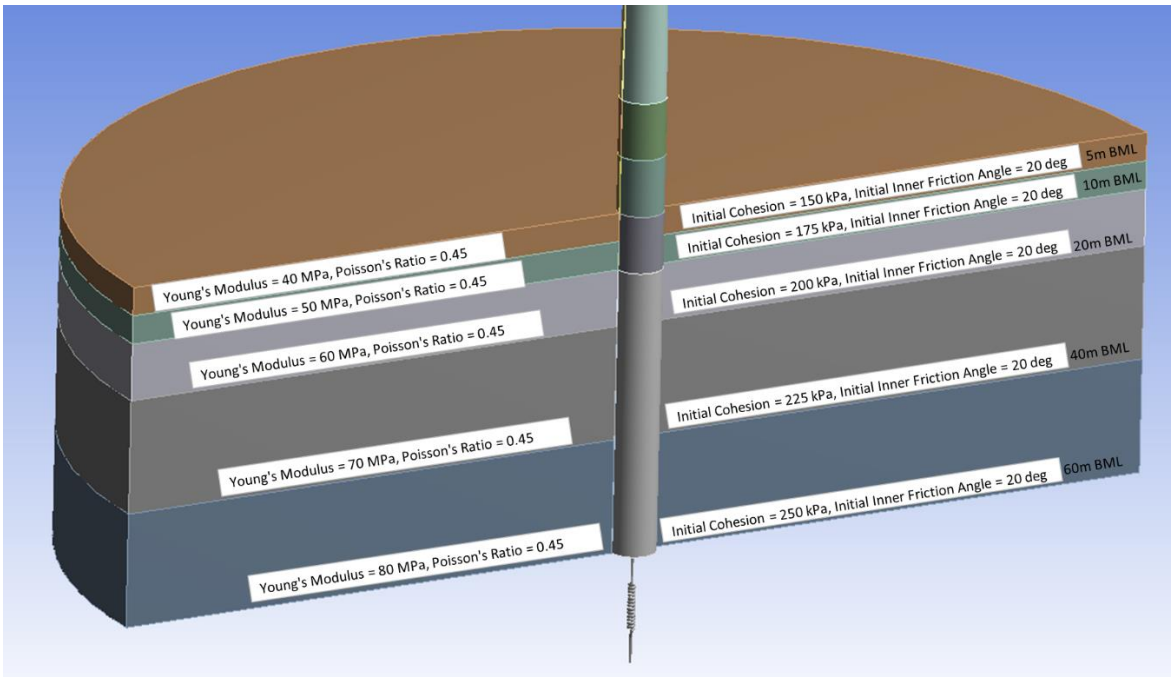

Figure 3.1 – Soil Model Profile

3.2.1 API Modelling Approach

For soft clay (s_u ≤100 kPa) subjected to static lateral loads, the ultimate unit lateral bearing capacity, p_uD has been found, according to the API standard, to vary between 8 s_uD and 12 s_uD, except in shallow depths where failure occurs in a different mode due to low overburden stress. The lateral bearing capacity can suffer from significant deterioration when subjected to cyclic loads below the static loads. The static API method is considered in this research and no cyclic modifiers have been applied in the generation of the p-y curves. The soil lateral bearing capacity, p_uD increases from 3 p_uD to 9 p_uD as z increases from 0 to z_R according to the following equation [45] [41]:

$$p_uD = 3\,s_uD + \gamma^I zD + J\,s_uz \;for\; z < z_R \quad (3)$$

$$p_uD = 9\,s_uD for\; z \geq z_R \quad (4)$$

where:

- p_uD is the ultimate resistance, units of force per unit length;
- s_u is the undrained shear strength of the soil at the point in question, in stress units;
- D is the pile outer diameter;
- γ^I is the submerged soil unit weight;
- J is the dimensionless empirical constant values ranging from 0.25 to 0.5 having been determined by field testing. J value of 0.5 is applied in this research;
- z is the depth below the original seafloor;
- z_R is the depth below soil surface to the bottom of the reduced resistance zone.

The lateral soil resistance-displacement relationships for piles in clay are generally non-linear. The p-y curves for short-term static loads and for cases where equilibrium has been reached when subjected to cyclic loads may be generated according to the relationship defined in the design code and presented in Table 3.3.

p/p_u	y/y_c
0.00	0.0
0.23	0.1
0.33	0.3
0.50	1.0
0.72	3.0
1.00	8.0
1.00	∞

Table 3.3 – p-y Curves for Short-term Static Loads [40]

where:

- p actual lateral resistance, (kPa)
- y actual lateral deflection, (m)
- y_c 2.5 ε_c D, (m)
- ε_c strain which occurs at one-half the maximum stress at laboratory unconsolidated undrained compression tests of undisturbed soil samples.

According to the API design methodology, the ultimate resistance is expected to be reduced to something considerably less, due to rapid deterioration under cyclic loadings, and it is recommended to be considered in cyclic design. Although cyclic loading and modifier is not considered in this research; in the absence of site-specific laboratory test date, ε_c is reasonably assumed as 0.02 for calculating yc and the corresponding soil deflection, y from the relationship given in Table 3.3. The relationship between the p/p_u *and* y/y_c and the soil spring forces, F, determined from the p values are based on the following equations:

$$\frac{p}{p_u} = \frac{1}{2}\left(\frac{y}{y_c}\right)^{1/3} \tag{5}$$

$$F\ (N) = P \times D_{O\_pile} \times L_{element} \tag{6}$$

The generated soil springs at selected depths, as used in the investigation according to API RP methodology, is presented Figure 3.2.

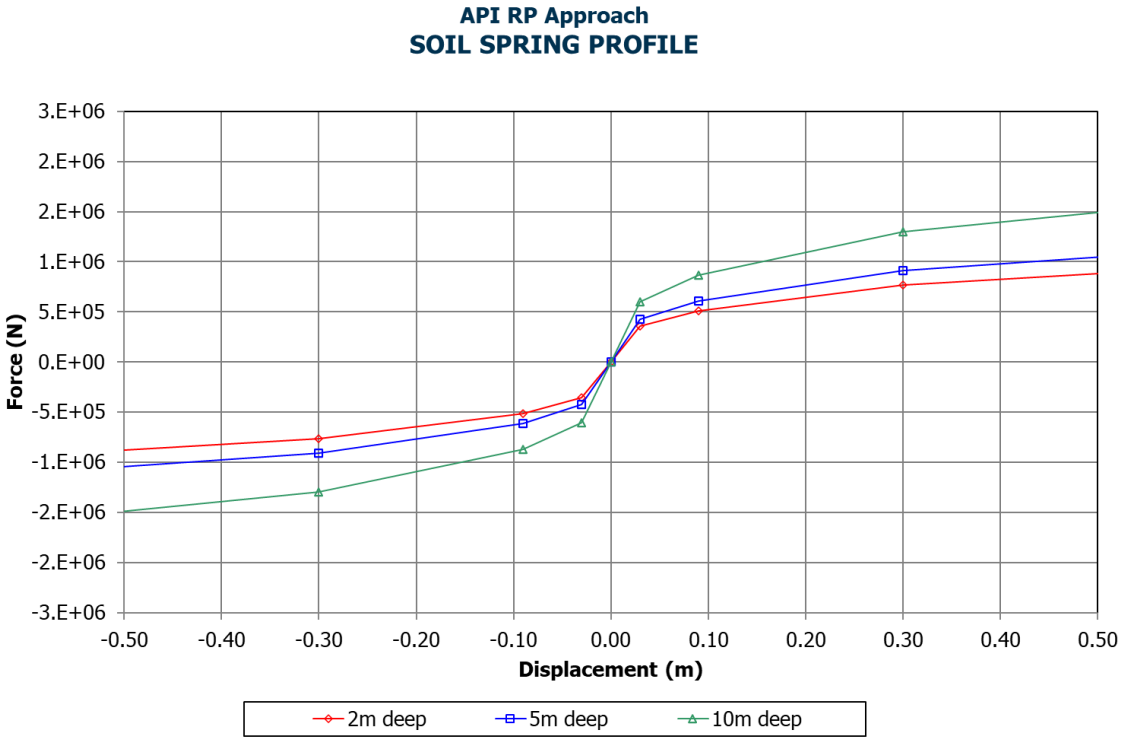

Figure 3.2 – Soil Spring Profile According to API RP

3.2.2 JeanJean Modelling Approach

The JeanJean modelling approach assumes that the shear strength profile increases almost linearly with depth. The method is more suitable for dynamic analysis of structures, subject to cyclic loads that can ultimately lead to fatigue damage [59]. The centrifugal curves from tests according to the JeanJean approach are stiffer than the API RP curves, and the ultimate pressure also exceeds the value of 9 p_uD given by the API RP. The average value of the ultimate pressure is 13.4 p_uD [54]. For shear strength profiles which increase almost linearly with depth, the ultimate unit pressure, P_{max}, can be calculated according to the following expressions:

$$P_{max} = N_p.\ S_u \tag{7}$$

$$N_p = 12 - 4\ .e^{\left(\frac{-\xi.Z}{D}\right)} \tag{8}$$

$$\xi = 0.25 + 0.55.\lambda, for\ \lambda < 6; and\ \xi = 0.5\ for\ \ \lambda \geq 6 \tag{9}$$

$$\lambda = \frac{S_{uo}}{S_{u1}.D} \tag{10}$$

where:

S_{u0} is the shear strength intercept at seafloor;
S_{us} is the rate increase of shear strength with depth;
D is the pile diameter;
z is the depth of interest.

The soil resistance, p, is calculated for a given lateral displacement y, over pile diameter, D, y/D of 0.002, 0.004, 0.008, 0.016, 0.064, 0.5, and 6. The selected y/D covers a lateral displacement range of 10mm and greater than 10m, considering a pile diameter of 5m or larger. The

$$\frac{P}{P_{max}} = \tanh\left[\frac{G_{max}}{100.S_u}.\left(\frac{y}{D}\right)^{0.5}\right] \tag{11}$$

where:

G_{max} initial or maximum shear modulus or small strain;
S_u shear strength.

The initial or maximum shear modulus or small strain can be determined from resonant column testing on samples taking during site-specific investigation. Alternatively,

$$\frac{G_{max}}{S_{uDSS}} \approx \frac{300}{PI/100} \tag{12}$$

where:

s_{uDSS} undrained shear strength from the direct simple shear tests;
PI plasticity index of the soil. In the absence of site-specific date, G_{max}/S_u is taken as 550 for calculating the plasticity index.

Finally, the soil spring forces are determined according to the equation:

$$F\ (N) = P \times D_{O\_pile} \times L_{element} \tag{13}$$

The generated soil springs according to the JeanJean approach at selected depths as used in the investigation is presented Figure 3.3.

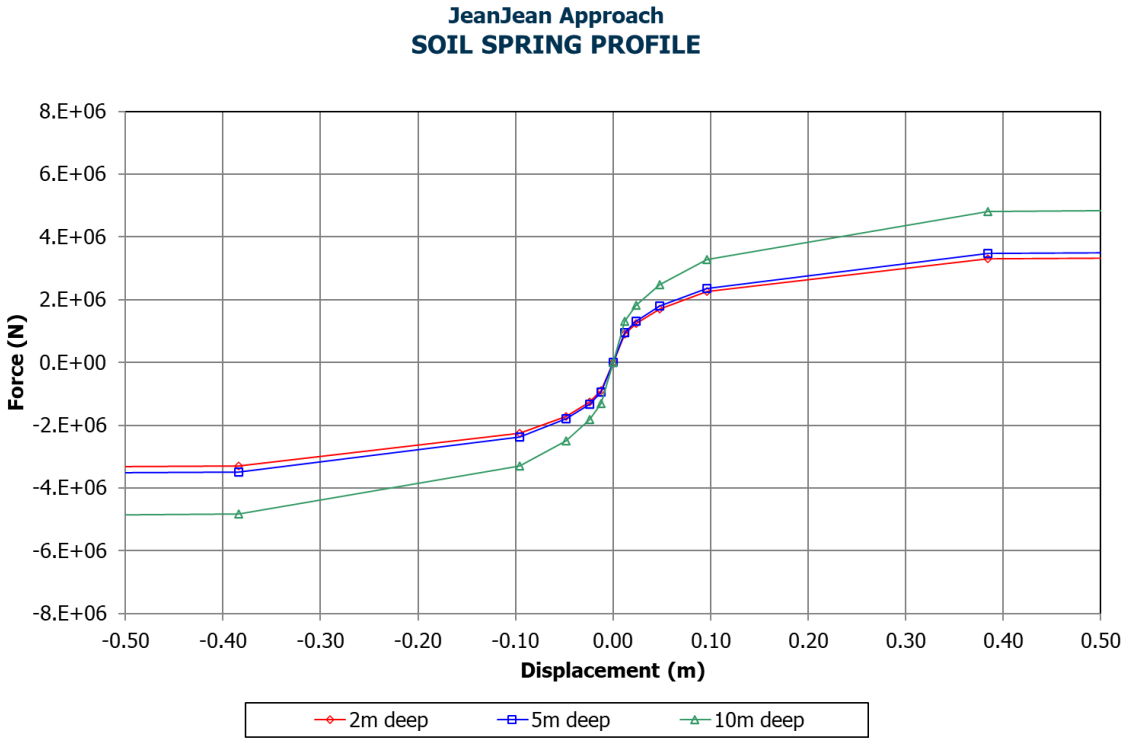

Figure 3.3 – Soil Spring Profile According to JeanJean

3.2.3 Finite Element Modelling Approach

The finite element modelling approach is conducted using Ansys Workbench - Static Structural. The model is made up of the tower supporting a lump mass representing the RNA mass. The tower is submerged in a water depth of 20m and embedded 60m below mudline. The foundation is modelled using soil mass extending 200 m in diameter (approximately 30 times the tower base outer diameter). The foundation is divided into several soil profiles to represent the different soil profiles and properties along the depth. The interaction between the structure and the soil is modelled using friction calculated based on the angle of internal friction of the soil. The base of the tower is supported on a spring for base bearing support. The interaction and connections of the different sections of the tower are achieved using bonded connections or workbench surface share tool to enable flexibility in meshing the different parts. The model showing sections of the soil and meshed profiles is presented in Figure 3.4.

Mesh sensitivity was completed for the solution, Figure 3.5. The mesh sensitivity is performed for different mesh sizes and combination, considering 750mm to 1500mm at different sections of the monopile. von Mises stress is extracted at the mudline where the bending moment is greater, for the different mesh configurations as presented in Figure 3.5. Details of the selected mesh sizes for the different sections of the OWT monopile structure used in this research are outlined below in this section.

Appropriate mesh adjustments were made for larger and heavier turbine models to accommodate the increased turbine capacity and convergence of the analytical solution. The total number of mesh elements varies and changes between models in line with the OWT monopile configurations such as diameters, thicknesses, water depths, and tower heights. The total number of mesh is between 22,788 for 5-MW OWT in 20m water depth to 51,024 for 20-MW OWT in 70m water depth. Free face Quad/Tri mesh type is used to model the tower and foundation structure. Based on findings from the mesh sensitivity, the structure and foundation model mesh sizes are as follows:

- Coarse mesh is used for the soil considering the diameter of 200 m and depth of 60 m. The model successfully solved and converged for the selected mesh size. Refined mesh dependent reactions are not extracted or required from the soil foundation.

- Monopile foundation and tower structure:
  - Between -60m to -10m below mudline: the circumferential mesh size is 250mm, and the longitudinal mesh size is 1000mm.
  - Refined mesh to capture desired reactions is applied between -10m below mudline to 10m above mudline: circumferential and longitudinal mesh size of 250mm is applied, respectively. This refinement allowed for stress, bending moment, deflection, and any other desired reactions to be extracted around the mudline region.
  - Between 10m to 20m above mudline: circumferential mesh size of 250 m and a longitudinal mesh size of 500mm is applied.
  - Circumferential mesh size of 250mm and longitudinal mesh size of 1000m is applied at 20m to the top of the structure.

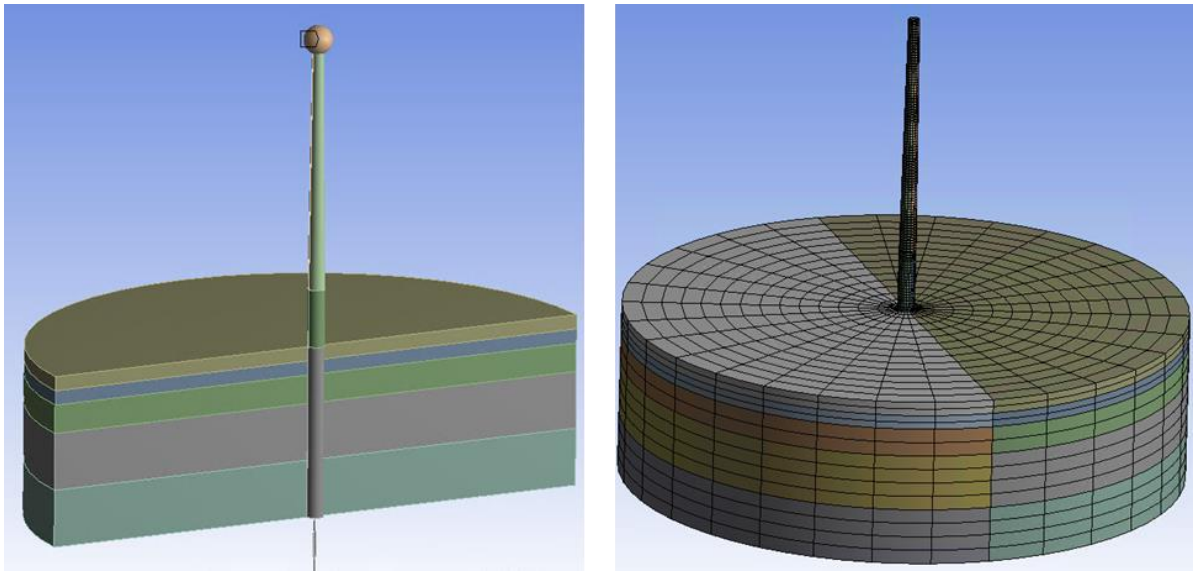

Figure 3.4 – FEA model Showing Soil and Meshed Profiles

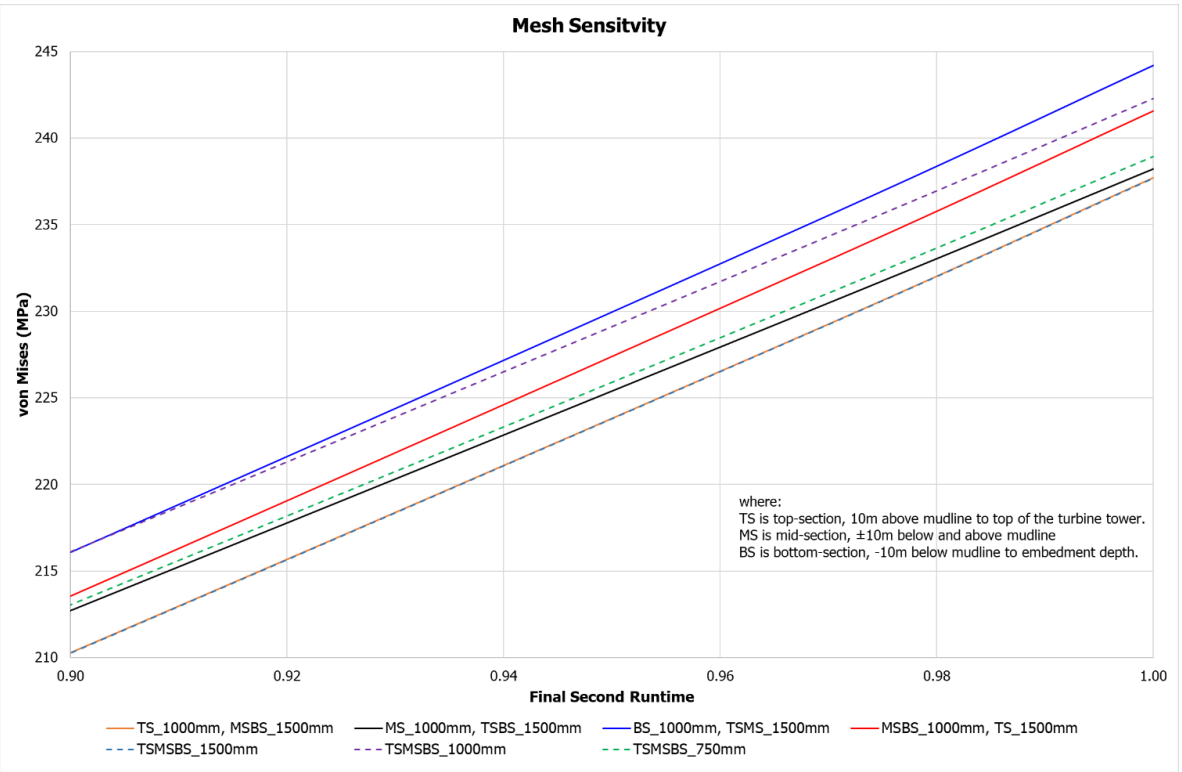

Figure 3.5 – Mesh Sensitivity

3.3 Soil Stiffness Parameter Sensitivity

Sensitivity is performed for the different soil modelling approaches stiffness parameters. For computational efficiency, the soil stiffnesses are compared for different soil strains ε_{50} for the API-RP-2A, and soil shear modulus (small strains) G_{max} for the JeanJean approach, while the response of the offshore wind turbine supported in a continuum mass soil model is investigated for different undrained Young's Modulus, E.

Soil strain, ε_{50} of 0.02 to 0.004, representing Soft Clay to Hard Clay are considered for the API p-y curve stiffness comparison [154], Figure 3.6. The JeanJean soil springs stiffness is compared for different values of G_{max}/C_u ranging from 450 to 650, Figure 3.7. Although the API-RP-2A soil stiffness parameter comparison shows a more notable variation in the load-displacement curves than the JeanJean comparison, it is worth noting that the soil strains used in generating the API p-y curves are not a corresponding match with the small strain used in the JeanJean. Furthermore, the difference (percentage increase) between the soil strain, ε_{50} used in the API-RP-2A differs from the percentage increase in the small strain, G_{max} used in the JeanJean approach. Hence, the presented soil stiffness parameter sensitivity should be considered independently for the different modelling techniques.

The continuum mass soil model sensitivity for different undrained Young's Modulus, considering ultimate limit state loads, is presented in Figure 3.8. The undrained Young's Modulus at the mudline is used for the plot, showing the response of the offshore wind turbine for mudline deflection and the first natural

mode. The base case undrained Young's Modulus is as presented in Table 3.2, having a value of 40 MPa at the mudline and 80 MPa at 60m monopile embedment depth below mudline. Four addition sets of undrained Young's Modulus are considered, increasing the base case by 25%, 50%, 75%, and 100%. The mudline deflection and first natural mode are observed to increase by approximately 3.3% and 1.1%, respectively, for every 25% increase in the soil undrained Young's Modulus. An increase in the undrained Young's Modulus does not equate to a corresponding change in magnitude in the offshore wind turbine displacement and natural frequency response.

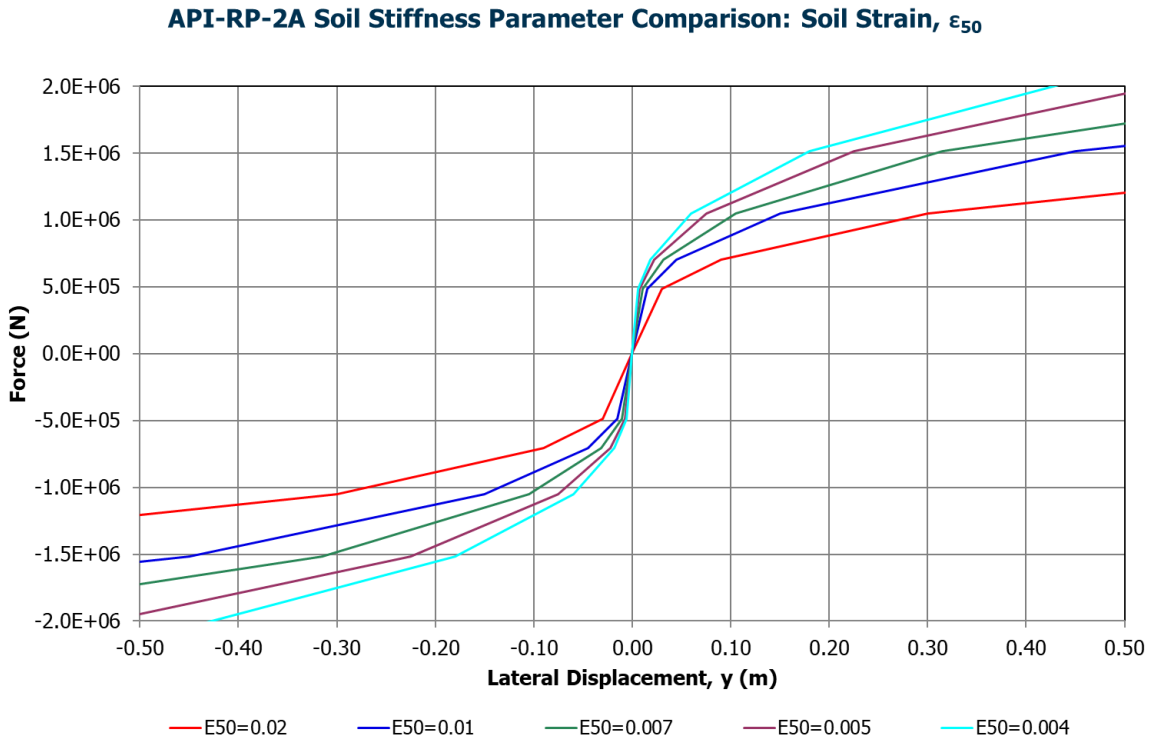

Figure 3.6 – API-RP-2A Soil Stiffness Parameter Comparison: Soil Strain, ε_{50}

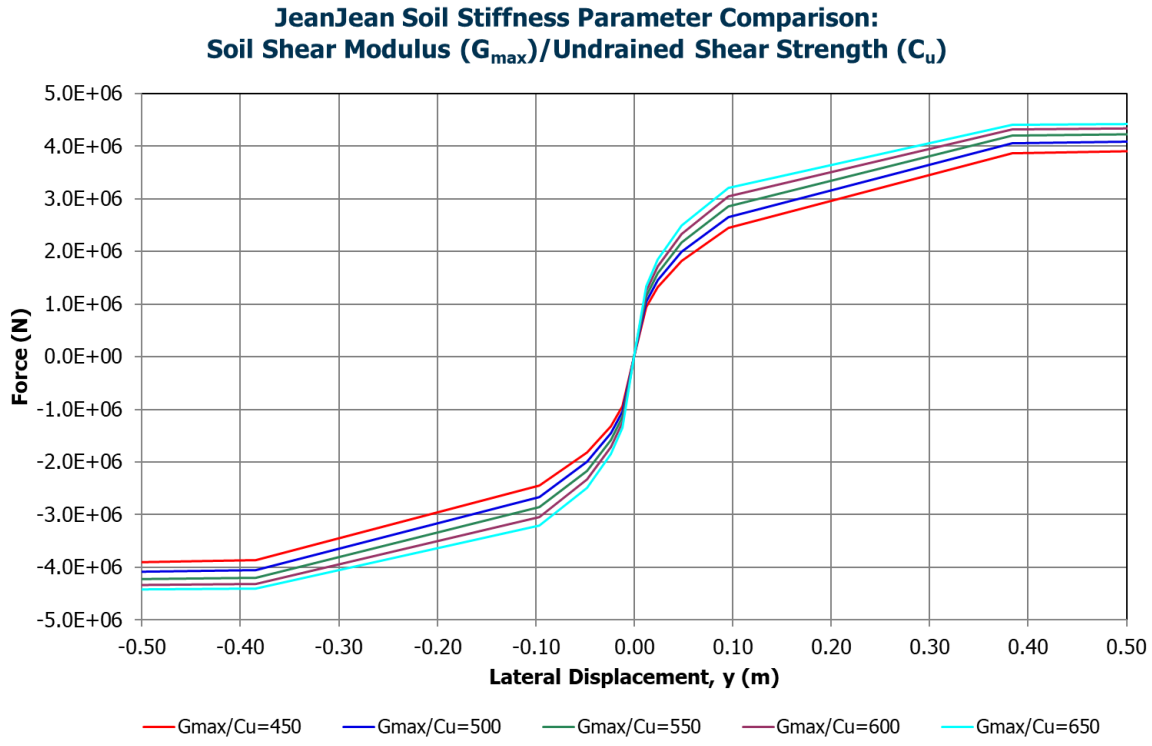

Figure 3.7 – JeanJean Soil Stiffness Parameter Comparison: G_{max}/C_u

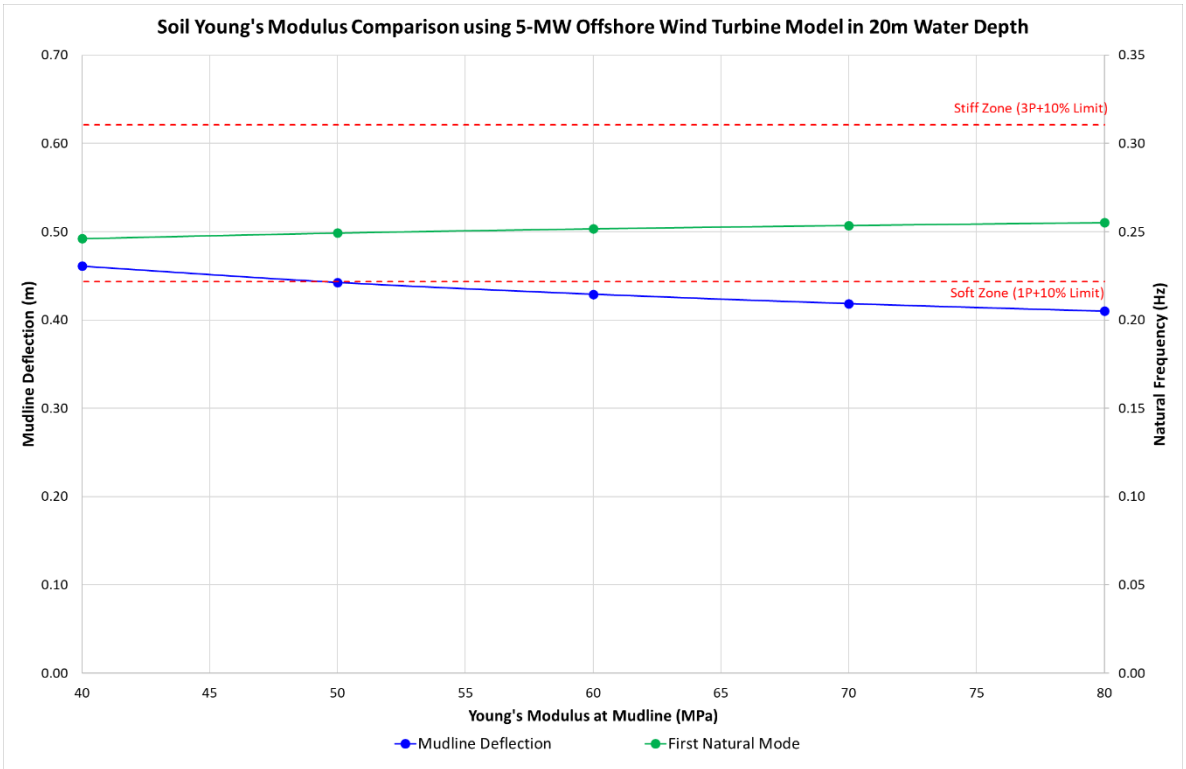

Figure 3.8 – Continuum Mass Soil Model Stiffness Parameter Comparison: Young's Modulus

3.4 Fundamental Frequencies and Safe Zone

Classical design aims to establish and fix the structure target frequency away from external loads. The target frequency of the structure depends on several variables: installation location, type and capacity of the turbine, wave period and spectrum, wind turbulence, and the operating range of the wind turbine (1P range). The rotational frequency of the rotor (1P) and blade passing frequency (3P for 3 bladed turbine) both depend on the wind turbine operating range. The safety margin on the target frequency of the structure is established so that the natural frequency of the turbine should not be within 10% of the 1P and 3P ranges. In addition, high energy content frequency bands of wind and wave loading are to be avoided to minimise the fatigue damage [11]. This usually leaves a narrow safety zone for the design of the turbine, considering the RNA, tower, and foundation systems. From an economic standpoint, a softer structure and underestimating the natural frequency of the OWT monopile is desirable; however, the safest design solution is a higher natural frequency target above the 3P range. Stiffer structure and a higher frequency target require expensive larger and thicker structures and foundation systems which has a corresponding cost impact on transportation and installation. The compromise to the soft or stiffer design is the soft-stiff design where the target natural frequency lies between the 1P and 3P external loads to avoid resonance as presented in Figure 3.9. The operating range is calculated from the turbine Cut-in and Rated frequencies.

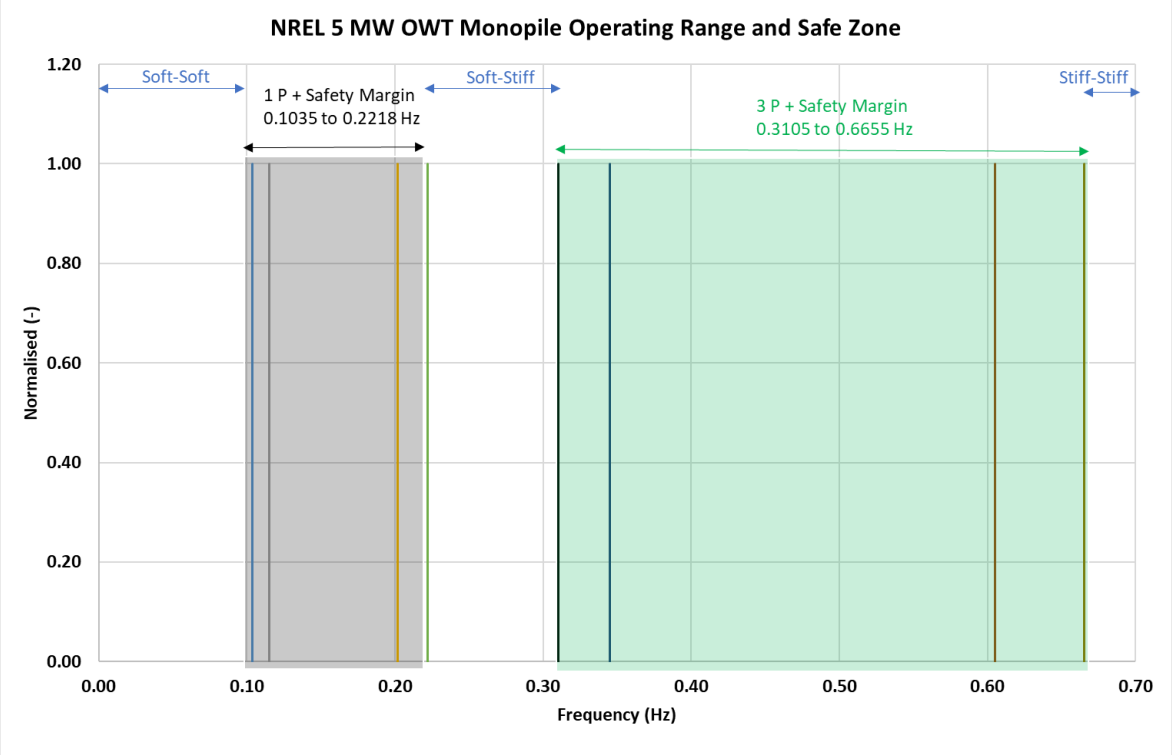

Figure 3.9 – NREL 5MW OWT Monopile Operating Range

3.5 Wind Spectrum

Wind spectrum is used to describe short-term stationary wind conditions. This is also known as the power spectral density of the wind speed, usually determined from available measured wind data for site specific scenarios. Several model spectra exist, and they generally agree in the high frequency range but exhibit significant differences in the low frequency range. Most of the available models may not be suitable for offshore applications as they have been calibrated to onshore or land-based wind data. For example, the Harris Spectrum was originally developed for wind over land. Furthermore, the Harris Spectrum and many other models are not recommended for use in the low frequency range, i.e., for $f < 0.01$ Hz. Most offshore wind turbines are installed in regions where the structure will experience wind loads, with frequency below the 0.01 Hz. Hence, it is important that the selected model spectra be appropriate for winds with frequencies below 0.01 Hz [155].

In this study, the empirical *Ochi and Shin spectrum*, applicable for the design of offshore structures is selected for the generation of the wind spectrum. This Ochi and Shin spectrum is known to have more energy content in the low frequency range ($f < 0.01$ Hz) than other models. Davenport, Kaimal and Harris spectra, are traditionally developed to represent wind over land or onshore applications. The *Ochi and Shin model spectrum* is developed from measured spectra over a seaway and can be calculated using the following equations:

$$\frac{fS(f)}{u^{*2}} = \begin{cases} 583f_* & for \quad 0 \le f_* \le 0.003 \\ \dfrac{420f_*^{0.7}}{(1+f_*^{0.35})^{11.5}} & for\ 0.003 < f_* \le 0.1 \\ \dfrac{838f_*}{(1+f_*^{0.35})^{11.5}} & for\ 0.1 > f_* \end{cases} \tag{14}$$

where:

$$f_* = \frac{f\,.Z}{U_{10}\,(Z)} \tag{15}$$

The generated wind spectrum according to the Ochi and Shin model, along with the external loads (1P and 3P) is presented in Figure 3.10.

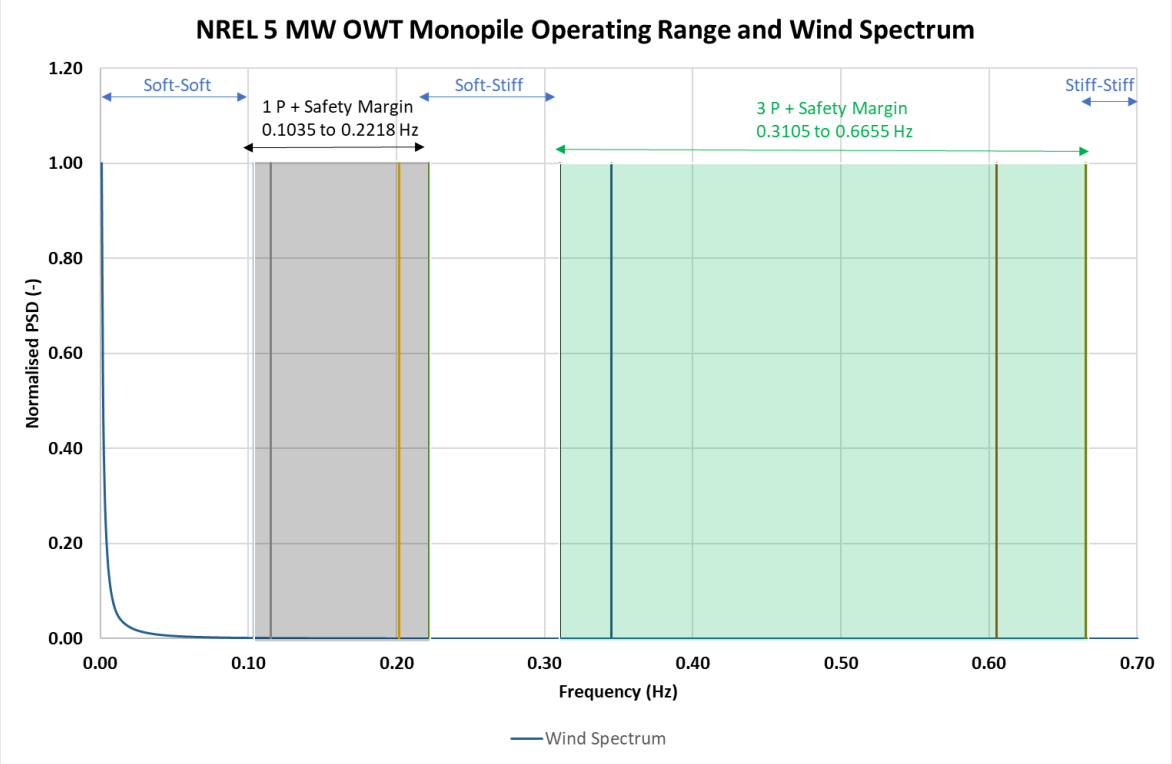

Figure 3.10 – NREL 5MW OWT Monopile Operating Range and Wind Spectrum

3.6 Wave Spectrum

The significant wave height H_s and the peak period T_p are important environmental parameters used to characterise stationary sea-states. Wave spectrum, also known as the power spectral density function of the vertical sea surface displacement is used to describe short-term stationary irregular sea-states. The JONSWAP spectrum is applied in generating the wave spectrum for this study. The JONSWAP spectrum is recommended for fully developed seas. In addition, it can be applied to describe developing sea-states in a fetch limited sea according to the following expression [155]:

$$S_J(\omega) = A_\gamma S_{PM}(\omega)\gamma^{exp\left[-0.5\left[\frac{\omega-\omega_P}{\sigma.\omega_P}\right]^2\right]} \quad (16)$$

where:

$S_{PM}(\omega)$ is Pierson-Moskowitz spectrum;
γ^I is non-dimensional peak shape parameter;
σ spectral width parameter;
σ = σ_a for ω ≤ ω_p
σ = σ_b for ω > ω_p
A γ = 1 – 0.287 ln (γ) is a normalising factor.

The generated wave spectrum according to the JONSWAP model, along with the external loads (1P and 3P) is presented in Figure 3.11.

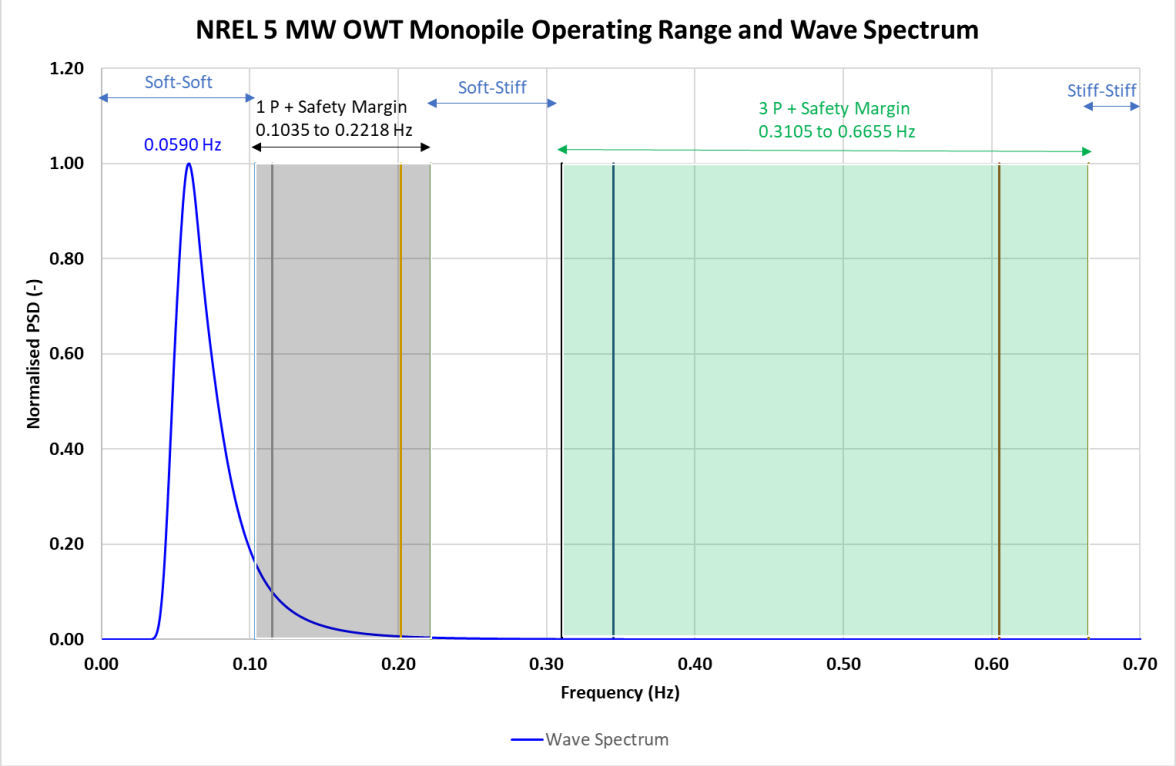

Figure 3.11 – NREL 5MW OWT Monopile Operating Range and Wave Spectrum

3.7 Findings and Discussions

The findings from the study and the discussion of the results are presented in this section by considering the 3D soil mass model, API-RP, and the JeanJean springs supported models. The responses and comparison of the models are also presented and discussed. The monopile is subject to the following external and machine loads according to [32]:

- Self-weight of the RNA is modelled using lump mass at the top of the tower;
- Maximum thrust force due to wind applied at the hub height;
- Horizontal wave force applied at the mean sea level;
- Wind pressure on the tower;
- Hydrostatic pressure.

The models were iteratively tested, and sensitivities performed for different total damping ratios, which includes steel damping, tower oscillation damping, aerodynamic, hydrostatic, and soil damping. A total damping ratio of 10% is selected and used in this research, considering sensitivity on the total damping as presented in Section 3.7.1, previous studies and guidance provided on damping estimation of offshore wind turbine structures [82] [12].

3.7.1 Sensitivities

Total Damping Sensitivity:

The offshore wind turbine monopile model was tested for different total damping, including 0%, 0.25%, 5%, 7.5%, 10%, and 12.5%. The sensitivity provides understanding into the influence of the total damping on the harmonic natural frequency response of the OWT monopile structure as presented in Figure 3.12. At 0% damping, the first frequency peak has a relatively low amplitude content and very high second frequency peak. By increasing the total damping, this natural response is improved. The structural response improvement contributed by damping attenuates and is similar for an applied total damping range of ≥5.0% to 12.5%. Based on previous research by Damgaard et al. (2012, [82]) and findings from this sensitivity, a total damping of 10% is selected and applied throughout this research.

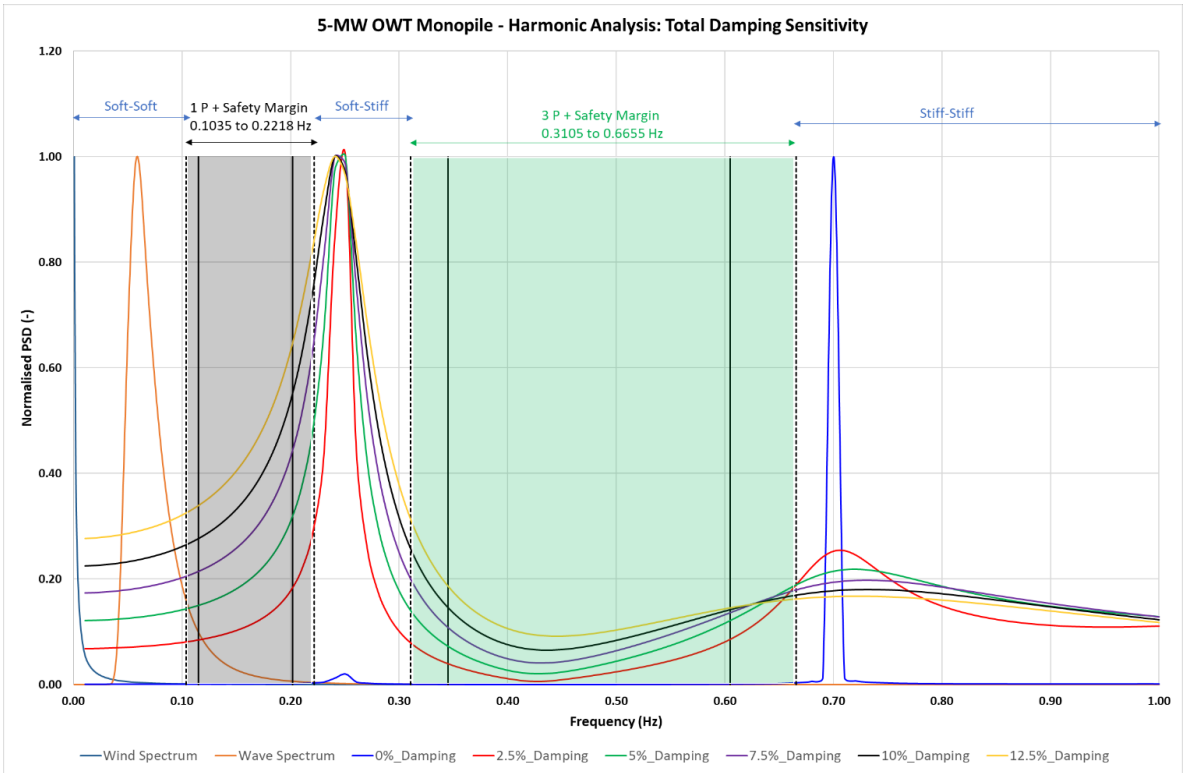

Figure 3.12 – Total Damping Sensitivity

3D Model Monopile Base Support Sensitivity:

The base-case 3D model used in this research is supported at the monopile base with axial soil springs to provide base bearing support. Sensitivity was performed for the monopile base bearing support approach considering the axial spring support, monopile base supported on 5m soil, and monopile base supported on 10m soil, Figure 3.13. The findings of the sensitivity are presented in Table 3.4. For conducting this sensitivity, the soil properties for the 5m and 10m layers below the monopile are taken to be the same as the immediate 20m layer above.

The three different monopile base modelling approaches show an agreement of less than 3% by comparing the structure's natural frequency for each model.

However, the difference in monopile deflection at the mudline is 7% for the 5m soil extension and 15% for the 10m soil extension, compared with the base case spring supported monopile base, respectively. The difference in the monopile deflection at the mudline can be primarily attributed to the soil deformation. For the base case monopile supported on springs, the soil vertical deformation measured at the mudline under full loading and under the soil self-weight only is -0.21m and -0.27m, respectively. This can be compared with the vertical deformation of -0.46m under full loading and -0.37m under soil self-weight for the monopile supported on 5m soil. The corresponding result for the model supported on 10m soil is presented in **Table *3.4***. Considering the findings from the sensitivity, the modelling approach where the base of the monopile is supported on axial springs is applied throughout this research. This is also to reduce the influence of the soil vertical deformation, both under full loading and soil self-weight only, which would require detailed geotechnical investigation and site-specific soil information to quantify the actual soil deformation and time-dependent settlement which are not covered within this research.

Description	Base of Monopile on Axial Spring	Base of Monopile on 5m Soil	Base of Monopile on 10m Soil
Monopile Deflection at Mudline (m)	0.46	0.49	0.53
Monopile Total Rotation at Mudline (°)	0.44	0.47	0.51
Natural Frequency (Hz)	0.2413	0.2382	0.2351
Soil Deformation Under Full Loading - Mudline (m)	-0.21	-0.46	-0.48
Soil Deformation under Soil Self-weight Only – Mudline (m)	-0.27	-0.37	-0.43

Table 3.4 – 3D Monopile Base Support Sensitivity

The corresponding OWT monopile shear and bending moment reaction loads at the mudline elevation are 6.38 MN and 250 MN-m, respectively.

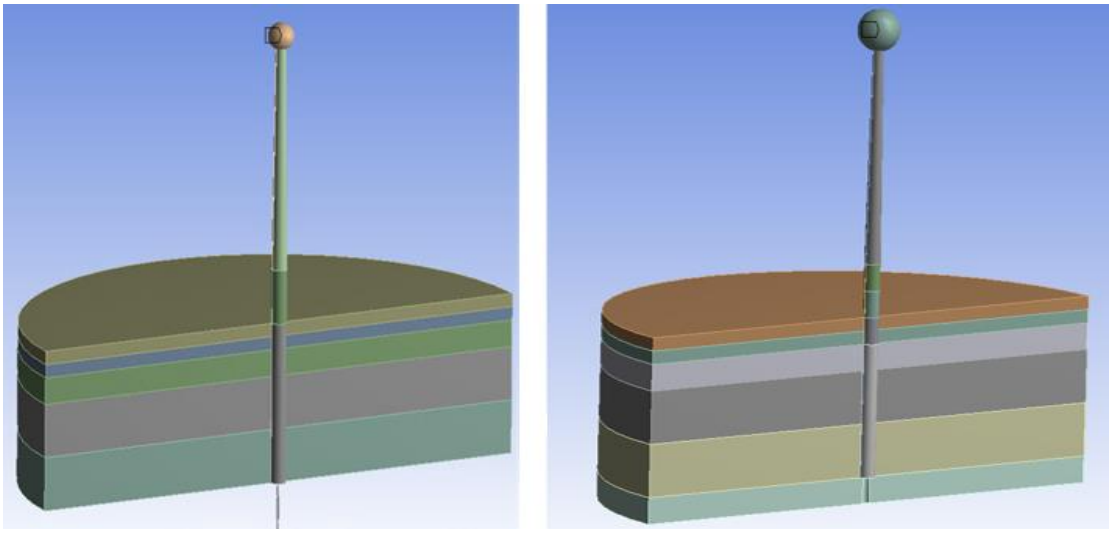

Figure 3.13 – Monopile Base Supported on Spring and Soil

3.7.2 Influence of Springs-Supported Modelling Techniques

Three springs-supported modelling techniques are conducted, and the results are compared and benched marked against the 3D soil mass model. Typically, and for a 1D/2D model, a single column of soil springs is applied along the length of the monopile foundation. However, the soil springs are applied and tested for more than one cardinal point along the monopile circumference considering the large diameter pile. The springs at each elevation along the monopile and at any point around the circumference are generated using similar properties and methodology, with zero tensile capacity. The models and findings are presented and described below:

- Base case near-face longitudinal primary springs(+x): the primary near-face springs are responsible for providing the main structural foundation support against the machine loads and environmental loads. The primary near-face springs are located opposite to the loading direction, providing support to the monopile generated through compressive soil strength as shown in Figure 3.14. The monopile deflection at mudline for the API-RP and JeanJean models are 0.76m (0.73°) and 0.71m (0.68°), respectively. Comparing the spring models against the 3D mass soil model, with a maximum deflection of 0.46m (0.44°), leads to an increase of 64% and 52% in deflection in the API-RP and JeanJean models, respectively.
- Far-face longitudinal springs in additional near-face primary springs (-x): far-face springs acts by generating additional resistance as the monopile tends to overturn or bend about the mudline. The far-face springs is illustrated in Figure 3.14. Introducing the far-face springs leads to an improvement of up to 2% on the base-case near-face, for the API-RP springs. However, the JeanJean springs showed an insignificant improvement on the base-case model.
- Side-face springs (skin friction resistance) in addition to both near- and far-face springs (±z): the side-face springs are introduced to generate skin friction resistance from the large monopile side-face contact interaction with the soil as the monopile responds to the imposed operational and environmental loads. The skin friction generated from the monopile side face contact and interaction with the soil leads to an improvement of 21% and 27% in deflection on the base-case considering the API-RP and JeanJean models, respectively. The side-face springs are often ignored for smaller monopile applications, for example, in the oil and gas sector. However, this is shown to be important as it leads to a significant improvement in the monopile structural response for springs-supported structure-foundation models.

Comparison of the 3D mass soil and API-RP springs-supported models performed as part of the PISA project supports the findings of this study. The ratio of horizontal load at the top of the OWT structure to the pile head displacement (force/displacement) was reported to be 19.38 for the 3D mass soil model and 8.75 for the API-RP model [8-10] [156]. This represents a 121% increase in 3D mass soil model stiffness on the API-RP spring-supported model stiffness.

A summary of the deflection and stress utilisation results considering the influence of spring-supported modelling techniques and 3D mass soil is presented Table 3.5. Stress utilisation is calculated based on the selected streel grade of 345 MPa. The stress infograph at the mudline for the 3D mass soil model and spring-supported models is presented in Figure 3.15.

Description	3D Mass Soil	API-RP Springs			JeanJean Springs		
		BC	FF	SF	BC	FF	SF
Deflection at ML (m)	0.46	0.76	0.75	0.59	0.71	0.71	0.52
Total Rotation ML (°)	0.44	0.73	0.71	0.56	0.68	0.67	0.49
von Mises Stress (MPa)	269	670	662	417	779	778	460
Stress Utilisation (%)	78	194	192	121	226	225	133

Notes: BC is Base-case near-face, FF is Far-face, SF is Side-face, ML is Mudline

Table 3.5 – Summary of Springs-Supported Modelling Techniques

The corresponding OWT monopile shear and bending moment reaction loads at the mudline elevation are 6.38 MN and 250 MN-m, respectively. These reactions loads are the same for the rest of the 5-MW OWT monopile findings presented throughout Section 3 of this thesis.

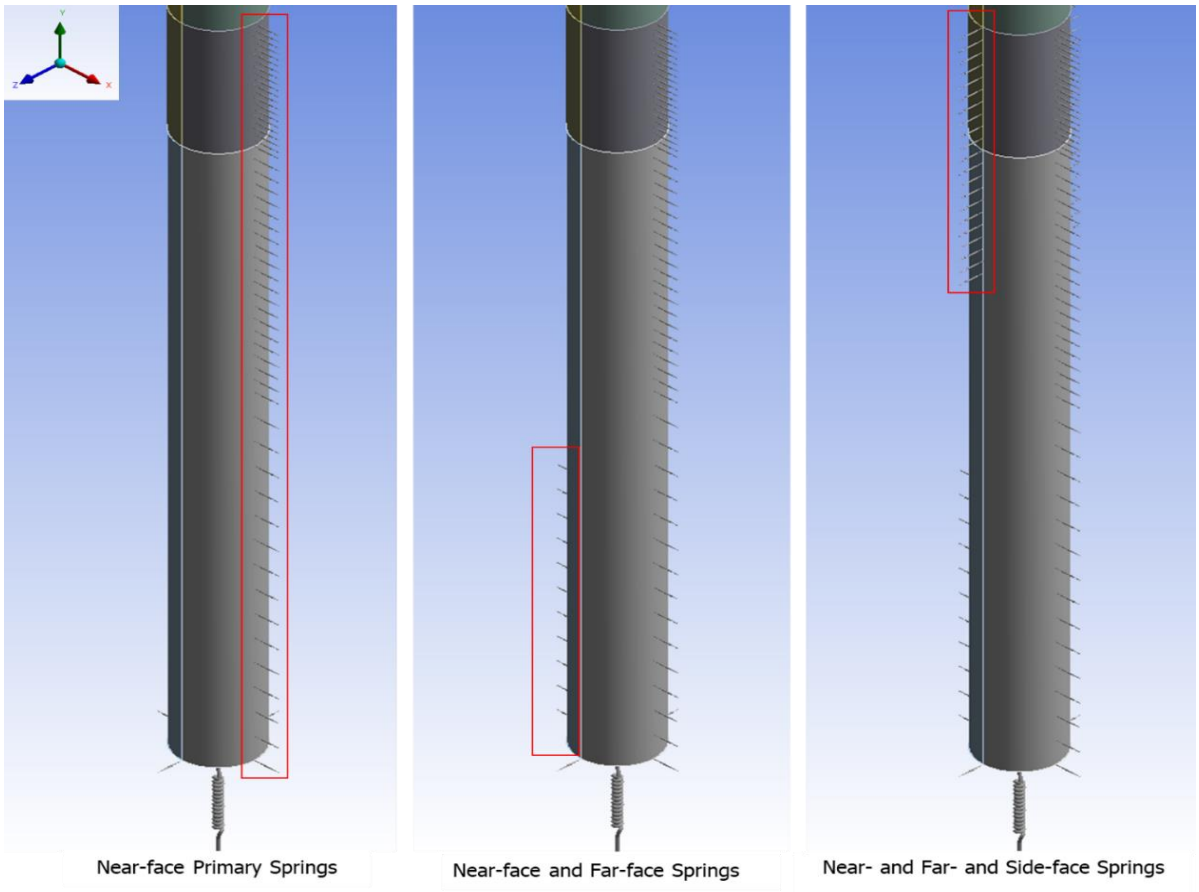

Figure 3.14 – Foundation Springs Supported Modelling Techniques

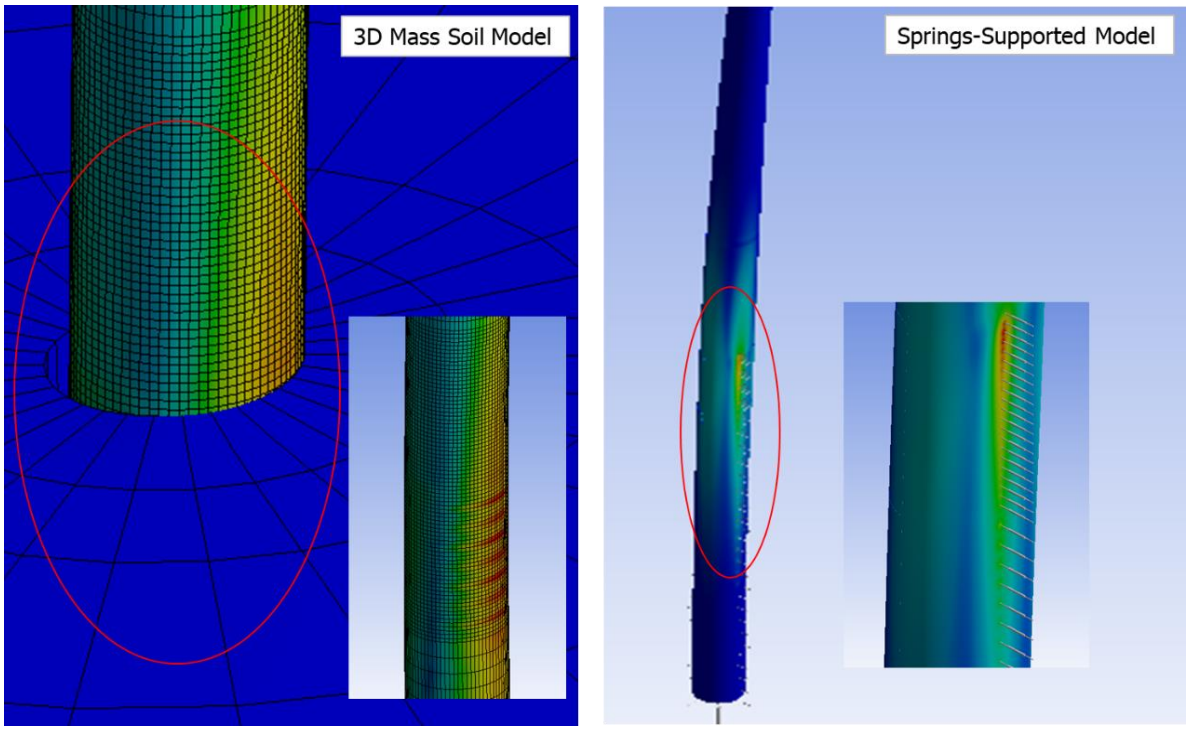

Figure 3.15 – 3D Mass Soil and Springs-Supported Models Stresses

3.7.3 Buckling of 3D Mass Soil and Springs-Supported Models

The first buckling mode is investigated in this study by considering the 3D mass soil model supporting the monopile, the API-RP and JeanJean springs-supported monopile models. The buckling is initiated by the compressive axial loads from the RNA, the monopile self-weight, and the bending loads. The bending loads are from the horizontal thrust force at the RNA, wind action on the tower above water level, and wave loads on the tower.

The monopile utilisation ratio due to buckling loads is 74% for the mass soil supported model. For the same loading conditions, the API-RP model buckling utilisation is 148% for the base-case near-face springs supported model described in 3.7.2. The JeanJean springs supported model buckling utilisation is 140%.

Summary of the buckling utilisation ratio for the different models is presented in Table 3.6.

Description	3D Mass Soil	API-RP Springs			JeanJean Springs		
		BC	FF	SF	BC	FF	SF
Buckling Utilisation (%)	74	148	146	176	140	140	178

Notes: BC is Base-case near-face, FF is Far-face, SF is Side-face

Table 3.6 – Summary of Spring-Supported Modelling Techniques

The buckling response of the springs supported models is two or more times poorer when compared with the mass soil model. The poor buckling performance of the springs supported model is primarily due to the local punching of the springs

on the monopile shell. The reduced buckling capacity is exacerbated when side-face springs are introduced to the model, aimed at generating additional resistance and stiffness from monopile-soil contact, but instead this leads to a reduced average buckling capacity of 23% on the base-case springs supported models. Study on wind turbine tower buckling behaviour based on energy method supports the findings on how bending moments affect the buckling evolution paths, leading to section distortions (oval-shaped) and curvature, resulting in change in the strain energy dissipation. The shell geometry along with local imperfections show a strong influence on the buckling and noticeable reduction in the monopile capacity during combined loading scenarios [157].

An infograph of the 3D mass soil model and the springs supported models buckling response is presented in Figure 3.16.

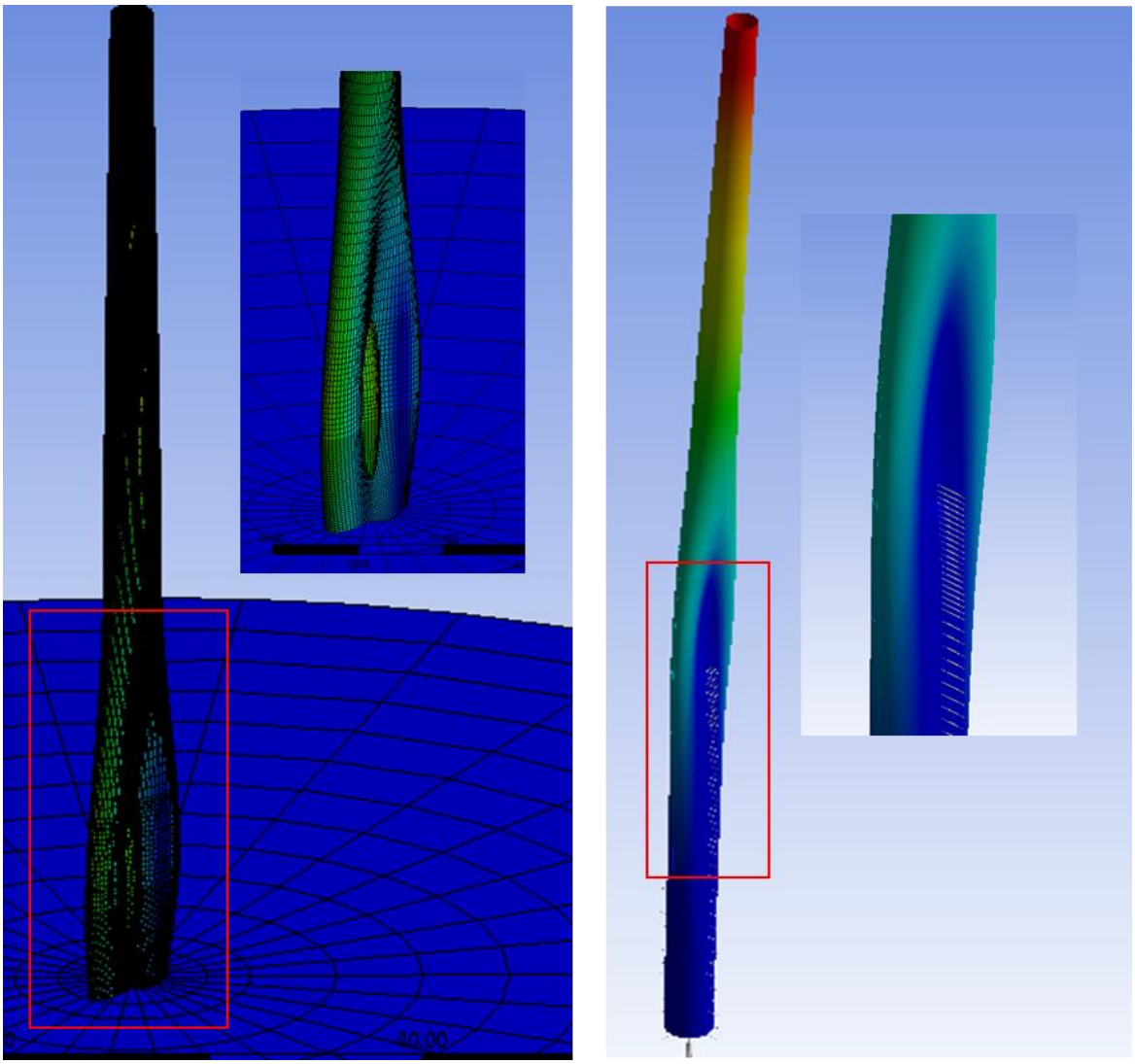

Figure 3.16 – 3D Mass Soil and Springs-Supported Models Buckling

3.7.4 Harmonic Response

The monopile structure is assessed for different modelling techniques in the frequency domain through the application of a forced frequency response, also known as the harmonic response analysis (a branch of linear dynamic analysis), to establish the structure excitation's natural frequency. As discussed in Section 3.4, this is fundamental for the design of the OWT monopile and avoidance of resonance which can lead to rapid damage and reduced operational life when the natural frequency or first bending mode shape of the structure is excited by external loads. The harmonic response analysis provides insight into the significance of the different modelling techniques and their responses to the external environmental and machine loads.

The first natural frequency mode for the mass soil model is 0.2460 Hz, located in the soft-stiff zone and away from the external loads, including the 1P and 3P loads. The API-RP and JeanJean springs supported models' first natural frequencies are 0.2021 Hz and 0.2132 Hz, respectively. They were found to be within the excitation region of the rotor rotational frequency (1P). The results from the harmonic response analyses showing the models first natural frequency and their interaction with external loads in frequency domain is presented in Figure 3.17.

The presentation in Figure 3.17 highlights the significance of the modelling techniques for the design of OWT monopile structure. For the same loading conditions, the mass soil model, although computationally expensive, indicates an improved model response and design in comparison with the springs supported models. Even after incorporating the three improvements outlined in Section 3.7.2 for the springs supported models, the API-RP and JeanJean models were still not sufficient to clear the "1P + Safety Margin" frequency excitation region, which will ultimately lead to reduced useful operational life of the monopile structure.

The springs supported models can still be applied in the design of OWT monopiles, but this would require significant deviation from current springs force-stiffness calculation and instead rely heavily on calibration using both the mass soil model and measured monitoring data to verify, investigate, and correct uncertainties in the design [133]. Engineering justification and benefit for undertaking the design and analysis using this method can be made on the grounds of reducing computational costs and improving efficiency considering the sheer number of modelling iterations, improvements, loading conditions, and combinations required for the complete structural design of OWT monopiles [156].

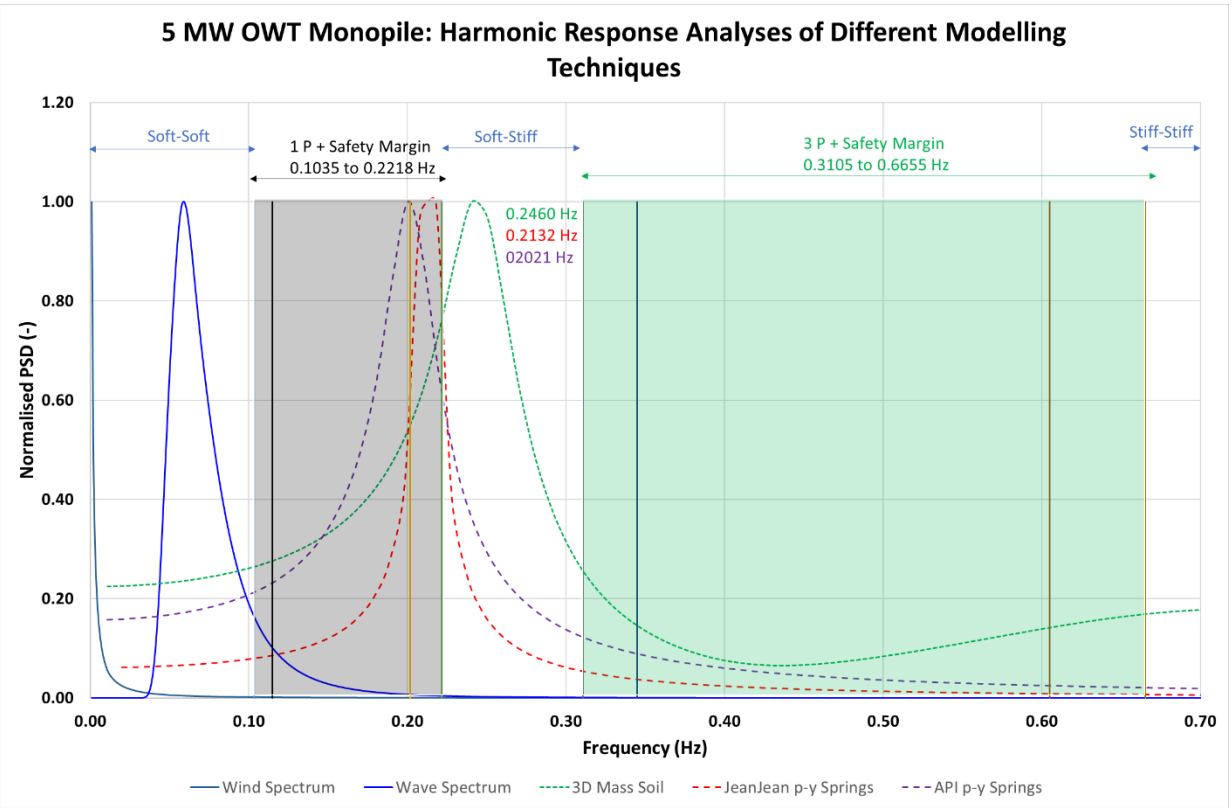

Figure 3.17 – Harmonic Response Analyses

3.8 Conclusions and Research Contribution

This research investigates the relationship between offshore wind turbine monopiles and the influence on the structural response considering external environmental loads and the turbine machine loads. The modelling approaches investigated in this study, include: the 3D mass soil supported monopile model, API-RP springs supported model, and JeanJean springs supported monopile model. The models are all 5 MW OWT monopiles, subjected to the same external environmental and machine loading conditions (maximum thrust force, wave force, wind pressure on tower, and hydrostatic pressure).

The following conclusions can be drawn from the investigation:

A. Three modelling improvements on the API-RP and JeanJean springs-supported monopile models were investigated. The study shows that the modelling refinements resulted in a corresponding average improvement of 24% on the base-case springs-supported models. Despite these improvements, the total deflections for the refined API-RP and JeanJean springs-supported models were observed to be 27% and 12% more than the 3D mass soil model, respectively.

B. The investigation further reveals the influence and significance of modelling techniques on the buckling capacity and the response of the monopile structure when subjected to external loads. The 3D mass soil model

monopile structure utilisation due to buckling is 74%. This compares with 148% and 140% for the API-RP and JeanJean springs-supported models, respectively, for the same design and loading conditions. The poor buckling capacity and response of the springs-supported models are exacerbated by the local punching of the springs on the monopile shell.

C. Harmonic response analysis is conducted with the aim of providing insights into the influence and significance of the modelling techniques on the monopile structural response when in frequency domain, factoring in the applied loads and operational conditions. The determination of the structural frequency response with respect to external loads is crucial in the design of the offshore wind turbine monopile, including the avoidance of resonance excitations that can rapidly reduce the design operational life. From the investigation, the following findings were made:
   i. The 3D mass soil supported model's first natural frequency mode is 0.2460 Hz, located in the soft-stiff zone and away from the external loads capable of causing resonance excitation, including the 1P (0.1035 Hz to 0.2218 Hz) and 3P (0.3105 Hz to 0.6655 Hz) loads for the 5 MW OWT.

   ii. The API-RP springs-supported model's first natural frequency mode is 0.2021 Hz which falls comfortably within the "1P + safety margin" excitation frequency zone.

   iii. Similarly, the JeanJean springs-supported model resulted in a natural frequency of 0.2132 Hz which is within the "1P + safety margin" excitation frequency zone.

D. Although, the springs-supported models may currently be suitable in other industries and applications, such as for the smaller pipes used in the Oil and Gas sector, this investigative study on the influence of modelling techniques shows that the springs-supported models would benefit from extensive refinement and calibration for offshore wind turbine monopile applications with larger and heavier structure sections. The PISA project for soil-structure modelling and interaction is an example of research progress aimed at addressing some of the modelling issues in the offshore wind turbine industry, including the influence on the structure fatigue life which is outside the scope of this study [8-10] [156].

E. Understanding the upper bound capacity limits of OWT monopile is an important and interesting question presently facing the industry. Although this is outside the scope of this study, extensive research and industry studies are required on the low technology readiness of future larger and heavier OWT monopile structure concepts. Some areas of interests include but are not limited to [12]:

i. Understanding the influence of modelling techniques and refinements on future monopile concepts.

ii. Applying the appropriate modelling techniques in defining the design envelope and limits of future concepts up to and including 20 MW OWT monopiles, and maybe higher.

iii. Understanding and outlining the limiting structural criteria, installation depth, and installation considerations such as acceptable and excessive pile inclination that may arise from driving larger diameter piles.

The unique knowledge contribution of this phase of the research are presented in Table 3.7.

Section	Unique Contribution	Contribution to Knowledge
Influence of soil-structure modelling techniques on offshore wind monopile structural response.	Modelled and compared three notable industry structural design and analytical approaches using 5-MW offshore wind monopile as case study: API p-y springs, JeanJean springs supported monopile, and 3D mass soil-monopile model.	Provides understanding and quantitative information on the modelling approaches and recommendations for offshore wind monopile application. Improvement techniques for springs supported monopiles such as the effective positioning of the springs around the circumference of the monopile foundation that would lead to a relatively improved structural response and result.
	Offshore wind monopile structural response comparison, focused on fundamental natural frequencies and the definition of safe zones from the expected external loads, using the three notable modelling methods.	The importance of the influence of modelling technique in the design of offshore wind monopiles. Provides quantitative information on how modelling techniques can lead to incorrect and expensive structural design of offshore wind monopiles. Provides direction on correct modelling approaches and design applications.
	Identified and categorised the primary and secondary governing design criteria and the influence of the different modelling methods on these criteria.	Provides focus and design priority for the governing criteria, including serviceability limit state and ultimate limit state.
	Established that the springs supported models in their current form are unsuitable for heavier and larger offshore wind turbine monopile structures, demonstrated using stress, deflection, buckling, and harmonic response outputs.	Saves valuable engineering manhours in avoiding unsuitable modelling techniques. Provides recommendations on how the springs supported models may be improved, where necessary, for providing quick indicative feasibility checks.

Table 3.7 – Unique Knowledge Contribution

4 OFFSHORE WIND MONOPILE STRUCTURAL RESPONSE UNDER 50-YEAR RETURN CONDITION

The submitted peer review journal article: Sunday K, Brennan F. OWT monopile structural response under 50-year return condition. Renewable and Sustainable Energy Reviews, 2022, was authored by myself as part of my research completed under the direction and consultation of my supervisor, Professor Feargal Brennan. The submitted article is incorporated and forms a significant part of the research on the response of offshore wind monopiles subjected to a 50-year return loading conditions as presented in this section.

4.1 Introduction

Previous study and design codes consider serviceability limit state design as the limiting structural design criterion for offshore wind monopiles. The structure response and limiting criteria has now become more complex in the new generation of larger and heavier offshore wind turbines such as ≥10 MW, required to deliver increasing capacity demand [11]. The monopile structure must be designed to resist the combined machine and environmental loads, including waves, wind, and a range of frequencies [14].

Modal analysis and harmonic response analyses are completed to establish the structure natural frequency and to define and avoid external frequency loads that can lead to resonance excitation. The process depends on the adopted soil-structure modelling technique, model verification benched marked against validated models, and validation by calibrating the analytical model to measured data.

Previous studies conclude that the accurate calculation of the natural frequency through modal analysis is important to avoid the external frequency loads that may lead to accumulated fatigue damage [58]. In addition, the structural response to external frequency loads is investigated through harmonic response analysis. Full-scale research conducted by Kuhn et al. (1997, [158]) and laboratory tests conducted by Bhattacharya et al. (2015) observed and concluded that the monopile structure's natural frequency can shift over time through soil softening or stiffening due to cyclic dynamic loading during the operational lifetime of the structure [11, 107].

The foundation models traditionally used in integrated analyses of OWT monopile foundations are simplistic and based on several assumptions, where the model and responses are commonly represented by the renowned non-linear p-y springs distributed along the length of the pile [13]. The p-y curves are generated in accordance with API-RP 2014 and as described in DNV-ST-0126. The p-y springs are limited to smaller pipe diameters, requiring rigorous validation for application on monopiles with greater than 1.0m diameters by way of testing, real-time structural monitoring, or the use of finite element analysis or other suitable means [39]. While the conventional p-y curve methodology has been successfully applied

for decades in capturing the soil-structural modelling and interaction for pile design in the oil and gas industry, the fundamental assumptions are less appropriate and unsuitable in their raw theory for OWT monopile foundation applications, and even more unsuitable for the new generation larger OWT structures [2, 151]. The application of the p-y method for offshore wind foundations requires improvement of the lateral soil reaction as well as three additional relevant soil reaction components, including a distributed moment, a base horizontal force, and a base moment.

The PISA research project has shown some notable progress in the modelling of soil-structure interaction toward design improvements for larger diameters offshore wind turbine monopiles. The PISA project introduces new methodology for calibrating one-dimensional Winkler-type soil reaction curves for generating springs that represent the soil stiffness and interaction with the monopile [8-10]. Further evidence on the short-comings of the p-y springs supported modelling techniques and applications, other important OWT structural design challenges faced by the industry, including design improvements and achievements by recent studies are captured by Sunday et al. (2021 [12], 2022 [13]). The large diameter of thin-walled piles is prone to a high risk of tip buckling during installation in dense sand or weathered bedrock [11]. Research conducted by Byrne et al. (2020) on more rigid, large diameter monopiles, suggests that rather than the pile (as in the case of slender piles), the soil may fail first due to a high induced overturning bending moment [9].

This article presents the response of offshore wind monopile structures under a 50-year return operational and environmental loading conditions and a road map for achieving an efficient and cost-effective engineering design solution. In addition, this study provides design direction to present and future research for the development of heavier and larger offshore wind turbine monopile structures for delivering the increased energy capacity, required to feed the demand for clean sustainable energy. The influence of installation water depth on the response of the 10 MW OWT monopile structure is also investigated, including 20m, 50m, and 70m, as illustrated in the structure overview in Figure 4.1. This article is structured into the following sections: Section 4.2 presents the design data and methodology based on a 10 MW offshore wind turbine structure. The modelling technique for the foundation, tower, and soil-structure interaction are covered in Section 4.3. The findings from the investigation, including response of salient individual and coupled design criteria are presented in Section 4.4 and the conclusions are outlined in Section 4.5.

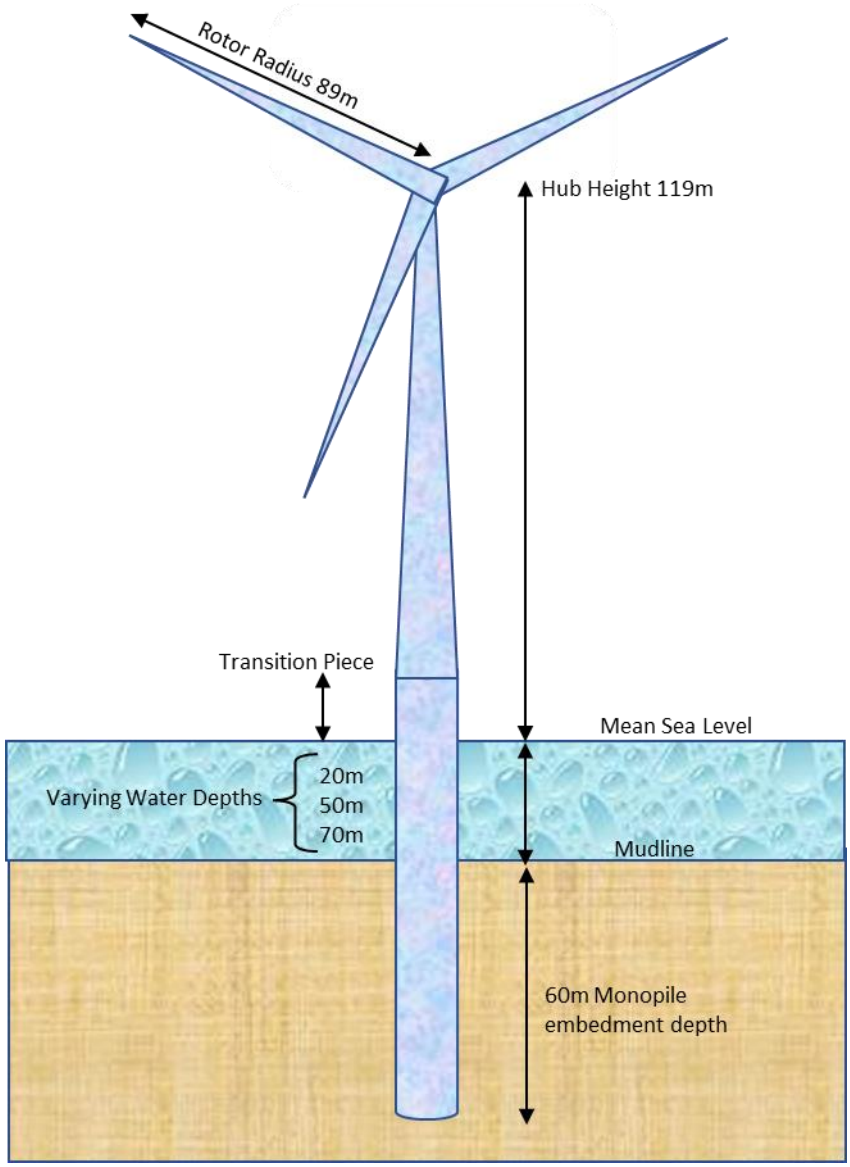

Figure 4.1 – Representative Sketch of the 10 MW OWT Monopile Structure

4.2 Design Data and Methodology

This study is based on the DTU 10-MW reference offshore wind turbine embedded 60m below ground level and at varying water depths of 20m, 50m, and 70m, respectively. The DTU 10-MW reference wind turbine is a conventional horizontal axis three-bladed and upwind type turbine on a tubular tower, supported by a large monopile embedded 60m the below seabed in this study. The pile penetration depth of 60m is selected to fix this variable, suitable for a workable design for including shallow to deeper waters. More information on the selection of embedded pile length is provided in Section 3.2. The original tower of the DTU 10-MW onshore turbine is truncated for the offshore environment with an air gap of 18m [159] [160]. The representative model is constructed in a finite element software package for the top structure, substructure, and the foundation system.

The design properties of the monopile and the soil structure are outlined in Table 4.1 and Table 4.2, respectively.

Description	Value	Units
Power Rating	10	MW
Turbine Class	IEC Class B	-
Rotor Diameter	178.3	m
Hub Height	119	m
Blade Mass	41000	kg
Rotor Nacelle Assembly Mass	674000	kg
Tower Mass	987000	kg
Cut-in, Rated Wind	4, 11.4	m/s
Cut-in, Rated Rotor Speed	6.0, 9.6	rpm
Cut-out Wind Speed	25	m/s
Shaft Tilt Angle	5	deg
Tower Top Diameter and Thickness	5.5, 0.02	m
Tower base Diameter and Thickness	8.3, 0.05	m

Table 4.1 – Properties of DTU 10-MW Offshore Wind Turbine Model [58] [159] [147] [161]

Description	Value	Units
Tower/Steel Structure Material Properties		
Density (Effective to account for paint, bolts, welds, flanges*)	7850 (8500*)	kg/m^3
Young's Modulus	210	GPa
Shear Modulus	80.8	GPa
Steel Grade	355	
Soil/Foundation Properties		
Installation Depth Below Mudline	60	m
Soil Density	1800 – 2000	kg/m^3
Undrained Young's Modulus	40 - 70	MPa
Poisson's Ratio	0.45	-
Soil Angle of Internal Friction	20	Deg
Undrained Shear Strength (S_U) (Cohesion)	150 – 250	kPa

Table 4.2 – Tower and Soil/Foundation Properties [11] [58]

The soil angle of internal friction of 20° is used to calculate the friction coefficient of 0.35 between the soil and monopile steel structure.

The DTU 10-MW wind turbine first rotor harmonics 1P range defined by the rotor cut-in and rated speeds is from 0.100 Hz to 0.160 Hz (0.090 Hz to 0.176 Hz, including 10% safety margin). The blade passing harmonics 3P range is from 0.300 Hz to 0.480 Hz (0.270 Hz to 0.528 Hz, including 10% safety margin). Damping ratio of 10% is considered in the modelling and analysis of the OWT monopile structure [12] [82]. The damping ratio used include the contribution from soil, hydrostatic, steel material, tower oscillation, and aerodynamic.

The thrust force (*Th*) is applied at the top of the wind turbine tower considering wind acting on the turbine rotor. The thrust force is estimated according to the following expression [41]:

$$\boldsymbol{Th = \frac{1}{2}\rho_a A_R C_T U^2} \quad (1)$$

Where: ρ_a is the density of air, A_R is the rotor swept area, C_T is the thrust coefficient, and U is the wind speed. The wind speed can range from cut-in to cut-out, with the appropriate thrust coefficient. The thrust coefficient can be approximated from the Thrust Coefficient Approximation Curve or by using equations. The thrust coefficient can be estimated for between cut-in and rated wind speed, and after rated wind speed when pitch control is active according to the following equations:

Between cut-in (U_{in}) and rated wind speed (U_R)

$$\boldsymbol{C_T = \frac{3.5\ [m/s]\ (2U_R + 3.5\ [m/s])}{U_R^2} \approx \frac{7\ [m/s]}{U_R}} \quad (2)$$

After rated wind speed, when pitch control is active, and power is assumed to be constant.

$$\boldsymbol{C_T = 3.5\ [m/s]\ U_R(2U_R + 3.5\ [m/s]).\frac{1}{U^3} \approx \frac{7\ [m/s]\ U_R^2}{U^3}} \quad (3)$$

Thrust coefficient for different wind scenarios and combinations, including turbulence, extreme, and gust can be estimated using the appropriate equations from literature and design codes. This is beyond the scope of this study.

The applied wave force is estimated by assuming linear wave theory such as the Morison's equation considering the sum of the drag force F_D and the inertia force F_I [61]:

$$\boldsymbol{dF_{wave}(z,t) = \frac{1}{2}\rho_w D_S C_D w(z,t)|w(z,t)| + C_m \rho_w A_S \dot{w}(z,t)} \quad (4)$$

Where: C_D is the drag coefficient, C_m is the inertia coefficient, and ρ_w is the density of seawater. The total horizontal force is then calculated by integrating over the water depth and applied at the mean water surface in in the FE model discussed in Section 4.3.

4.3 Foundation-Structure Interaction Modelling and Verification

Ansys finite element package is used for this investigation, including modelling and analysis of the offshore wind monopile. The offshore wind turbine Rotor Nacelle Assembly (RNA) is captured using lump mass supported on the tower. The modelling includes configurations submerged in 20m, 50m, and 70m water depth, for monopile foundations that are installed at 60m below the soil surface. Based on

the soil angle of internal friction of 20° outlined in Table 4.2, a friction coefficient of 0.35 is calculated and applied in the model to simulate the interaction between the soil and monopile structure. Spring elements are used to provide end bearing support to the monopile and tower structure.

The OWT global model and meshed profiles showing the lump mass (representing the RNA), the tower, and foundation are presented in Figure 4.2. Free face Quad/Tri mesh type is used to model the tower and foundation structure and model mesh sensitivity was completed for the solution. The model was verified by conducting global sensitivities as outlined in Section 3.2.3, and verified against published literature and case studies [11] [58] [12].

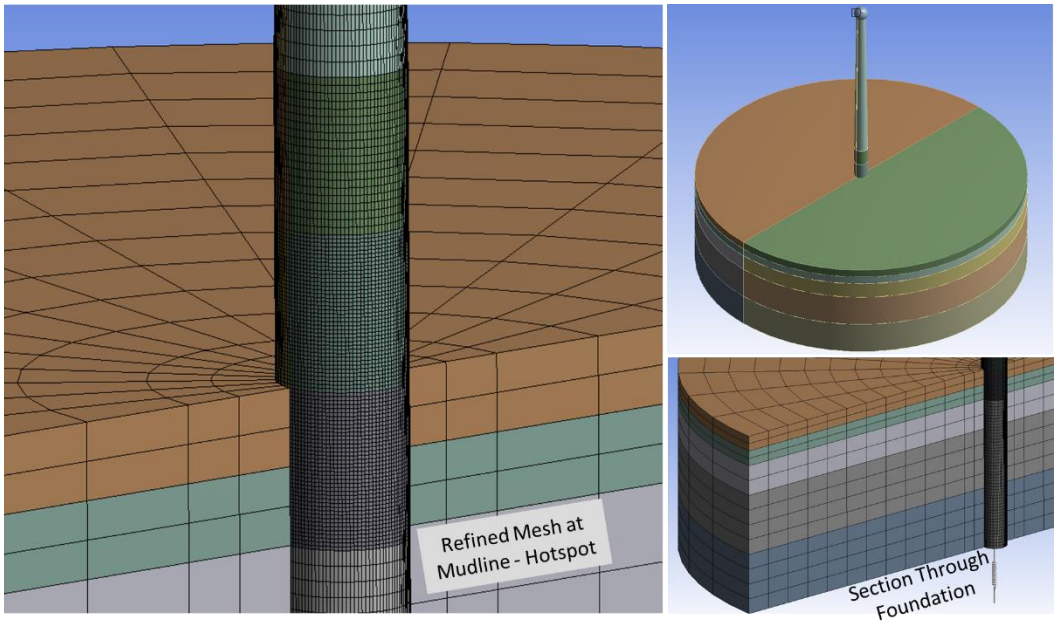

Figure 4.2 – FEA Global Model and Meshed Profiles

The analytical model verification was performed in two stages:

- Fixed base model with lump mass representing the Nacelle mass and hub mass. The first natural frequency is 0.3474 Hz compared with 0.355 Hz according to the study by Senanayake et al. (2017, [58]). This shows a 2% agreement in the analytical models' responses.
- The second stage involves improving on the modelling and analysis by including the flange connection between the tower above water and foundation, fixing the foundation base at the mudline installed in a 20m water depth. The first natural frequency is 0.288 Hz compared with 0.302 Hz according to the study by Senanayake et al. (2017, [58]). This shows a <5% agreement in the analytical models' responses.

The effects of waves and currents are neglected at this stage for simplicity and to determine the natural frequencies. The mode shapes and natural frequency are shown in Figure 4.3 and presented in Table 4.3.

Figure 4.3 – Mode 1, 2, and 3 Infograph - NREL 5 MW OWT

Mode Number	Fixed Base			Fixed Base at 20m Water Depth		
	Frequency		Period	Frequency		Period
	(Hz)	(rad/sec)	(s)	(Hz)	(rad/sec)	(s)
1	0.3474	2.1828	2.8785	0.2883	1.8114	3.4686
2	3.0310	19.0443	0.3299	2.2165	13.9261	0.4512
3	8.6498	54.3483	0.1156	6.1501	38.6422	0.1626

Table 4.3 – NREL 5 MW OWT Monopile Model Verification

4.4 Findings and Discussions

Results from the study are presented and discussed in this section. The environmental and external loads applied to the structure include the thrust force at the hub centre and the self-weight of the rotor-nacelle-assembly. In addition, the wind force on the structure is applied as pressure on the super-structure above the mean sea level, wave action at the mean sea level, and hydrostatic loads based on the water depth [32].

The shear and bending moment reaction loads at the mudline elevation for the 10-MW OWT monopile findings presented in this section are given in Table 4.4.

10-MW OWT Monopile Reaction Loads	Water Depth		
	20 m	50 m	70 m
Shear (MN)	9.23	9.23	9.23
Bending Moment (MN-m)	430.40	707.32	891.94

Table 4.4 – 10-MW OWT Monopile Reaction Loads at Mudline

4.4.1 Harmonic Response and Natural Frequency

Harmonic response analysis is performed to understand the structure's natural frequency and to define the range of the external frequency loads that can lead to resonance excitation and ultimately fatigue damage on the OWT monopile. Findings from the harmonic response assessment showing the natural frequency and external frequencies are presented in Figure 4.4. The tower and foundation structure are soft when the natural frequency response is below the 1P rotor passing frequency, and stiff when above the 3P blade passing frequency. Although both options are a workable design solution, they each have economic and engineering implications, hence, a suitable solution is a structure configuration where the natural frequency is between the 1P and 3P loads.

Harmonic response of the 10-MW OWT presented in Figure 4.4 shows that the external loads and resonance initiation regions are avoided for the 20m and 50m water depths, for the same monopile diameter of 8.3m and respective thicknesses of 60mm and 90mm. However, for 70m with the same pile diameter, it is within the 1P external loading region with a high likelihood of resonance occurrence, even for thicknesses of up to 110mm. This result demonstrates the impact of water depths on the OWT, even with increasing pile thickness. The structural design of the OWT can be improved regarding the natural frequency response by increasing the thickness; however, this study has shown that this specific design change has a reduced effect and in fact can be limited with respect to water depth, as the turbine structure is installed in deeper waters as elaborated in Figure 4.5. To achieve a workable design solution at deeper water depths, both the turbine monopile thickness and the diameter must be increased as shown in Figure 4.6, for all water depths considered in this study. This structural design response improvement technique leads to higher fabrication costs and installation challenges. Furthermore, this can lead to a deterioration in the buckling response for increased monopile diameter as demonstrated and explained in Section 4.4.2.

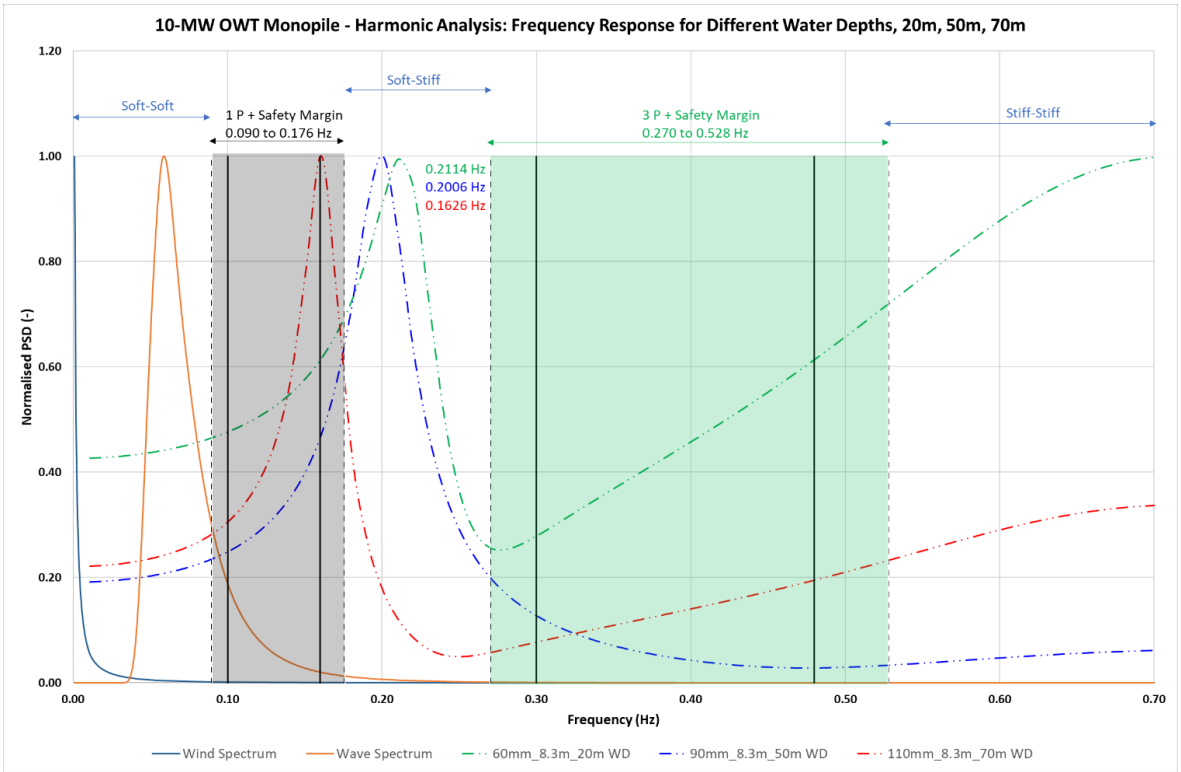

Figure 4.4 – Harmonic Response at Different Water Depths

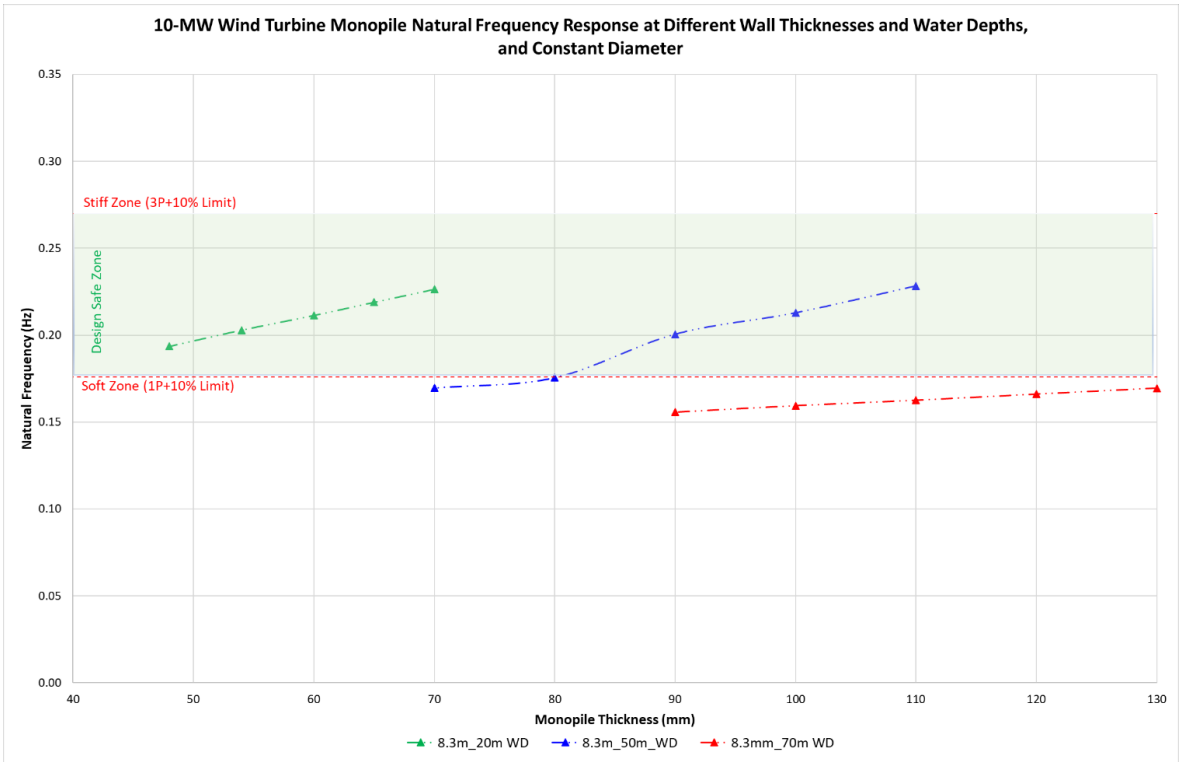

Figure 4.5 – Natural Frequency Response at Different Wall Thicknesses and Constant Diameter at Water Depths

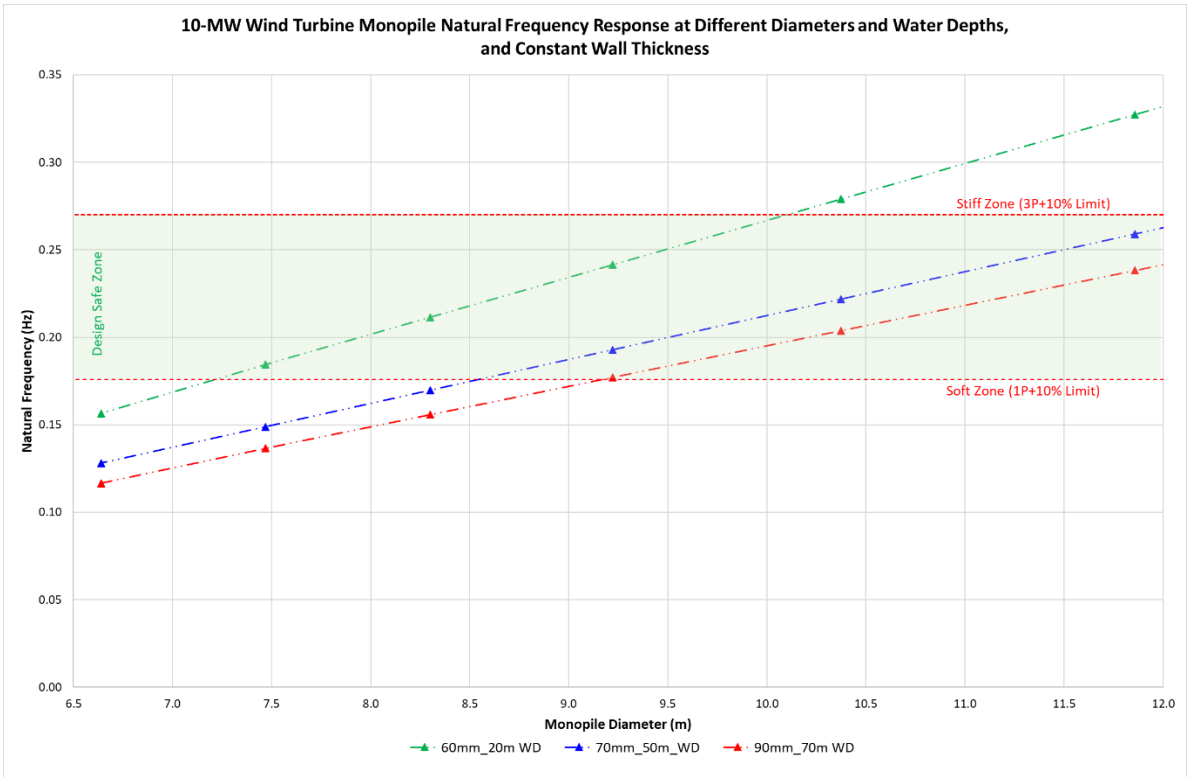

Figure 4.6 – Natural Frequency Response at Different Diameters and Constant Thickness at Water Depths

4.4.2 Buckling Behaviour

Findings from the buckling investigation, including the first and subsequent buckling modes are considered; the onerous and representative results are presented and discussed in this section. Although this study does not account for geometric imperfection due to manufacturing or transportation/installation [157], the bending loads due to thrust force at the hub height introduces eccentricity and affects the buckling evolution paths. This exacerbates the compressive buckling loads from the weights of the tower and monopile and the machine loads at the top of the tower.

The base-case model diameter is 8.3m, according to the DTU 10-MW offshore wind turbine model, outlined in Table 4.1. This diameter is factored by 0.9 and a 0.8 to build two representative model configurations of 7.47m and 6.64m with varying thicknesses, respectively. The buckling utilisation for base-case scenario, calculated as the inverse of the buckling safety factor is 76%, 28%, and 17% for 20m, 50m, and 70m water depths, respectively. The base-case monopile configuration consists of an 8.3m shell diameter for all water depths but with varying wall thicknesses which are 60mm, 90mm, and 110mm in order of increasing water depths. Summary of the buckling utilisation ratio for the different model configurations and water depths is presented in Table 4.5.

Description	20m Water Depth		50m Water Depth		70m Water Depth	
Monopile Diameter (m)	Wall Thickness (mm)	Utilisation (%)	Wall Thickness (mm)	Utilisation (%)	Wall Thickness (mm)	Utilisation (%)
8.30	60	76	90	28	110	17
	54	126	80	41	100	22
	48	284	70	63	90	30
7.47	60	58	90	24	110	16
	54	88	80	35	100	20
	48	167	70	53	90	26
6.64	60	49	90	21	110	17
	54	68	80	29	100	29
	48	108	70	44	90	24

Table 4.5 – Summary of Buckling Utilisation

Under a 50-year return loading, it is observed that buckling is exacerbated as the diameter of the monopile increases, for the same shell thickness. For example, considering 60mm wall thickness, the buckling utilisation is observed to increase from 49% for 6.64m diameter, 58% for 7.47m diameter, and 76% for 8.30m diameter. The structural response and trend regarding the buckling behaviour of the 10-MW OWT are predicted to be similar for the different installation water depths of 20m, 50m, and 70m. On the other hand, the buckling response is shown to improve by increasing the wall thickness, considering constant monopile diameter. The response is consistent for the different water depths considered in this study.

A plot of the buckling utilisation showing the structural response and trend for the case of different monopile diameters and constant thickness at respective water depths is presented in Figure 4.7. Similarly, the OWT monopile structural response for buckling considering different wall thicknesses and constant monopile diameters at respective water depths is presented in Figure 4.8.

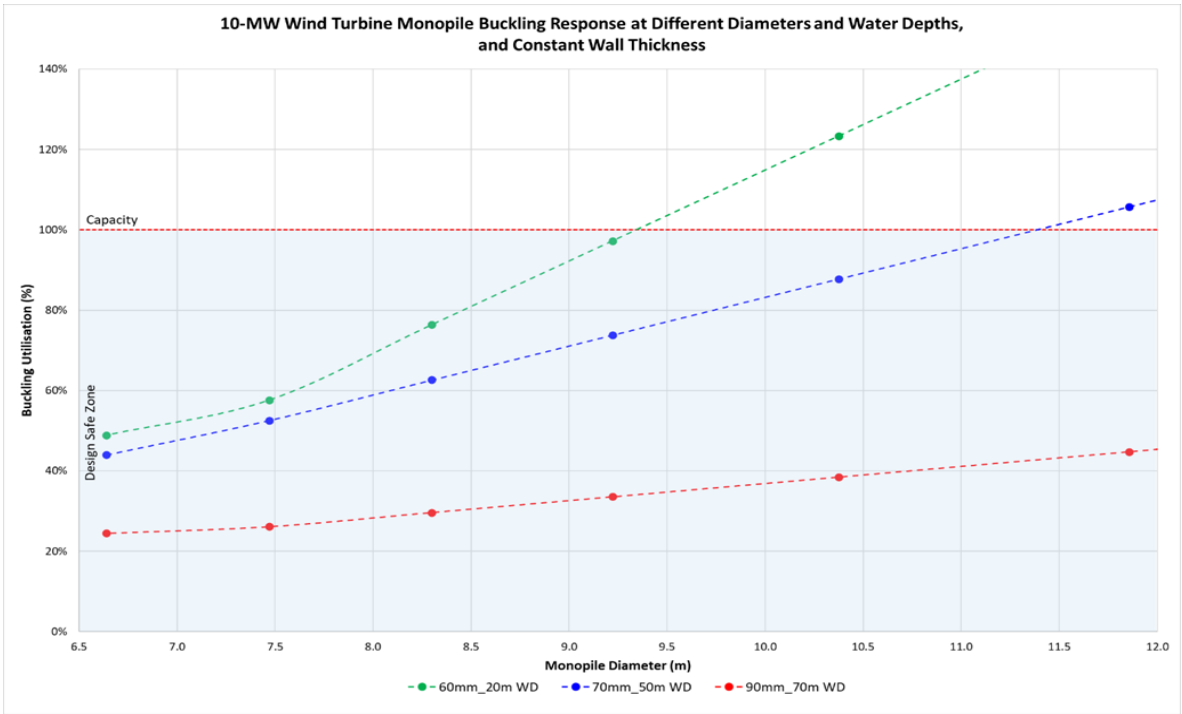

Figure 4.7 – Buckling Response at Different Diameters and Constant Thickness at Water Depths

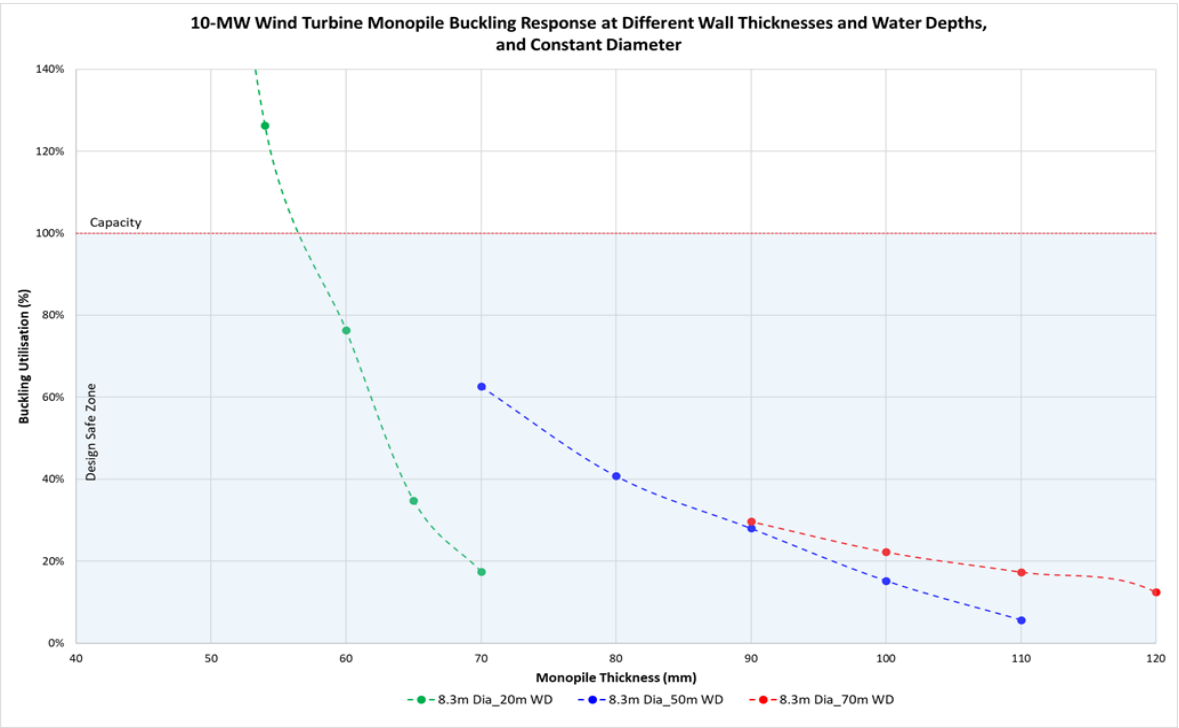

Figure 4.8 – Buckling Response at Different Wall Thicknesses and Constant Diameter at Water Depths

4.4.3 Stress and Deflection

The results of this study have shown that stresses, primarily due to bending, shear and torsion are not the governing failure mode and design criteria as explained

and presented in this section. The result and trend are consistent across the water depths investigated, monopile diameter, and thickness. In fact, stresses can be considered as less concerning in the design of the 10-MW OWT regarding strength and serviceability design; the structure is well within utilisation for the base case diameter of 8.3m and reduced diameter across water depths to at least 7.5m diameter. The structural response regarding stress improves when either or both the monopile diameter and thickness are increased. The stress utilisation for the different water depths and selected thickness, across different monopile diameters is presented in Figure 4.9. The stress utilisation for different wall thicknesses and constant monopile diameter with respect to water depths is presented in Figure 4.10. Although fatigue design is not part of this research, the presented stress output gives some indication that fatigue will not be a driving challenge provided resonance is avoided or properly designed.

The deflection follows a similar trend as the stresses which are expected for a cantilever structure supported at and below the mudline. The deflection for different diameters (and constant thickness) and for different thicknesses (and constant diameter) are presented in Figure 4.9 and Figure 4.10, for the water depths investigated in the study. The maximum deflection (or displacement) for the base case diameter of 8.3m occurs at the smallest monopile wall thickness of 48mm, 70mm, and 90mm, for water depths of 20m, 50m, 70m respectively. For these parameters, the maximum deflections at the mudline elevation are 0.32m, 0.38m, and 0.42m. These correspond to total rotation of 0.31 deg, 0.36 deg, and 0.40 deg, respectively. The deflections should be within allowable limits for most 10-MW OWT structures but must be verified on a site and manufacturer specific basis. Deflection as set out in the Section 4.1, is known to be the governing criterion for OWT in the range of 2-MW to around 5-MW and may be related to the functionality of the RNA; however, the strict limits for the complete OWT complete structure are often not met and there are no clear guidelines regarding the source and reasons for such strict limits.

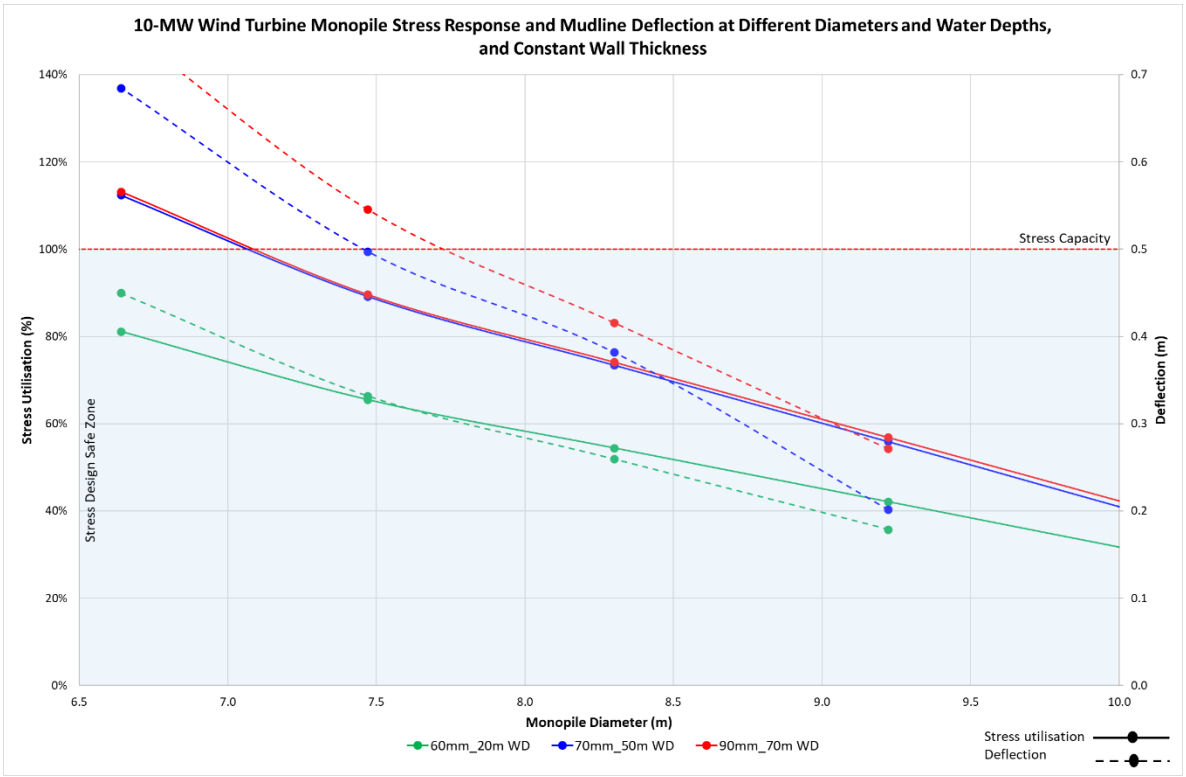

Figure 4.9 – Stress and Mudline Deflection at Different Diameters and Constant Thickness at Water Depths

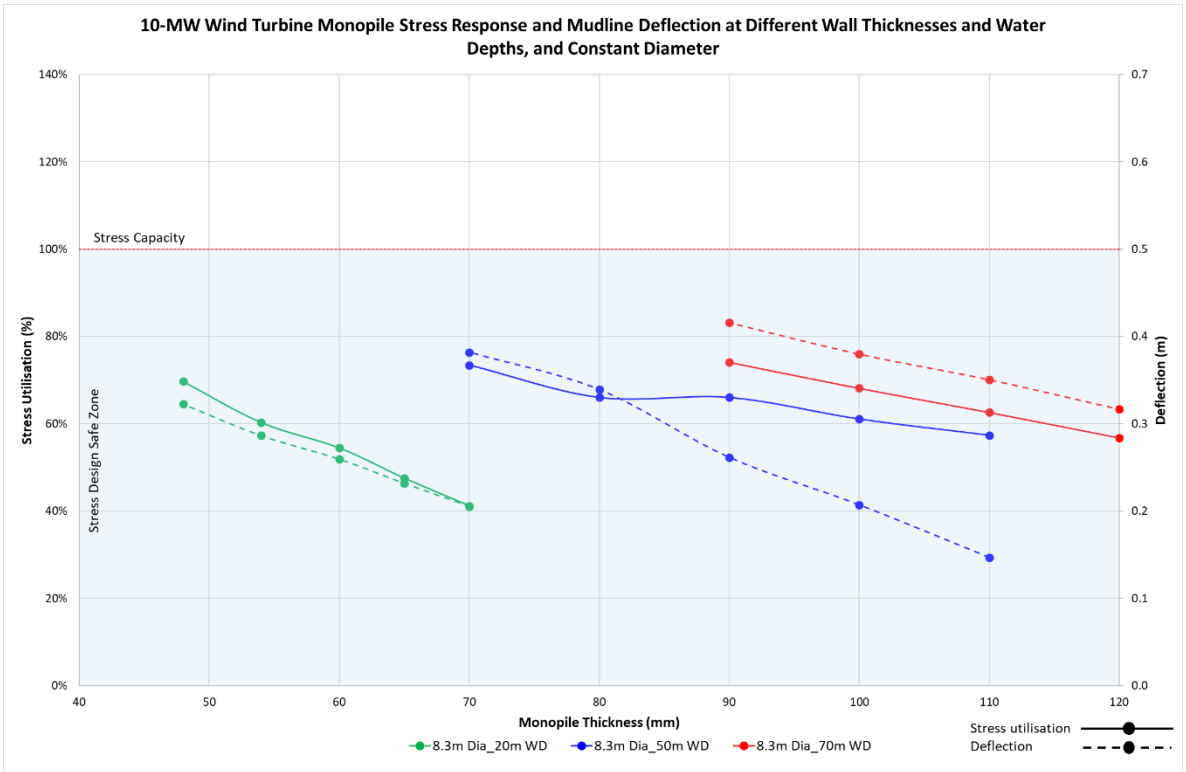

Figure 4.10 – Stress and Mudline Deflection at Different Wall Thicknesses and Constant Diameter at Water Depths

4.4.4 Coupled Response

The coupled response is aimed at presenting the combined response of the OWT considering harmonic response (natural frequency), buckling, and stress. To elaborate on the impact of thickness in the study, 60mm, 90mm, and 110mm are selected for water depths of 20m, 50m, and 70m, respectively. Considering the constant monopile thicknesses and for different diameters, the coupled response of the OWT structure is presented in Figure 4.11. The structure's natural frequency is the limiting design criterion considering the lower bound monopile diameter. The diameter is limited at approximately 7.25m, 7.75m, and 9.0m for water depths of 20m, 50m and 70m, respectively. Below these diameters, the OWT natural frequency falls within the target 1P external load, susceptible to resonance excitation. The buckling and stress are well within the allowable capacity for the selected design thickness and water depths.

Considering the OWT monopile upper bound diameter, the governing criteria are both the buckling and the natural frequency. The stress as explained in Section 4.4.3 is not a driving or governing design criterion in a coupled response scenario. The 20m water depth configuration is limited at the upper bound diameter by a buckling response, followed closely by natural frequency. At 50m water depth, the governing criterion shifts to the natural frequency alone, while the buckling and stress are well within allowable utilisation. At 70m water depth, the OWT coupled structural response is within the suitable design region for all three structural failure modes considered in this study. The primary reason for selecting 110mm thickness at 70m water depth is to achieve a workable design solution, controlled by the lower bound diameter at approximately 9.0m for natural frequency, to ensure that the structure clears the 1P external load resonance excitation frequency.

The observed trend is supported by the selected constant diameter configuration of 8.3m and at different monopile thicknesses as shown in Figure 4.12. The limiting criteria are primarily the buckling and natural frequency responses. The upper bound exceedance is shown to be at approximately 9.25m and 9.75m diameters for 20m and 50m water depths configurations, Figure 4.11.

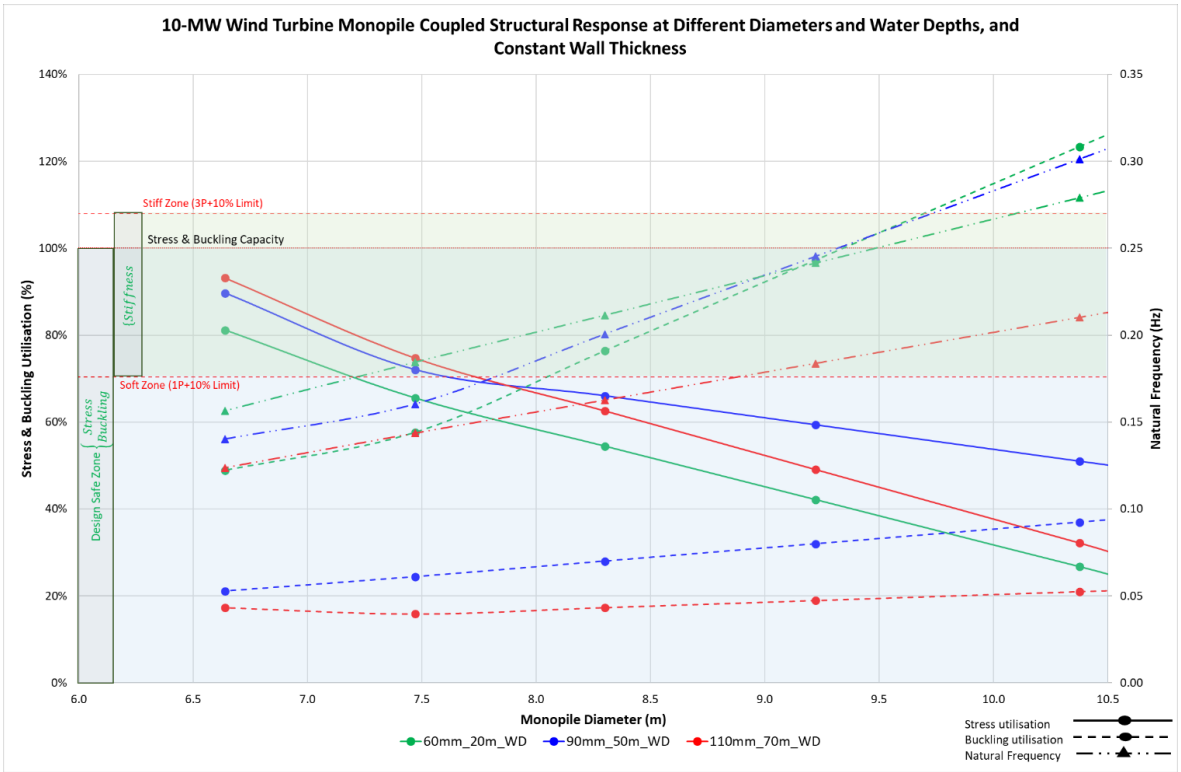

Figure 4.11 – Structural Response at Different Diameters and Constant Thickness at Water Depths

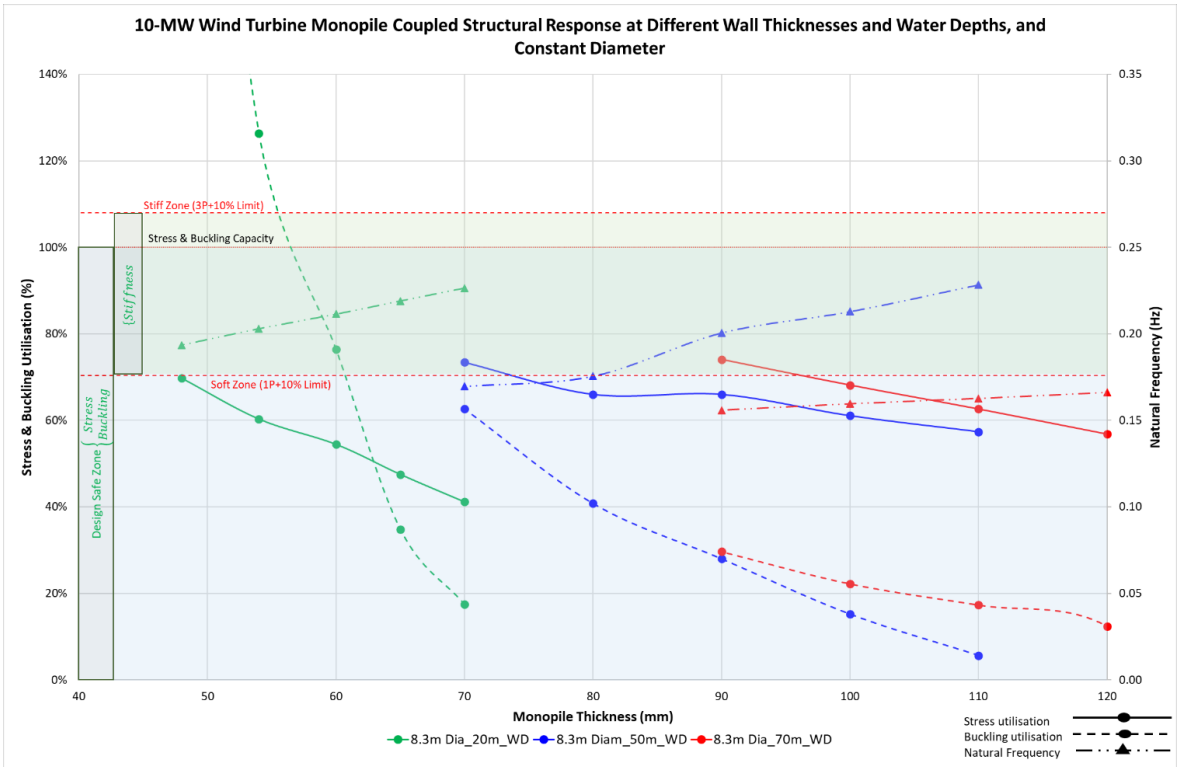

Figure 4.12 – Structural Response at Different Wall Thicknesses and Constant Diameter at Water Depths

4.5 Conclusions and Research Contribution

This research investigates the structural response of a 10-MW OWT monopile configuration under 50-year return environmental and turbine machine loading conditions. The structural response is focused on the primary design criteria, including the outcome of the harmonic analysis, natural frequency of the structure, buckling behaviour, stress utilisation and deflection. A coupled response of the design criteria is also investigated to give a global understanding of the design of the 10-MW OWT structure, which may also be applied to other OWT monopile configurations. The study is performed for 20m, 50m, and 70m water depth configurations, considering different monopile thicknesses and diameters. The conclusions from this study are presented as follows:

A. The harmonic response analysis and natural frequency shows that the external loads and resonance initiation regions are avoided for 20m and 50m water depths, considering 8.3m monopile diameter, and thicknesses of 60mm and 90mm, respectively. However, the harmonic response for the 70m water depth configuration falls within the 1P external loading region, which is likely to initiate resonance excitation, even for monopile thicknesses of up to 110mm. The study demonstrates that to achieve a suitable design solution at deeper water depths, both the monopile thickness and diameter must be increased, leading to higher costs and installation challenges such as fabrication, transportation, and installation.
   A.1. In addition to the OWT structural response improvement techniques as discussed above, active/passive structural damping design solutions can be considered and implemented to improve and control dynamic responses.
   A.2. It is worth noting that the OWT structural response and results presented in this study are sensitive and subject to site-specific soil structure properties, soil-structure interaction modelling approaches and interpretation. It is recommended to use the information presented in this study as a useful indicative guide and a road map for feasibility design underpinned by site-specific assessment.
   A.3. The turbine pile drivability and susceptibility to buckling due to pile hammer and associated installation challenges are not investigated within this study.
   A.4. Therefore, it is recommended that these design challenges be considered in future research projects to provide enhanced understanding and leading to design improvements.
B. The buckling behaviour is demonstrated to be less important to the design of OWT monopiles when compared with natural frequency response design criterion. The monopile utilisation due to buckling is satisfied at all water depths considered, up to and including 70m and for the base case monopile diameter of 8.3m. The buckling response is improved by increasing the monopile wall thickness and using a constant diameter. But the response is affected by increasing the monopile diameter.
   B.1. The OWT buckling response and interpretation presented in this study assume that the OWT structure is designed to resist pile driving and installation related buckling.

C. The stress utilisation and deflection are not the governing or driving structural design criteria in the 10-MW OWT structure. The structure is within capacity regarding induced stresses for the base case scenario and all water depths considered in the study.
D. Considering the coupled structural response, the structure's natural frequency is the governing design criterion for lower bound monopile diameter at all water depths investigated within the study. The upper bound monopile diameter is defined based on the natural frequency and buckling as the limiting or governing design criteria.
E. Definition of the offshore wind turbine monopile capacity envelope, how large and how heavy, and how deep we can install the larger and heavier future concepts are important future research questions, including installation related challenges.
F. The presented stresses give an indication that fatigue design will not be a challenging design criterion provided resonance due to external loads is avoided or properly designed.
    F.1. This study and the interpretation of the results assume that the OWT structure is defect-free; hence, defects that may exacerbate and accelerate fatigue damage such as manufacturing flaws, installation flaws, flaws initiated and progressed during operations, and corrosion must be assessed on a site-basis.
    F.2. The coupled structural response due to fatigue design is not part of this investigation; however, it is recommended to be considered in future research for clarity and detailed design assurance.

The unique knowledge contribution of this research is presented in Table 4.6.

Section	Unique Contribution	Contribution to Understanding
Offshore wind monopile structural response under 50-year return condition	Identified the benefits of using refined 3D modelling approach in achieving a more accurate and representative structural assessment of offshore wind monopile.	Highlights the importance of appropriate modelling approaches in structural assessment of offshore wind turbines which would result in cost-effective engineering design solutions.
	Knowledge on offshore wind monopile structural response using 10-MW turbine as a case study.	The knowledge and understanding will improve the engineering of offshore wind monopiles by highlighting the critical and driving parameters.
	Outlined the importance of structure's natural frequency and the buckling behaviour in the global response of offshore wind monopiles under a 50-year return loading condition.	Provides clear direction and focus on the main structural design issues under 50-year return conditions.
	Demonstrates the use and importance of harmonic response analytical tools in understanding the structural dynamic behaviour.	Highlights the importance of frequency domain analysis and application to offshore wind monopile global design.
	Demonstrates that in an idealised defect-free condition, stresses and fatigue damage is likely to be of design concern.	Useful knowledge and information for the feasibility design, including tower and monopile sizing.
	Provides knowledge and understanding of the dynamic response direction with respect to changes in the section diameter and thickness, separately and together.	Useful information for initial design and sizing of offshore wind monopiles and how to make effective design changes and reduce costly design iterations.

Table 4.6 – Unique Knowledge Contribution

5 THE OFFSHORE WIND MONOPILE STRUCTURAL DESIGN ENVELOPE

The submitted peer review journal article: Sunday K, Brennan F. Offshore wind monopile structural design envelope. Royal Society Publishing, 2022, was authored by myself as part of my research completed under the direction and consultation of my supervisor, Professor Feargal Brennan. The submitted article is incorporated and forms a significant part of the research on the offshore wind monopile structural design envelope as presented in this section.

5.1 Introduction

This research study was driven by the growing interest in new offshore wind turbine monopiles with low to medium commercial maturity and technological readiness. Such interest centres around an understanding of how far and how deep the new concept OWT monopiles can be in order for them to be successfully installed and operated. In 2020, the average installation depth below mean sea and distance from shoreline in Europe was 36m and 44km, respectively [162]. Offshore wind turbine monopiles of up to 10-MW are now operational; however, the extent of their structural capacity in deeper waters and the governing criteria are unclear. The same question applies to even larger and heavier OWT structures of up to 20-MW capacity and beyond. Upscaling and preliminary design studies on new generation turbine capacities such as 20-MW are currently being conducted. Recent studies include multidisciplinary design optimisation to define the aeroservoelastic design of the rotor and tower subject to blade-tower clearance, structural stresses, modal frequencies, tip-speed, and fatigue damage at selected sections [163] [164], and the design and structural analysis of a three-spar type 20-MW floating wind turbines [165]. The question as to how far and how deep the monopiles can be installed is complicated by the need to understand the effect of installation water depth on these larger and heavier structures. This includes OWT monopile structural design challenges relating to manufacturing, transportation, and operations as outlined in previous in-depth review studies and gap analysis of OWT monopiles [12] [166]. Research conducted by Arany et al. (2015) concluded that larger diameter thin-walled piles are susceptible to tip buckling during installation in dense sand or weathered bedrock [11].

Increased capacity and larger supporting structures have resulted in a corresponding increase in wind load, design, and performance related challenges. These challenges are made worse by the dynamic sensitive nature of offshore wind turbine monopile structures under the imposed action of coupled cyclic and varying environmental and machine loads from a wide range of frequency bands. The external loads and frequency bands are primarily the wind action on the structure, wave forces, the rotor and blade frequencies [14]. Research by Arany et al. (2015) identified the serviceability limit state as the controlling design principle for offshore wind turbines [11]. While this finding may be valid for offshore wind turbine monopiles up to 8-MW, and possibly 10-MW, this conclusion is yet to be tested and verified for the new generation of offshore wind turbine monopiles with an increased capacity of up to 20-MW which have a larger and heavier monopile

structure and tower diameter and thickness. The natural structural frequency and deflection (tilt and rotation) are the governing parameters for main serviceability limit state. These parameters have been tested and verified for both current and new OWT monopile structures through harmonic response analyses and modal analyses to isolate the monopile structural natural frequency from the frequencies of the imposed loads.

Research performed by Senanayake et al. (2017) concluded that correct estimation of the structural response and natural frequency can be the deciding factor between an over-conservative expensive design or an accurate cost-effective design solution [58]. Laboratory tests undertaken by Bhattacharya et al. (2015) and research by Kuhn et al. (1997) deduced that the OWT monopile natural frequency can change with respect to time due to either soil stiffening or softening from cyclic dynamic loading during the operational design life [11, 158]. Previous research has revealed that the structure's modal frequency is sensitive to soil properties, modelling techniques, and soil-structure interaction [13]. The renowned non-linear p-y springs distributed along the pile length, traditionally and successfully used in the oil and gas sector, are also being utilised in the design of OWT monopile structures. Nevertheless, this soil modelling method has primarily been tested and validated for pile diameter ≤1.0m, and has been shown by numerous research studies to be based on fundamental theoretical assumptions that are inappropriate and unsuitable for larger diameter OWT monopile foundation applications, including current and future OWT monopile installations [39] [2]. The ongoing PISA project and other research projects has revealed notable improvements in simplistic offshore wind monopile foundation modelling methods which have been supported and calibrated using field tests and measurements [8-10].

This study addressed and elucidated the structural response of current (5-MW and 10-MW) and future generation (15-MW and 20-MW) offshore wind turbines under 50-year return operational and environmental loading conditions in installation water depths of 20m, 50m, and 70m. A secondary aim was to provide a direction for future research and development work along with structural design improvements in the offshore wind turbine sector. This will provide the required clean energy capacity to meet global demand in line with climate change and sustainability. This article is structured in terms of the following sections. Section 5.2 presents the design data and methodology based on 5-MW, 10 MW, 15-MW, and 20-MW offshore wind turbine structures. The modelling technique for the foundation, tower, and soil-structure interaction is presented in Section 5.3. The results of the investigation, including the response of salient individual and coupled design criteria, are discussed in Sections 5.5 and 5.6. Other salient structural assessment observations are presented in Section 5.11. The conclusions and research contributions are presented in Section 5.12.

5.2 Design Data and Methodology

The models were based on validated 5-MW NREL and DTU 10-MW reference models, 15-MW reference model, and 20-MW upscaled offshore wind monopile models installed at 60m below the seabed at varying water depths of 20m, 50m, and 70m, respectively. The 20-MW upscaled model configuration was generated according to the upscaling procedure for wind turbine and upscaling law using scaling factor k which is normally determined by the power rating of new and initial wind turbine designs. The power is usually the predefined value of the desired upscaled turbine [161] [167]. The reference and upscaled wind turbine models were a conventional horizontal axis three-bladed and upwind type turbine on a tubular tower, supported by a large monopile embedded 60m below the seabed. The original tower, the DTU 10-MW onshore turbine, was truncated for the offshore environment with an air gap of 18m [159] [160]. The representative models were constructed in a finite element software package for the top structure, substructure, and the foundation system. The fundamental design data are presented in Table 5.1. The tower and soil-foundation design information are outlined in Table 5.2.

Description	**Value**				**Units**
Power Rating	**5**	**10**	**15**	**20**	MW
Turbine Class		IEC Class B	IEC Class IB	IEC Class IB	-
Rotor Diameter	126	178.3	240	270	m
Hub Height	87.6	119	150	175	m
Blade Mass	-	41000	65000	-	kg
Rotor Nacelle Assembly Mass	406780	674000	10170000	1250000	kg
Tower Mass	347000	987000	860000	-	kg
Cut-in, Rated Wind	3, 11.4	4, 11.4	3, 10.59	3, 10.50	m/s
Cut-in, Rated Rotor Speed	6.9, 12.1	6.0, 9.6	5.0, 7.56	5, 7.25	rpm
Cut-out Wind Speed	25	25	25	25	m/s
Shaft Tilt Angle	5	5	6	7	deg
Tower Top Diameter and Thickness	3.87, 0.025	5.5, 0.02	7.94, 0.02	8, 0.03	m
Tower base Diameter and Thickness	6, 0.05	8.3, 0.05	10, 0.05	11, 0.07	m

Table 5.1 – Turbine Data for NREL 5-MW, DTU 10-MW, IEA 15-MW, and Upscaled 20-MW [159] [160] [58] [147] [161] [153]

Description	Value	Units
Tower Material Data		
Density (Effective to account for paint, bolts, welds, flanges*)	7850 (8500*)	kg/m^3
Young's Modulus	210	GPa
Shear Modulus	80.8	GPa
Steel Grade	355	MPa
Soil Properties and Foundation Data		
Embedment Depth	60	m
Density	1800 – 2000	kg/m^3
Undrained Young's Modulus	40 - 70	MPa
Poisson's Ratio	0.45	-
Friction Angle	20	Deg
Undrained Shear Strength (S_U) (Cohesion)	150 – 250	kPa

Table 5.2 – Tower and Soil-Monopile Foundation Design Data [11] [58]

The thrust force (*Th*) applied at the hub height is calculated according to the equation [41]:

$$\boldsymbol{Th = \frac{1}{2}\rho_a A_R C_T U^2} \quad (1)$$

where ρ_a is the density of air, A_R is the rotor swept area, C_T is the thrust coefficient, and U is the wind speed. The wave action on the structure is calculated using the Morison's equation on linear wave theory [61].

5.3 Foundation-Structure Interaction Modelling

The 5-MW, 10-MW, 15-MW, and 20-MW analytical models, including the tower and monopile foundation structures, were generated and investigated in global space using the finite element modelling package, Ansys Workbench - Static Structural. The models were investigated for 20m, 50m, and 70m installation water depths using different combinations of monopile, and tower diameters and thicknesses supported in a soil mass. The OWT monopiles were embedded 60m below the mudline for all load cases and model configurations. Initially, similar model combinations were investigated to consider different modelling techniques for the soil-structure arrangement using Winkler type p-y curves and JeanJean springs/curves [13].

The foundation structure was modelled according to the different soil formation and profiles and characteristic through depth properties. The interaction of soil-monopile interface and behaviour was generated and modelled based on friction action, calculated according to the soil properties presented in Table 5.2. The Rotor Nacelle Assembly (RNA) at the top of the offshore wind turbine structure was represented in the model by a lump mass. End bearing support to the monopile, and the tower were generated using spring elements with appropriate non-linear stiffness properties. The connections between the different structural

members, the soil-structure interface and interactions were completed using finite element analytical share and bonding tools [13].

The OWT global model and meshed profiles depicting the RNA load, the turbine tower, and foundation are presented in Figure 5.1. Sensitivity analysis was completed for the mesh definition for the top structure and soil-foundation systems. Industry case studies and published literatures were used to verify and validate the models and structural response [12] [11] [58] [13] [159].

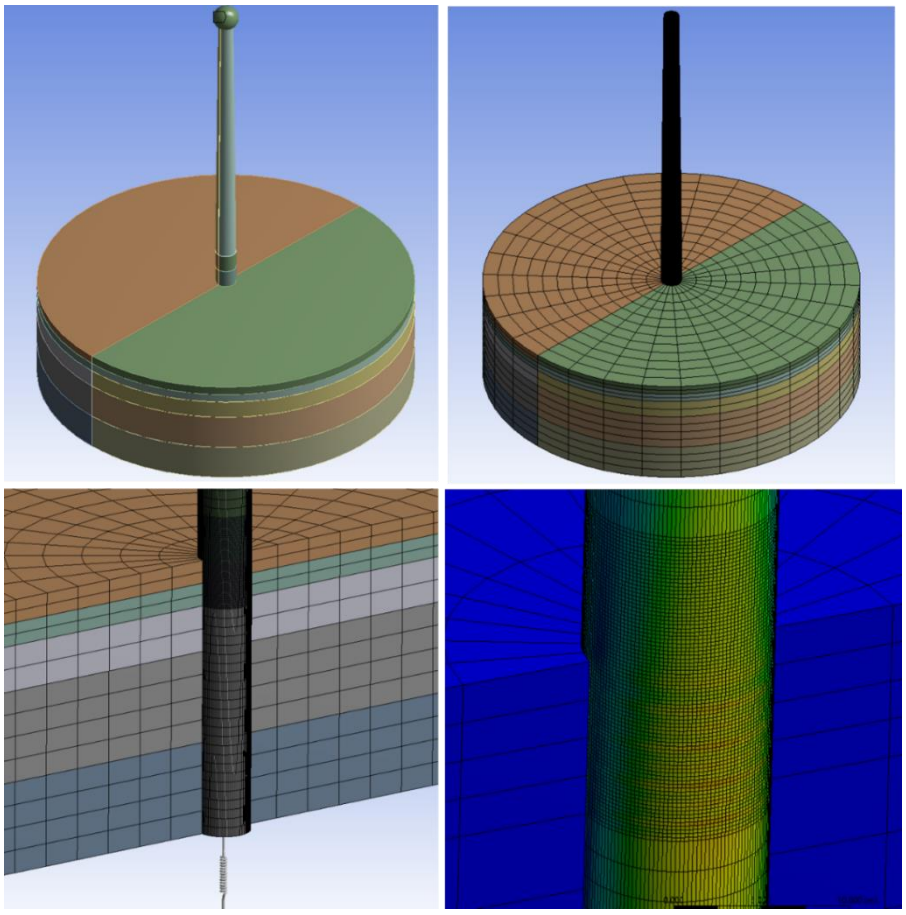

Figure 5.1 – Representative Finite Element Analysis Global Model and Meshed Profiles

5.4 Foundation Ultimate Limit State Geotechnical Design Checks

Geotechnical design checks are carried out to estimate the moment of resistance, M_R, and lateral load carrying capacity, H_R. The Moment-Lateral resistance is used to determine the soil capacity and soil failure around the pile due to external loads. This is different from structural failure criteria of the monopile structure such as stress and buckling. The combination or interaction of the moment of resistance and lateral resistance of the soil can be used to define the safe zone, such that loads that fall within the interaction diagram are considered safe. The soil Moment-Lateral resistance can be calculated using three different methods according to Aleem et al. (2022, [168]):

1. The Simplified Method based on Limit Equilibrium which can easily be completed using spreadsheet type program.
2. Standard Method based on the Beam on Winkler Foundation or p-y curve method where standard of bespoke p-y curves can also be used.
3. Advanced Method based on finite element analysis where the curves are generated based on selected failure criterion and the soil constitutive model.

The simplified method is used for determining the soil capacity to support external moment and lateral loads for a 50-year return period. This represents typical foundation loads and a conservative approach that may serve as the basis for feasibility and conceptual design of offshore wind turbine monopiles. The Simplified Method approach is shown to have a good agreement and indication of the soil capacity compared with the Standard and Advanced Method according to study completed by Aleem et al. (2022, [168]) . Detailed geotechnical analysis for model optimisation and final design may be required to address other load cases and combinations. Detailed design would require detailed site-specific environmental data, turbine properties.

The lateral resistance to monopile in clayey soil can be calculated according to Broms (1964, [169]) and considering the pressure distribution presented in Figure 5.2. This method ignores any reduction in capacity in the clay soil that are induced due to the vertical loads.

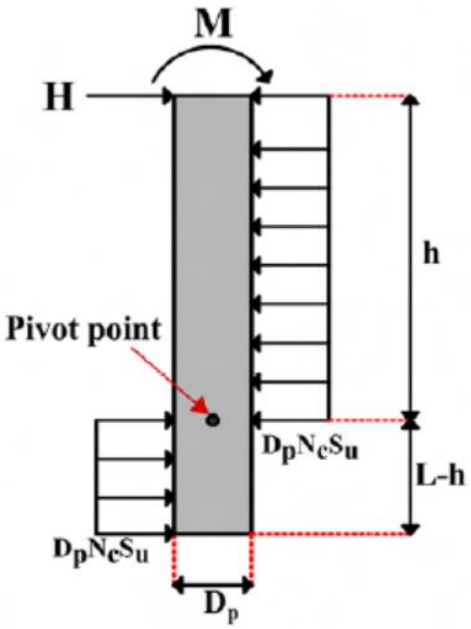

Figure 5.2 – Rigid Monopile in Clayey Soil [168]

Considering horizontal equilibrium:

$$H = hD_PN_CS_U - (L-h)D_PN_CS_U = (2h-L)D_PN_CS_U \quad (2)$$

Considering moment equilibrium and taking moment about the pivot point:

$$M + Hh = \frac{h^2}{2}D_PN_CS_U - \frac{(L-h)^2}{2}D_PN_CS_U \quad (3)$$

Combining the horizontal and moment equilibrium equations above, yields:

$$M = \frac{(L^2-2h^2)}{2}D_PN_CS_U \quad (4)$$

When H= 0, and the pivot point is h = L/2, then M_R can be calculated:

$$M_R = \frac{L^2}{4}D_PN_CS_U \quad (5)$$

Similarly, when M= 0, and the pivot point is h = L/$\sqrt{2}$, then H_R can be calculated:

$$H_R = \left(\sqrt{2}-1\right)LD_PN_CS_U \quad (6)$$

where:

h is the assumed pivot point in m.
L is the embedded depth of the monopile in m.
S_U is the undrained shear strength of soil in kPa.
N_C is the lateral bearing factor = P_U/S_u.
P_U is the ultimate soil resistance in kPa.

Considering the Simplified Method, the soil resistance (moment-lateral capacity) between the mudline and $1.5D_p$ is ignored for cohesive soil as suggested by Broms (1964, [169]). Hence, the distribution below 1.5Dp is constant at $9S_uD_p$. The Geotechnical design check for the 5-MW, 10-MW, 15-MW, and 20-MW offshore wind turbine monopiles is presented in Figure 5.3. The soil is shown to have sufficient resistance to support the imposed external loads for all wind turbine configurations. The minimum Load Utilisation Ratio, LU, is 10.6 factor of safety, which represents the 5-MW monopile configuration embedded 60m below mudline, calculated according to the following expression [168]:

$$LU = \frac{Resistance\ (R)}{Action\ (A)} = FOS = \sqrt{\frac{(H_iM_RH_R)^2 + (M_iM_RH_R)^2}{\frac{(M_iH_R + H_iM_R)^2}{\sqrt{\left(M_i^2 + H_i^2\right)}}}} \quad (7)$$

The pile penetration depth of 60m is selected to fix this variable, suitable for a workable design, considering the range of pile diameters, thicknesses, and water

depths of up to 70m. The influence of the embedded depth and undrained shear strength on the soil load utilisation ratio can be tested by reducing the pile penetration depth for the 5-MW offshore wind turbine monopile configuration to the minimum pile length of 25m for the pile to be considered "infinitely long". Hence, the load utilisation ratio, reduces to 2.2 factor of safety for 25m pile penetration length. The calculation for the minimum pile length is presented in Section 3.2. The factor of safety reduces further to <1.0 by considering the minimum pile length of 25m and 75kPa undrained shear strength at $1.5D_p$. The undrained shear strength at $1.5D_p$ used for the rest of this research is 175kPa.

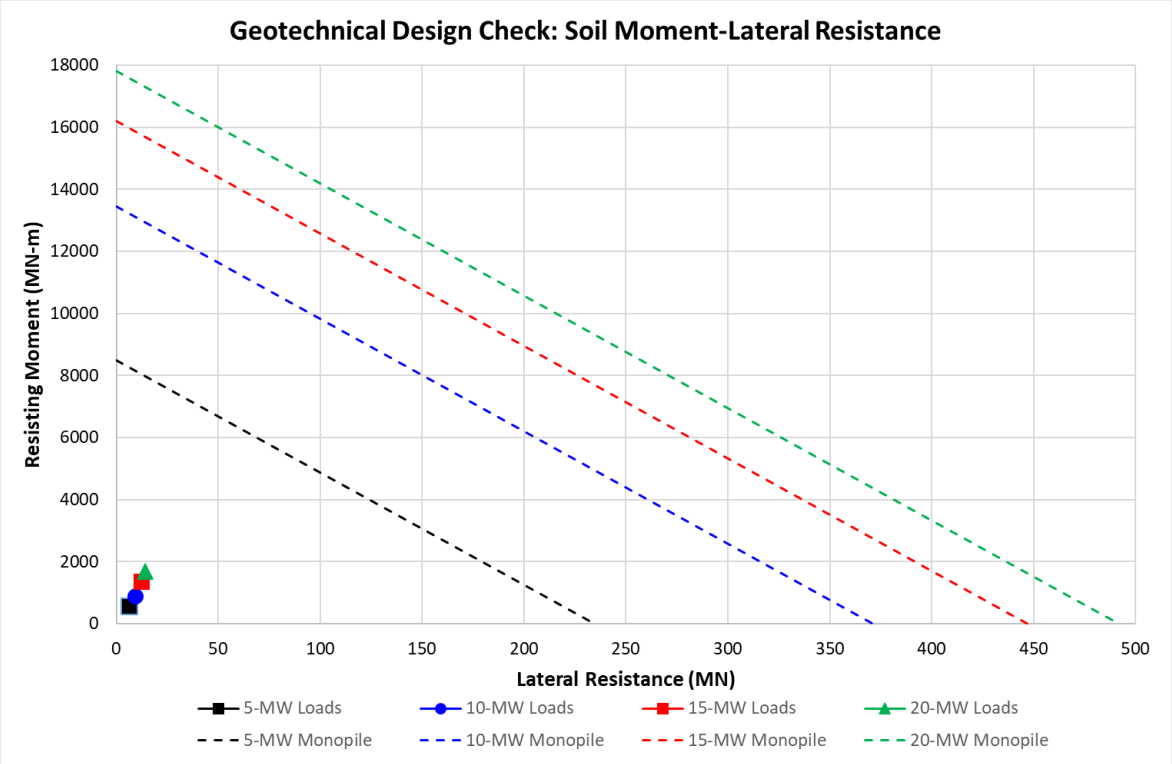

Figure 5.3 – Geotechnical Design Check: Soil Moment-Lateral Resistance

5.5 Findings and Discussion

The interpretation and discussion of the results for the 5-MW, 10-MW, 15-MW, and 20-MW capacity OWT monopiles are presented in Sections 5.6 through 5.9. The findings were used to generate the OWT monopile structural design envelopes for the turbine capacities considered. The design envelope covered 20m, 50m, and 70m installation water depths. The appropriate design range of monopile diameters and wall thicknesses selected were captured in the offshore wind monopile design envelope. The monopile was subjected to a 50-year return environmental and rotor-nacelle-assembly loads and a total damping of 10% in accordance with [12] [32] [82].

Although the interpretation of the results and the structural design envelope apply to monopiles of 5-MW to 20-MW OWT, it is important to note that the turbine structure and foundation system response are dynamically sensitive to the soil

properties, modelling techniques, and environmental conditions. The design envelope presented in this article serves as a useful feasibility design tool, but it is essential that it is verified on a site basis using site-specific design data and information.

5.6 Current Gen: 5-MW Findings and Discussions

This section presents the structural design envelopes for 5-MW offshore wind turbines at 20m, 50m, and 70m installation water depths. Selected design configurations are used to demonstrate each of the installation water depths, as presented in Sections 5.6.1 to 5.6.3.

The shear and bending moment reaction loads at the mudline elevation for the 5-MW OWT monopile findings presented in this section are given in **Table *5.3***.

5-MW OWT Monopile Reaction Loads	Water Depth		
	20 m	50 m	70 m
Shear (MN)	6.38	6.38	6.38
Bending Moment (MN-m)	249.67	441.21	568.90

Table 5.3 – 5-MW OWT Monopile Reaction Loads at Mudline

5.6.1 5-MW 20m Installation Water Depth

The design envelope of the 5-MW OWT monopile installed at a 20m water depth is defined for 5m to 8m monopile diameters and wall thicknesses of 40mm to 60mm. The selected range of configurations is based on iterative investigation leading to definition of the appropriate and allowable design window/boundaries. The design envelope is generated according to the four main governing criteria: natural frequency, stresses, buckling, and deflection. The deflection correlated with and followed a similar trend to the stresses; hence, it was excluded from the envelope for clarity and simplicity of presentation. Additionally, the deflection limit is turbine model specific and defined by the manufacturer or specified in the design codes. The deflection limit is often extremely strict and exceeded, and thus remains a subject of debate in the design of OWT.

The maximum OWT monopile deflection at the mudline is presented in Table 5.4.

Monopile Deflection at Mudline (Degree)			
Diameter (m)	Thickness (mm)		
	50mm	45mm	40mm
6.0m	0.44	0.49	0.56
5.4m	0.58	0.64	0.73
4.8m	0.80	0.89	1.02

Table 5.4 – 5-MW OWT Monopile Deflection at Mudline in a 20m Water Depth

For a 20m water depth, 6m and 7m monopile diameters were used to demonstrate the 5-MW design envelope as presented in Figure 5.4. At a 6m monopile diameter, the structure was suitable for 50mm to 60mm wall thicknesses. It was unsuitable

for 45mm wall thicknesses and less. The first natural buckling mode was the governing design criterion. Although the turbine capacity at 40mm wall thickness was marginal, the turbine was within the capacity for natural frequency and stresses for 40mm to 60mm wall thicknesses.

When the monopile diameter was increased to 7m, the turbine became suitable only for 50mm wall thicknesses. The failure mode became complex because of a combination of the first buckling mode and the natural frequency. The turbine is susceptible to buckling at 50mm to 60mm thicknesses. Superimposed over the natural frequency boundary of 40mm to 50mm thicknesses, the recommended design is 50mm wall thickness at 7m monopile diameter. An improvement in the stresses is evident at all wall thicknesses as the diameter increases Figure 5.4.

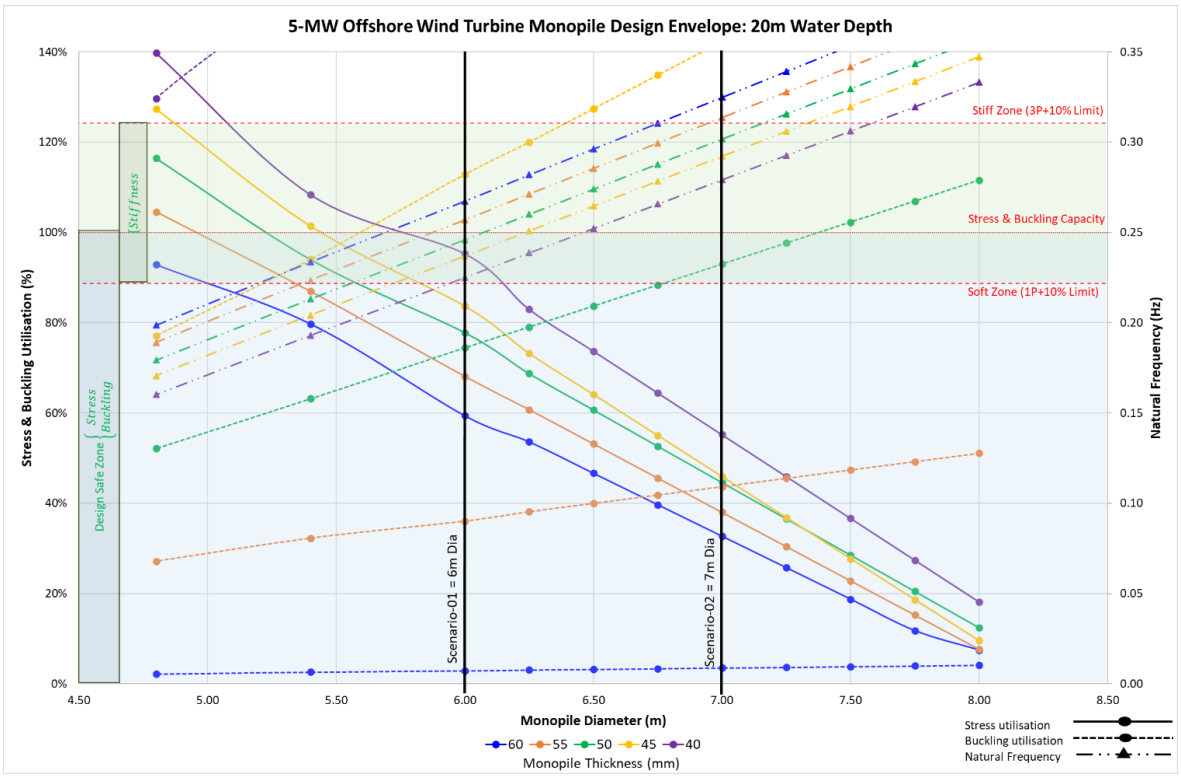

Figure 5.4 – 5-MW OWT Monopile Design Envelope for a 20m Water Depth

5.6.2 5-MW 50m Installation Water Depth

The design envelope of the 5-MW OWT monopile installed at a 50m water depth was defined for 5m to 8m monopile diameters, assuming wall thicknesses of 40mm to 60mm. The maximum OWT monopile deflection at the mudline is presented in Table 5.5. The maximum deflection must be considered along with the design envelope presented in Table 5.5.

Monopile Deflection at Mudline (Degree)			
Diameter (m)	Thickness (mm)		
	50mm	45mm	40mm
6.0m	0.80	0.91	1.47
5.4m	1.08	1.22	1.63
4.8m	1.52	1.72	2.11

Table 5.5 – 5-MW OWT Monopile Deflection at Mudline in a 50m Water Depth

Similar to the 20m installation water depth in Section 5.6.1, 6m and 7m monopile diameters are used to demonstrate the 5-MW design envelope for a 50m installation water depth, as presented in Figure 5.5. At a 6m monopile diameter, the OWT monopile was marginally suitable at a 60mm wall thickness for natural frequency, but fully suitable at a 55mm wall thickness. Below 55mm, the turbine was unsuitable primarily due to the first buckling mode, followed by natural frequency in the soft-soft zone for reduced wall thicknesses.

For a larger monopile diameter of 7m, the turbine was unsuitable at all wall thicknesses. The limitation at 55mm and 60mm wall thicknesses was governed by the natural frequency. Although the turbine was within the allowable design limit at 50mm wall thickness for natural frequency and stress, it was an unsuitable configuration because of a shift in the governing criterion to the first buckling mode. Below a 50mm wall thickness, both the natural frequency and the buckling governed the design envelope. Hence, the OWT monopile is unsuitable for a 7m monopile diameter and 50m installation water depth. The recommended design is 55mm wall thickness at 6m monopile diameter or other suitable configurations selected from the design envelope in Figure 5.5.

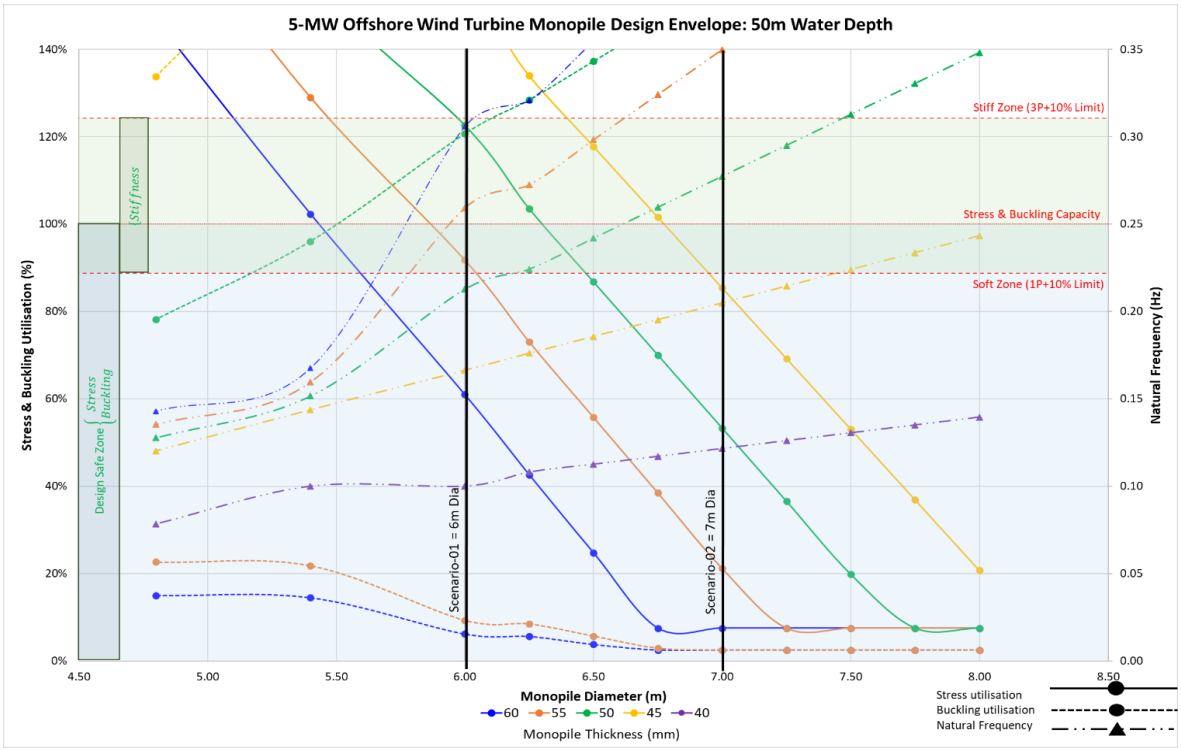

Figure 5.5 – 5-MW OWT Monopile Design Envelope at a 50m Water Depth

5.6.3 5-MW 70m Installation Water Depth

Due to the limitations and narrowed permissible design envelope presented for the 50m water depth in Section 5.6.2, a 70m water depth is unsuitable for 5m to 8m monopile diameters and for 40mm up to 60mm wall thicknesses. However, efficient, and workable design solutions and an allowable envelope are possible at this depth, as shown and defined for the 10-MW capacity OWT monopile in Section 5.7. The design envelope for a 10-MW OWT monopile at a 70m water depth, as presented in the next section, can be reasonably extended, and applied, subject to good engineering judgement, in the feasibility design of a 5-MW OWT monopile at a similar installation water depth of 70m.

5.7 Current Gen: 10-MW Findings and Discussions

This section presents the structural design envelopes for 10-MW offshore wind turbine installed at 20m, 50m, and 70m water depths. The design envelopes for the three installation water depths are presented in Sections 5.7.1 through 5.7.3.

The shear and bending moment reaction loads at the mudline elevation for the 10-MW OWT monopile findings presented in this section are given in Table 5.6.

10-MW OWT Monopile Reaction Loads	**Water Depth**		
	20 m	**50 m**	**70 m**
Shear (MN)	9.23	9.23	9.23
Bending Moment (MN-m)	430.40	707.32	891.94

Table 5.6 – 10-MW OWT Monopile Reaction Loads at Mudline

5.7.1 10-MW 20m Installation Water Depth

The 10-MW design envelope was defined by a lower bound monopile diameter of 6.75m and upper bound diameter of 10.5m, assuming wall thicknesses of 48mm to 70mm. The boundary was defined following iterative assessment to determine the permissible design window. The maximum OWT monopile deflection at the mudline for selected representative configurations is presented in Table 5.7. The deflection should be compared with the turbine manufacturer specification considering the monopile and tower, and the industry code allowable general deflection limit.

Monopile Deflection at Mudline (Degree)			
Diameter (m)	**Thickness (mm)**		
	60mm	54mm	48mm
8.30m	0.25	0.27	0.31
7.47m	0.32	0.35	0.40
6.64m	0.43	0.48	0.55

Table 5.7 – 10-MW OWT Monopile Deflection at Mudline in a 20m Water Depth

The 10-MW installed at a 20m water depth is explained for 7m and 9m monopile diameters in Figure 5.6. At a 7m monopile diameter, the OWT was suitable for

70mm thickness and marginal for 65mm, as governed by the natural frequency soft-soft resonance initiation zone (1P + 10%). The turbine structure was unsuitable for wall thicknesses below 65mm. Buckling failure mode was initiated at 50mm and deteriorated for reduced wall thicknesses. The structural response to stresses at a 7m diameter was within the permissible stress utilisation for wall thicknesses from 48mm to 70mm.

By increasing the turbine diameter to 9m, the OWT structure was within the allowable design window for wall thicknesses of 60mm to 70mm inclusive. The structure became unsuitable for reduced wall thicknesses, notably at 54mm. The governing criterion shifted from the natural frequency, as the failure mode at a 7m monopile diameter, to the first buckling mode as the diameter increased to 9m. This behaviour demonstrates the dynamic and sensitive response of the OWT monopile. Simply increasing either the diameter/thickness or both does not necessarily translate into a suitable engineering solution but may reduce the resistance of the structure to external environmental conditions and turbine loads. Other suitable recommended OWT structural configurations can be selected from the design envelope for 10-MW capacity at a 20m water depth presented in Figure 5.6.

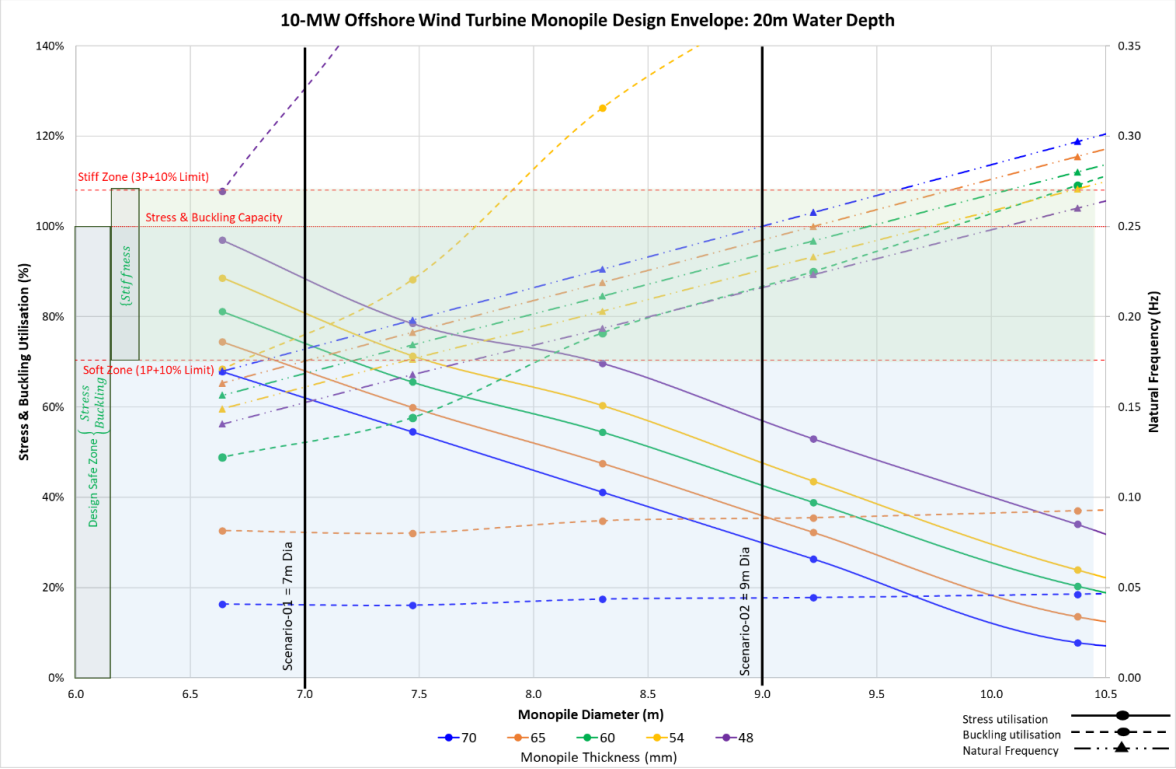

Figure 5.6 – 10-MW OWT Monopile Design Envelope at a 20m Water Depth

5.7.2 10-MW 50m Installation Water Depth

The maximum deflection of the turbine structure for the 50m water depth is presented for increased wall thickness. This is in line with design changes made to generate the structural design envelope as the OWT monopile is installed in deeper

waters. The maximum OWT monopile deflection at the mudline for selected representative configurations is presented in Table 5.8. The deflection clearly improved as diameter and wall thickness increased.

Monopile Deflection at Mudline (Degree)			
Diameter (m)	Thickness (mm)		
	90mm	80mm	70mm
8.30m	0.25	0.32	0.36
7.47m	0.38	0.42	0.48
6.64 m	0.52	0.58	0.65

Table 5.8 – 10-MW OWT Monopile Deflection at Mudline in a 50m Water Depth

For an indicative configuration of 7m monopile diameter, the OWT structure was unsuitable for all wall thicknesses investigated, including 70mm to 110mm, as shown in Figure 5.7. The driving criterion at this lower bound monopile diameter was the first natural frequency mode. The first buckling mode and stresses were both within the allowable design capacity.

At 9m monopile diameter, the OWT structure was suitable for the design envelope wall thicknesses presented in Figure 5.7. The natural frequency remained the governing criterion for the presented configurations. Notably, the first buckling mode was likely to overtake the natural frequency at higher diameter and reduced thickness subject to the selected configuration and optimisation of steel volume and other site-specific objectives.

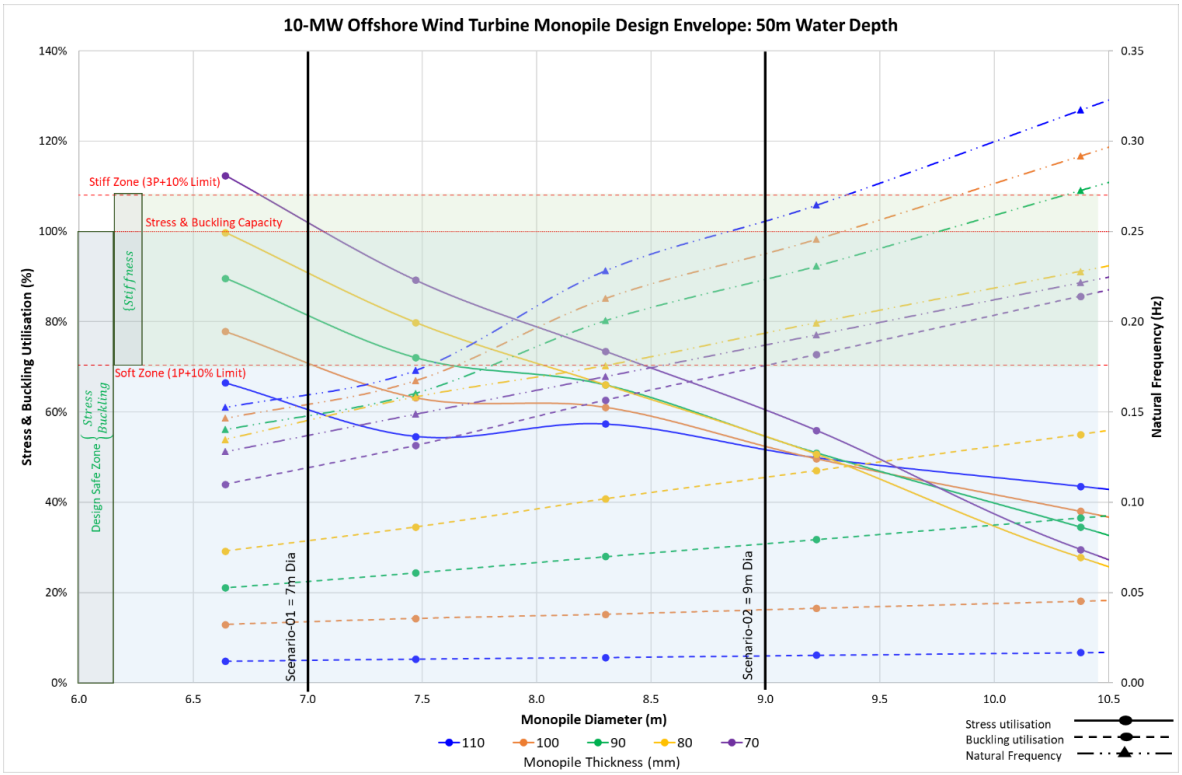

Figure 5.7 – 10-MW OWT Monopile Design Envelope at a 50m Water Depth

5.7.3 10-MW 70m Installation Water Depth

This section discusses the 10-MW capacity installed at a 70m water depth. The maximum OWT monopile deflection at the mudline is presented in Table 5.9. For the same lower and upper bound diameters of 6.64m (wall thickness 90mm) and 8.30m (for wall thickness 110mm), the maximum deflection was 0.72° and 0.33°, respectively. As predicted in previous sections, the deflection improved for increased diameter and wall thickness.

Monopile Deflection at Mudline (Degree)			
Diameter (m)	Thickness (mm)		
	110mm	100mm	90mm
8.30m	0.33	0.36	0.40
7.47m	0.44	0.47	0.52
6.64 m	0.60	0.65	0.72

Table 5.9 – 10-MW OWT Monopile Deflection at Mudline in a 70m Water Depth

Similar to the 50m water depth, the indicative 7m monopile diameter configuration was unsuitable for all wall thicknesses investigated, including 70mm to 110mm, as presented in Figure 5.8. Furthermore, increasing the monopile wall thickness for the 7m diameter led to marginal and expensive design improvement. It is necessary that the monopile diameter is increased and matched with a suitable wall thickness to enable a noticeable cost-effective improvement in the design. The limiting criterion at 7m diameter was the first natural frequency mode. The first buckling mode and stresses were both within the permissible design capacity.

For an increased monopile diameter of 9m, the OWT structure was within the allowable design window for 70mm through to 110m wall thicknesses, as presented in Figure 5.8. The trend depicts the natural frequency as the first limiting factor up to a certain diameter which may shift to the first buckling mode for an increased monopile diameter. Nevertheless, this will only become evident with expensive and larger structure design configurations.

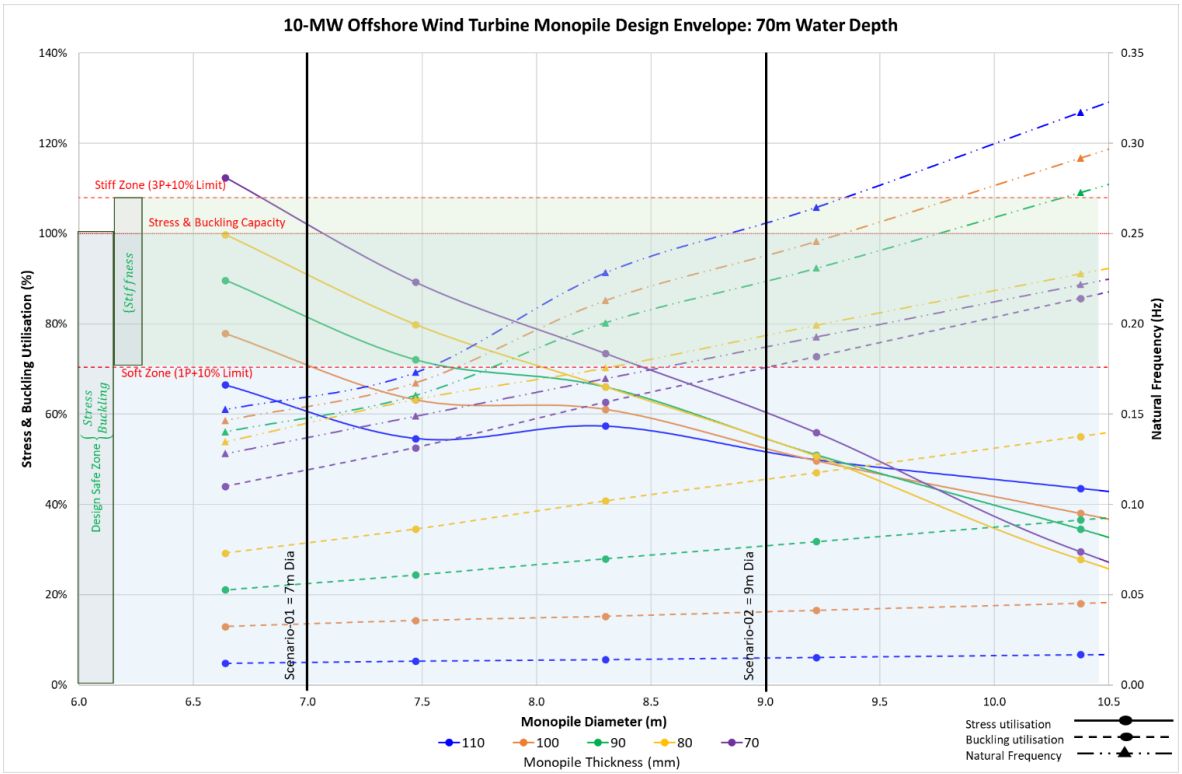

Figure 5.8 – 10-MW OWT Monopile Design Envelope at a 70m Water Depth

5.8 Future Gen: 15-MW Findings and Discussions

Sections 5.8.1 through 5.8.3 considers the future generation of 15-MW OWT monopile structural design responses and the allowable envelope definition for 20m, 50m, and 70m water depths.

The shear and bending moment reaction loads at the mudline elevation for the 15-MW OWT monopile findings presented in this section are given in Table 5.10.

15-MW OWT Monopile Reaction Loads	Water Depth		
	20 m	50 m	70 m
Shear (MN)	12.35	12.35	12.35
Bending Moment (MN-m)	749.26	1119.69	1366.64

Table 5.10 – 15-MW OWT Monopile Reaction Loads at Mudline

5.8.1 15-MW 20m Installation Water Depth

The monopile diameter increased in line with the 15-MW turbine capacity to achieve a suitable permissible design window/envelope based on the governing structural criteria. The deflection at the mudline for a 10m monopile diameter and wall thickness of 70mm is 0.30^{O}. Reducing the diameter and wall thickness to 8m and 50mm, respectively, caused a deflection of 0.67^{O}. Details of the deflections for 8m to 10m diameter for 50mm to 70mm wall thicknesses are presented in Table 5.11.

Monopile Deflection at Mudline (Degree)			
Diameter (m)	Thickness (mm)		
	70mm	60mm	50mm
10.0m	0.30	0.32	0.39
9.0m	0.37	0.43	0.49
8.0m	0.50	0.54	0.67

Table 5.11 – 15-MW OWT Monopile Deflection at Mudline in a 20m Water Depth

The 8.5m and 11m indicative design monopile diameters were selected from the design envelope to provide an overall explanation of the 15-MW OWT monopile design envelope for a 20m water depth. For the 8.5m monopile diameter, the recommended design limit is 70mm wall thickness, governed by the first buckling mode. However, the 60mm wall thickness configuration should be considered with caution, as the structure at this stage began to become unstable when resisting buckling loads, as illustrated in Figure 5.9. At a lower wall thickness of 50mm, stress was also a limiting criterion.

By increasing the OWT monopile diameter to 11m, the structural response improved for some thickness configurations, whereas it deteriorated for the others. The governing criteria also shifted between the first buckling mode and the natural modal frequency. The structure became susceptible to resonance excitation loading in the stiff zone (3P + 10%) for 90mm and 80mm wall thicknesses, which is likely to have exacerbated the fatigue damage. At the lower bound thicknesses, the suitability of the turbine structure was limited by the first buckling mode for 60mm thickness and below. This resulted in a narrow allowable design window configuration of 11m diameter and 70mm wall thickness. Other optimal design configurations can be selected from the design envelope, as depicted in Figure 5.9.

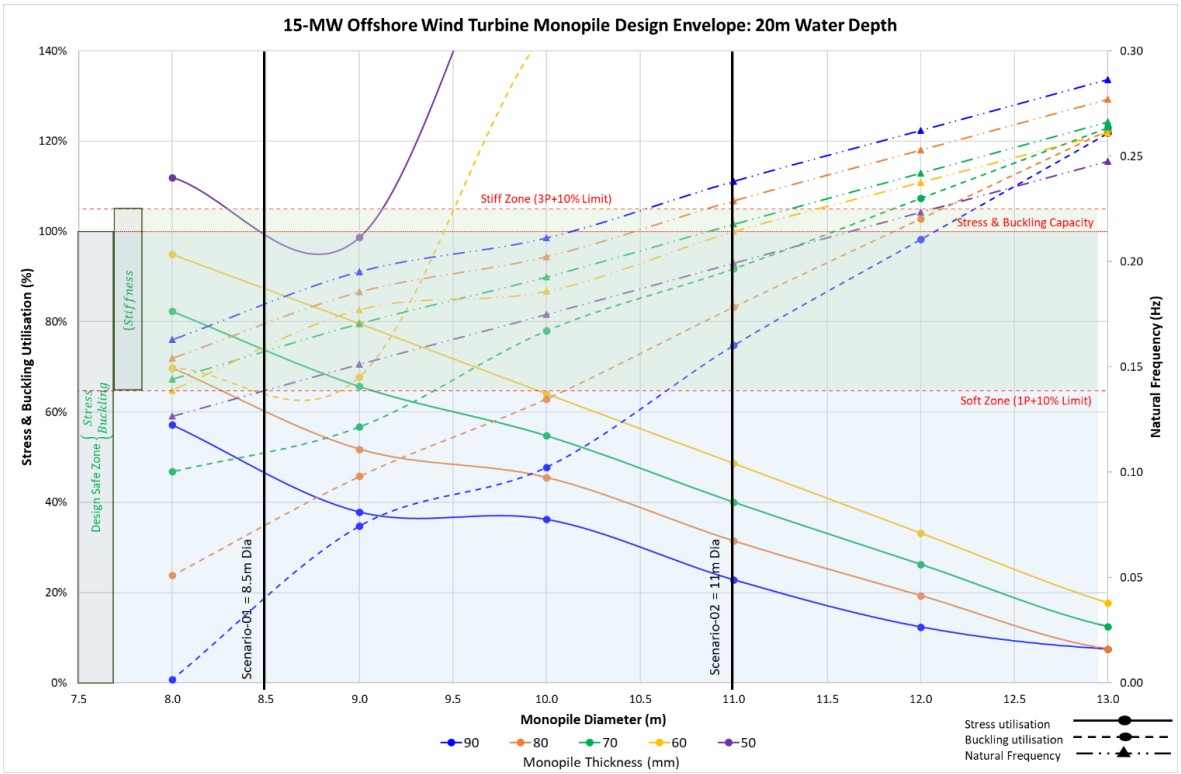

Figure 5.9 – 15-MW OWT Monopile Design Envelope at a 20m Water Depth

5.8.2 15-MW 50m Installation Water Depth

Details of the deflection at the mudline for a 15-MW OWT turbine installed at a 50m water depth for 8m to 10m monopile diameters and 50mm to 70mm wall thicknesses are presented in Table 5.12. A simple comparison of 20m and 50m water depths in Table 5.11 and Table 5.12, respectively, reveals a noticeable increase in the deflection for deeper installation water depths.

Monopile Deflection at Mudline (Degree)			
Diameter (m)	Thickness (mm)		
	70mm	60mm	50mm
10.0m	0.44	0.50	0.56
9.0m	0.56	0.63	0.79
8.0m	0.77	0.86	0.94

Table 5.12 – 15-MW OWT Monopile Deflection at Mudline in a 50m Water Depth

The design configuration at 8.5m monopile diameter for 50mm to 90mm wall thicknesses was unsuitable, and limited by a combination of the natural frequency, buckling, and stresses, as shown in Figure 5.10. A diameter greater than 8.5m is advisable with appropriate thickness. This can be selected from the design envelope.

With respect to an 11m monopile diameter design configuration, the 15-MW OWT in 50m water depth was suitable for 80mm and 90mm wall thicknesses. At a 70mm wall thickness and below, the structure was limited by the first buckling mode, followed by stresses below 60mm wall thicknesses, as depicted in Figure

5.10. The recommended suitable design lies between 80mm to 90mm, possibly 100mm, thickness for an 11m monopile diameter. Other workable design configurations can be identified from the design envelope.

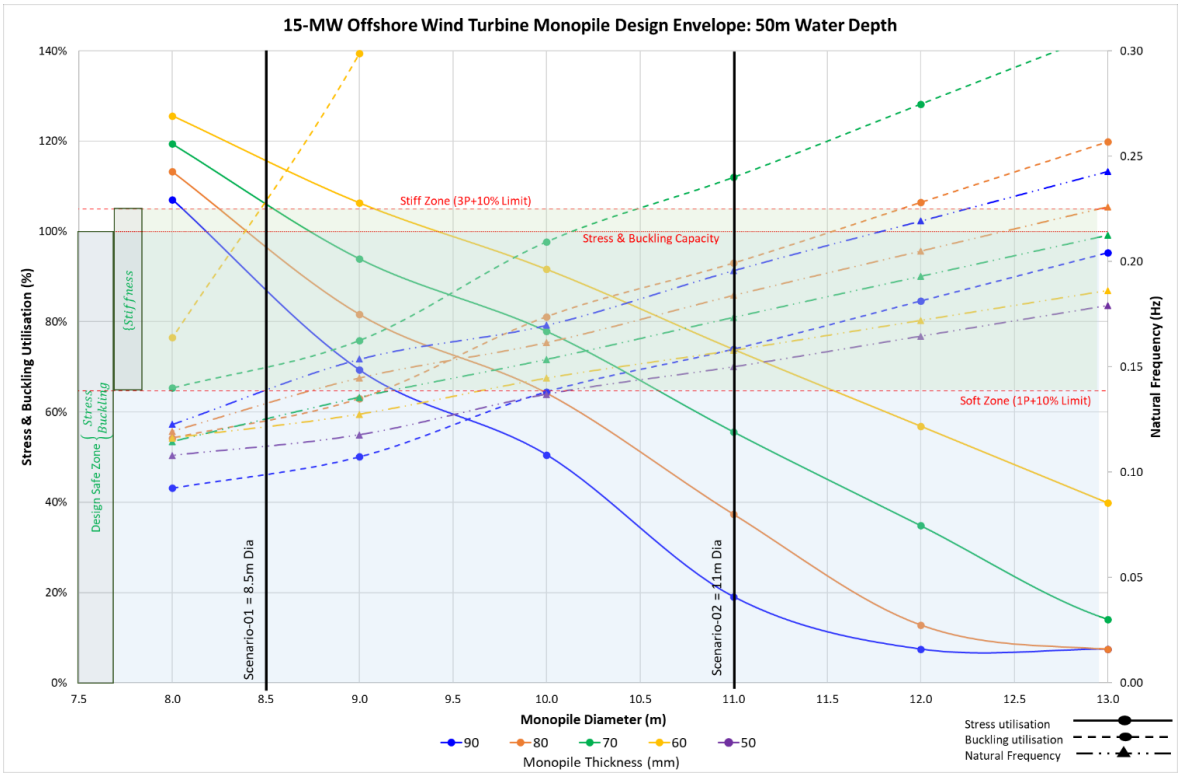

Figure 5.10 – 15-MW OWT Monopile Design Envelope at a 50m Water Depth

5.8.3 15-MW 70m Installation Water Depth

For a deeper installation water depth of 70m, the deflection at the mudline for a 15-MW OWT representative configurations of 8m to 10m monopile diameters and 70mm to 90mm wall thicknesses are presented in Table 5.13. By increasing the wall thickness from 70mm at a 50m water depth to 90mm at a 70m water depth, similar monopile mudline displacements of 0.44° and 0.46°, respectively, were achieved.

Monopile Deflection at Mudline (Degree)			
Diameter (m)	Thickness (mm)		
	90mm	80mm	70mm
10.0m	0.46	0.50	0.55
9.0m	0.49	0.52	0.60
8.0m	0.67	0.71	0.76

Table 5.13 – 15-MW OWT Monopile Deflection at Mudline in a 70m Water Depth

Similar to the 15-MW at 50m installation water depth, an 8.5m monopile diameter design configuration was unsuitable at 70mm to 110mm wall thicknesses. The selected design configuration was governed by the natural frequency and stresses, as depicted in Figure 5.11.

To improve the structural response and design outcome, it is essential that larger monopile diameters are considered and selected, along with an appropriate wall thickness. For instance, for the 11m monopile diameter presented in Figure 5.11, the structure was suitable regarding natural frequency and stresses for 70mm to 110mm wall thicknesses. Furthermore, buckling was satisfactory for 80mm to 110mm wall thicknesses. Nevertheless, the design was limited by buckling at a reduced wall thickness of 70mm. Other suitable design configurations at 70m water depth can be selected from the design envelope presented in Figure 5.11.

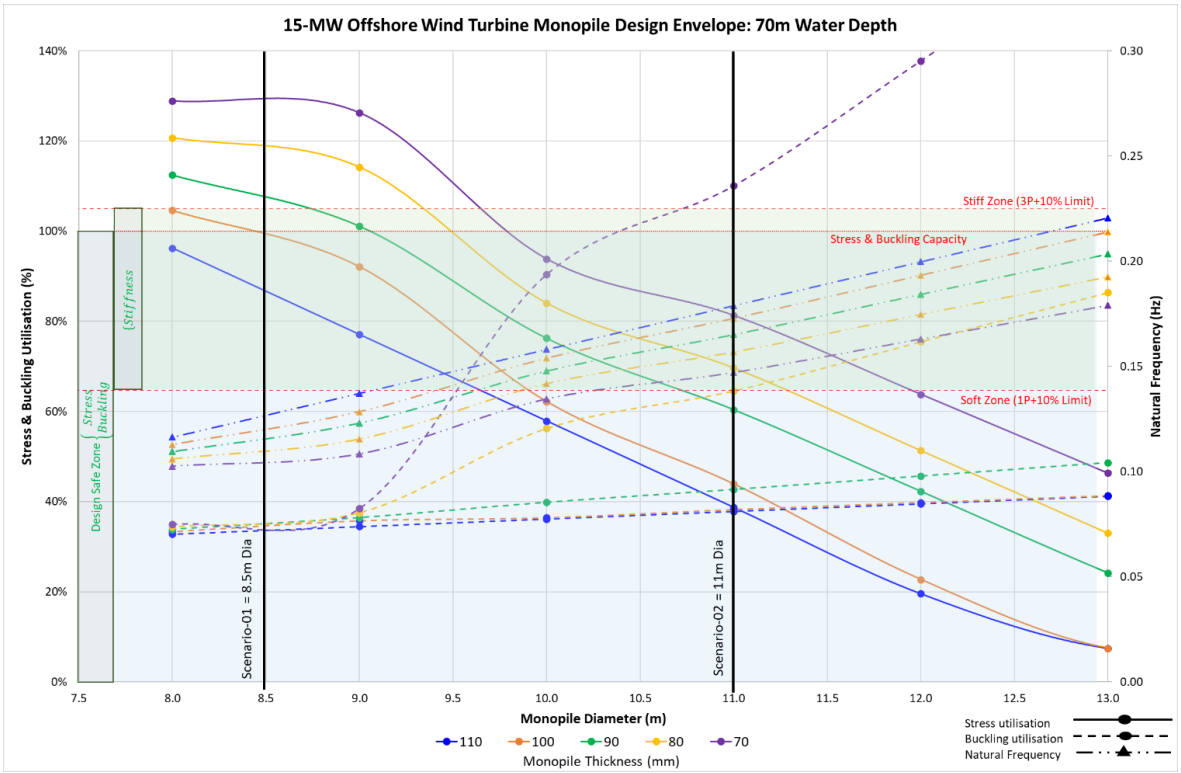

Figure 5.11 – 15-MW OWT Monopile Design Envelope at a 70m Water Depth

5.9 Future Gen: 20-MW Findings and Discussions

In this section, the structural response and allowable design envelope for the upscaled 20-MW OWT monopile is presented. The 20-MW OWT monopile is also investigated for 20m, 50m, and 70m water depths, considering the structural response to external loads in the frequency domain, susceptibility to buckling, stresses, and maximum displacement at the top of the tower.

The shear and bending moment reaction loads at the mudline elevation for the 20-MW OWT monopile findings presented in this section are given in Table 5.14.

20-MW OWT Monopile Reaction Loads	Water Depth		
	20 m	50 m	70 m
Shear (MN)	14.28	14.28	14.28
Bending Moment (MN-m)	975.06	1403.45	1689.04

Table 5.14 – 20-MW OWT Monopile Reaction Loads at Mudline

5.9.1 20-MW 20m Installation Water Depth

The tower diameters and thicknesses investigated for the 20m water depth increased in line with the turbine capacity and loads. The monopile mudline deflection for representative configurations of 9m to 11m monopile diameters and wall thicknesses of 60mm to 80mm are presented in this section. The monopile deflection at mudline was 0.34° for an 11m diameter and 80mm thickness, while a deflection of 0.62° was recorded for a 9m diameter and 60mm wall thickness. Details of the deflection for the representative configurations are presented in Table 5.15.

Monopile Deflection at Mudline (Degree)			
Diameter (m)	**Thickness (mm)**		
	80mm	70mm	60mm
11.0m	0.34	0.35	0.38
10.0m	0.42	0.45	0.48
9.0m	0.48	0.57	0.62

Table 5.15 – 20-MW OWT Monopile Deflection at Mudline in a 20m Water Depth

Figure 5.12 presents illustrative examples of the upscaled 20-MW OWT design envelope at a 20m water depth for 9m and 12 m monopile diameters. For a 9m monopile diameter, the turbine was suitable for 80mm to 100mm wall thicknesses. The turbine structure became unstable for wall thicknesses of 70mm and below due to external lower bound natural frequency in the soft zone (1P+10%) in addition to susceptibility to buckling. The design envelope suggests there is available scope to increase the wall thickness to accommodate other design-related issues where necessary, including for transport and installation scenarios.

Regarding the 12 m monopile diameter, the turbine structure was suitable regarding natural frequency susceptibility to resonance and stresses, including 60mm to 100mm wall thicknesses. The governing design criterion was the structure's first natural buckling mode. The 20-MW OWT became unstable at 70mm wall thickness and below, limited solely by buckling. Other suitable design configurations for a 20m water depth can be selected from the design envelope illustrated in Figure 5.12.

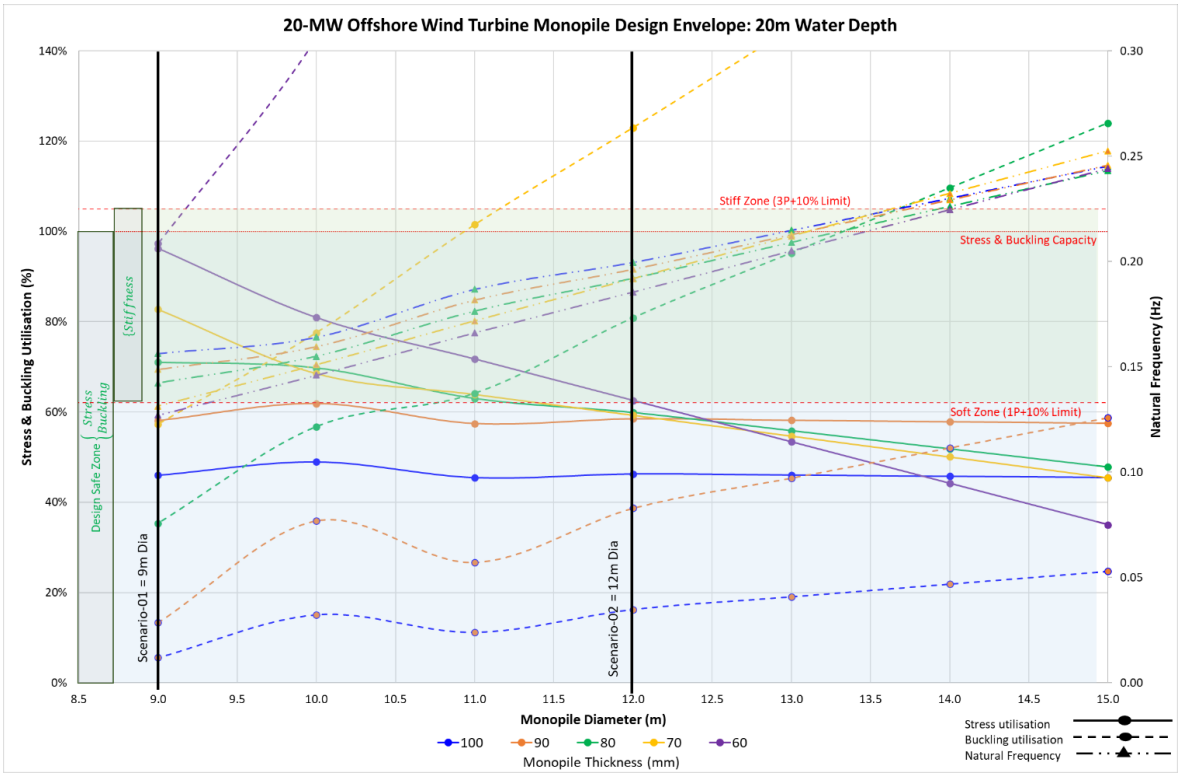

Figure 5.12 – 20-MW OWT Monopile Design Envelope at a 20m Water Depth

5.9.2 20-MW 50m Installation Water Depth

For a 50m installation water depth, a configuration range similar to that in Section 5.9.1 was used, which is presented in this section for demonstration. The maximum deflection at the mudline for the different configurations is presented in Table 5.16. The displacement at the mudline increased by approximately 30% when the turbine was installed in deeper waters of 50m, compared with the 20m water depth presented in Section 5.9.1.

Monopile Deflection at Mudline (Degree)			
Diameter (m)	Thickness (mm)		
	80mm	70mm	60mm
11.0m	0.46	0.50	0.56
10.0m	0.49	0.61	0.68
9.0m	0.75	0.82	0.92

Table 5.16 – 20-MW OWT Monopile Deflection at Mudline in a 50m Water Depth

As presented in Figure 5.13, for a 9m monopile diameter, the 20-MW OWT structure was governed by the natural frequency susceptibility to resonance in the soft zone (1P+10%) for 60mm to 100mm thicknesses. This was further limited by stresses below 80mm wall thickness and buckling below 70mm thickness. Based on the design findings presented in the envelope, increasing the wall thickness at 9m monopile diameter resulted in minimal to insignificant design improvement.

Hence, a larger OWT monopile diameter is required for the 20-MW OWT. For a 12 m monopile diameter, the structure was suitable for natural frequency and stresses for 70mm to 100mm wall thicknesses. The suitable wall thickness that satisfies all the design criteria considered in this study is between 80mm to 100mm, as presented in Figure 5.13. The wall thickness can be increased further based on site-specific design requirements and a value engineering assessment.

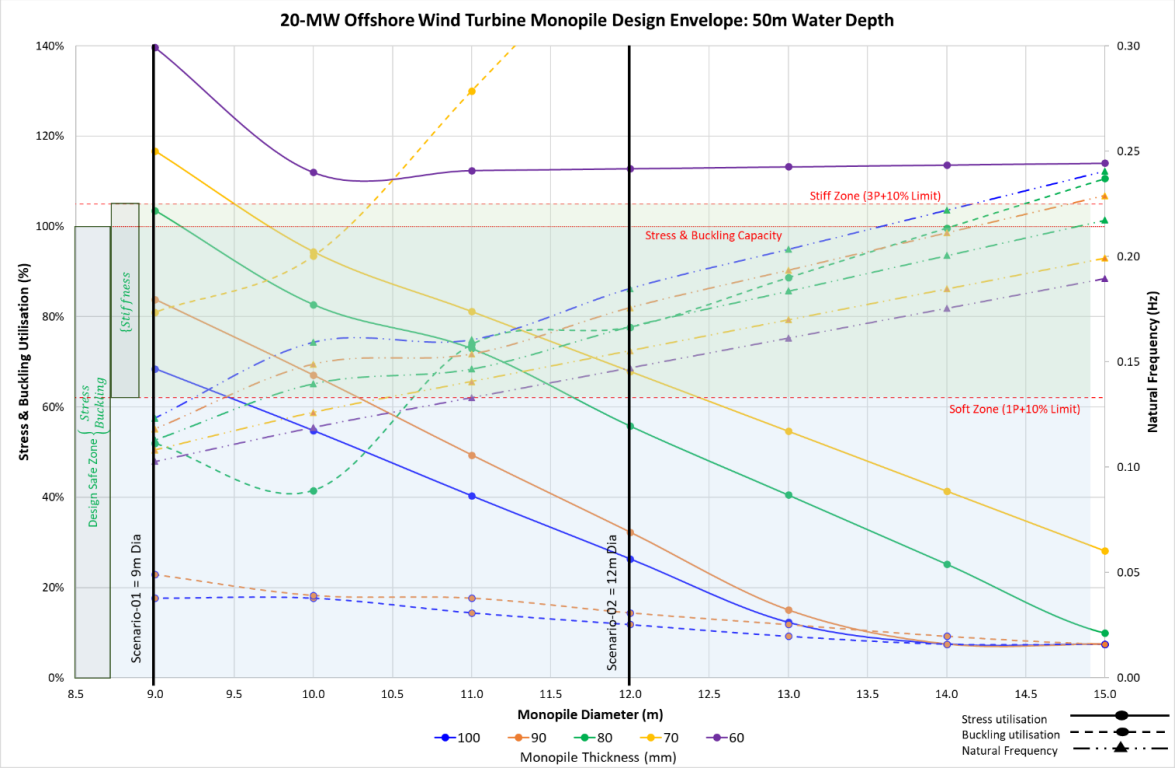

Figure 5.13 – 20-MW OWT Monopile Design Envelope at a 50m Water Depth

5.9.3 20-MW 70m Installation Water Depth

The 20-MW OWT structure configuration at a 70m water depth was limited to a 10m monopile diameter. The deflection at the monopile mudline for 10m to 12 m diameters and 60mm to 80mm wall thicknesses is presented in Table 5.17. An increase in the monopile diameter is required, based on design outcome, to support the increased capacity load in deeper waters, given the structural response for 20m and 50m water depths presented in earlier sections.

Monopile Deflection at Mudline (Degree)			
Diameter (m)	Thickness (mm)		
	80mm	70mm	60mm
12.0m	0.46	0.50	0.57
11.0m	0.49	0.52	0.56
10.0m	0.53	0.56	0.59

Table 5.17 – 20-MW OWT Monopile Deflection at Mudline in a 70m Water Depth

Although the analytical solution successfully converged for a 10m monopile diameter at a 70m water depth, the structure was unsuitable for 60m to 100mm

wall thicknesses governed primarily by the natural frequency, as shown in Figure 5.14. By considering even larger diameters, for instance, 12m, the limiting criteria shifted to the buckling mode and stresses for wall thicknesses of 70mm and below. The structure was suitable for wall thicknesses of 80mm to 100mm, and possibly a higher justifiable wall thickness. As Figure 5.14 illustrates, the monopile diameter may also be increased or reduced from the indicative 12m. However, it is necessary for the selected configuration to be assessed using site-specific data.

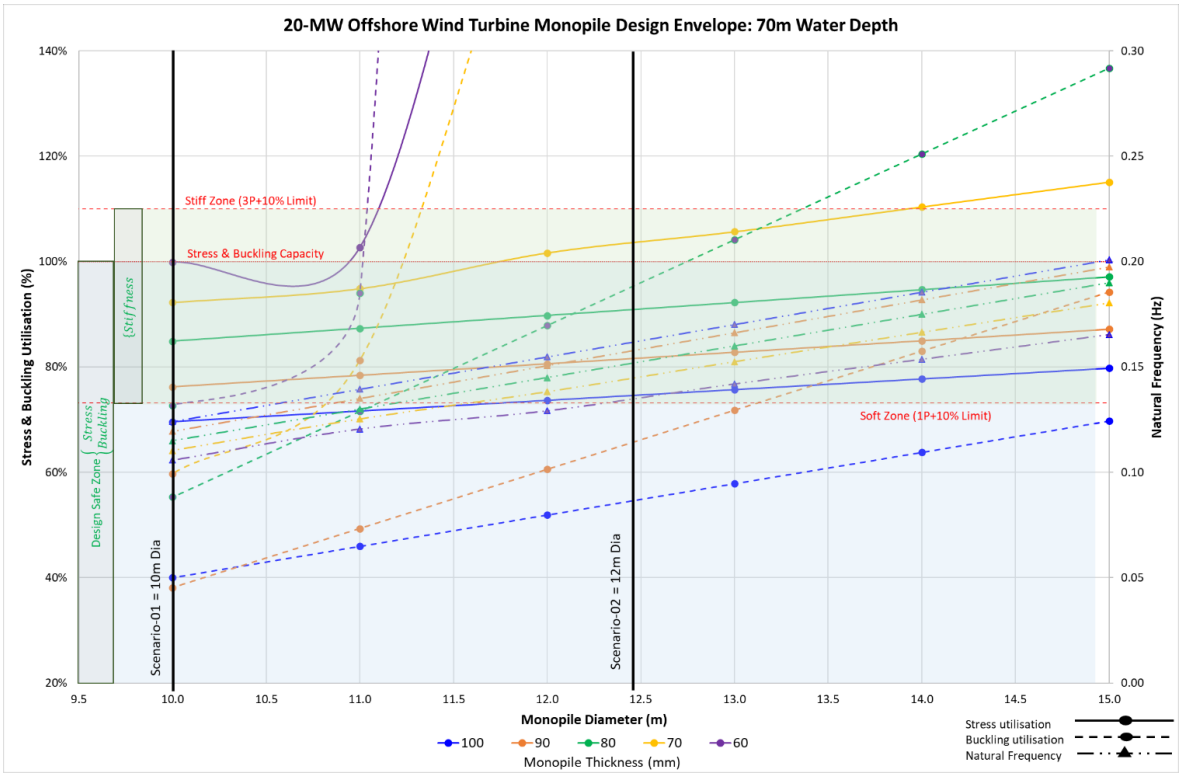

Figure 5.14 – 20-MW OWT Monopile Design Envelope at a 70m Water Depth

5.10 Optimum 5-MW to 20-MW OWT Monopile Configuration

Optimum offshore wind turbine monopile configurations for 5-MW to 20-MW capacities are presented in Figure 5.15, Figure 5.16, and Figure 5.17, installed in 20m, 50m, and 70m water depths, respectively. The optimum configurations are based on the offshore wind turbine monopile design envelopes presented above in this Section 5. Lower bound and upper bound configurations are included to generate a reasonable design range. It is worth noting that the optimum configurations presented in this section do not account for manufacturing, installation, and costs analysis and optimisation.

The optimum OWT configurations are to serve as a useful tool for feasibility and conceptual design and feed into detailed design of offshore wind turbine monopile structures. It is essential that the configurations are tested and verified on a site basis using site-specific design data and information.

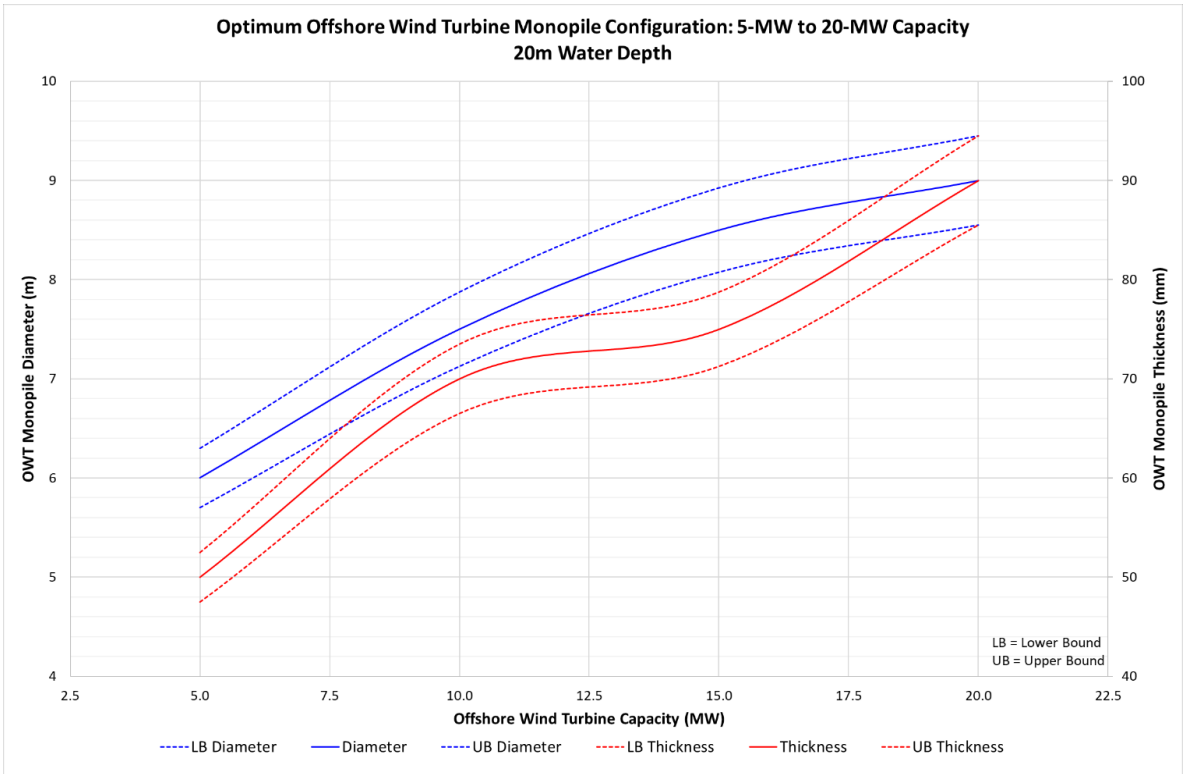

Figure 5.15 – Optimum 5 to 20-MW OWT Configuration in 20m Water Depth

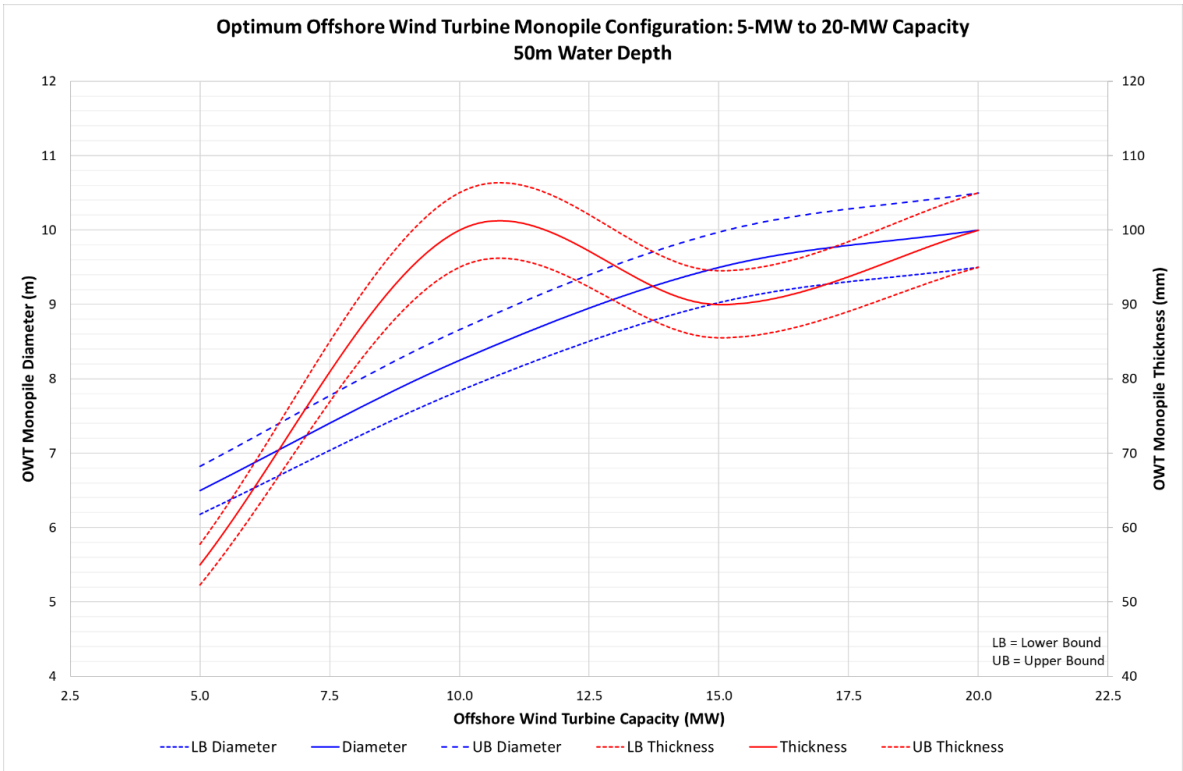

Figure 5.16 – Optimum 5 to 20-MW OWT Configuration in 50m Water Depth

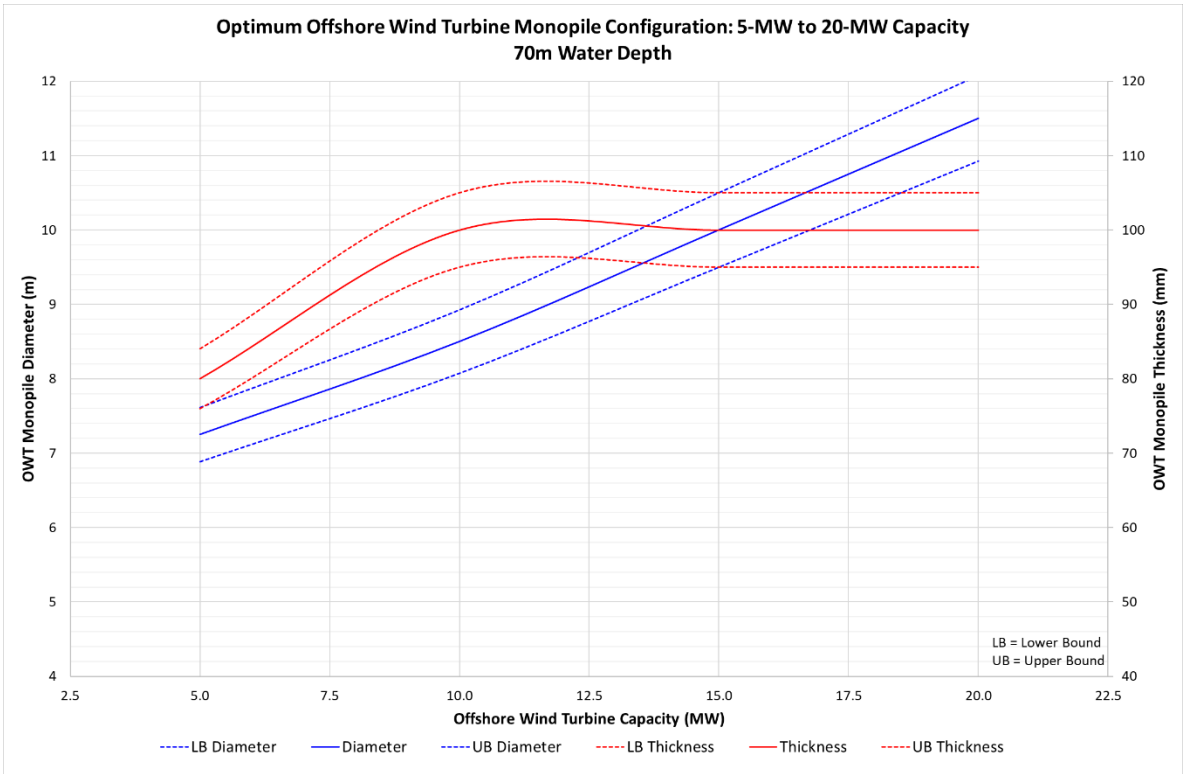

Figure 5.17 – Optimum 5 to 20-MW OWT Configuration in 70m Water Depth

5.11 Other Salient Structural Assessment Observations

Other important observations from the results are presented in this section. These do not fall within the detailed scope of this research; therefore, they have not been subjected to detailed investigation, but are recommended for future research and development.

a) Total damping of 10% was used in this research. This comprised the tower oscillation damping, steel material damping, aerodynamic damping, hydrodynamic damping, and soil damping. It was influenced by the character of the individual loads, and can be determined from structural analytical investigations, sensitive checks, full-scale tests, and where necessary, assumptions are made. The findings from this study (including earlier research contributions) imply that the impact of total damping significantly decreased for new generation larger and heavier wind turbines of 15-MW to 20-MW OWT monopiles. In some instances, total damping contributed to the non-convergence of the analytical solution. Although sensitivities were performed, the application of total damping and the extent of its influence in assessing new generation larger and heavier OWT monopiles are a subject for future detailed research.

b) According to the results, the stresses indicate that fatigue damage is not a concern of design criteria provided that resonance due to external loads is avoided or properly designed. Modal analysis and harmonic response analyses were performed to define and isolate the systems natural

frequency from of the frequencies of external loads that may lead to resonance excitation and accelerated fatigue damage.

The harmonic response analysis for the new generation of 15-MW and 20-MW OWT monopiles are presented in Figure 5.18 and Figure 5.19, respectively, for representative suitable structure configurations. A 10m monopile diameter by 70mm wall thickness for 20m, 50m, and 70m water depths were selected and presented for the 15-MW capacity. For the 20-MW capacity, the selected configuration across the water depths was 11m monopile diameter by 80mm wall thickness. The outcome of the harmonic response analysis supported the use of the design envelope and indicated how the selected suitable configuration avoids the external loads that can cause resonance initiation and accumulated stresses resulting in fatigue damage.

Therefore, according to the findings, stresses are not the governing design criteria across the OWT monopile configurations presented in the design envelope, especially for the new generation monopiles, and the likelihood of stress accumulation resulting in significant fatigue damage being low. It is important to note, however, that the coupled structural response leading to fatigue damage design was not part of this investigation. Future research on this topic is therefore recommended to provide clarity and detailed design assurance. The interpretation of the results from this study assumed that the OWT structure was defect-free; hence, it is essential that defects which may exacerbate and accelerate fatigue damage such as manufacturing flaws, installation flaws, flaws initiated and progressed during operations, and corrosion are assessed on a site-basis.

c) Offshore wind turbine monopile structural design improvement did not necessarily equate to simply increasing the structure size and section properties. In some instances, due to the complex, non-linear, sensitive, and dynamic nature of the OWT monopile structure, increasing either the thickness or monopile diameter initiated a different failure mode or led to minimal/insignificant benefits. Therefore, a well-informed and justified selection of suitable configurations from the design envelope is required for engineering feasibility design.

d) Failure caused by the structural first buckling mode was a serious concern in the design of the OWT monopile, particularly for the new larger and heavier OWT monopiles. Although suitable structure configurations were available for selection from the design envelope in resisting the first buckling mode, pile installation-related buckling was not investigated as part of this research study. Hence, it is necessary that detailed design of the OWT monopile structure include an assessment and design to resist pile installation-initiated buckling.

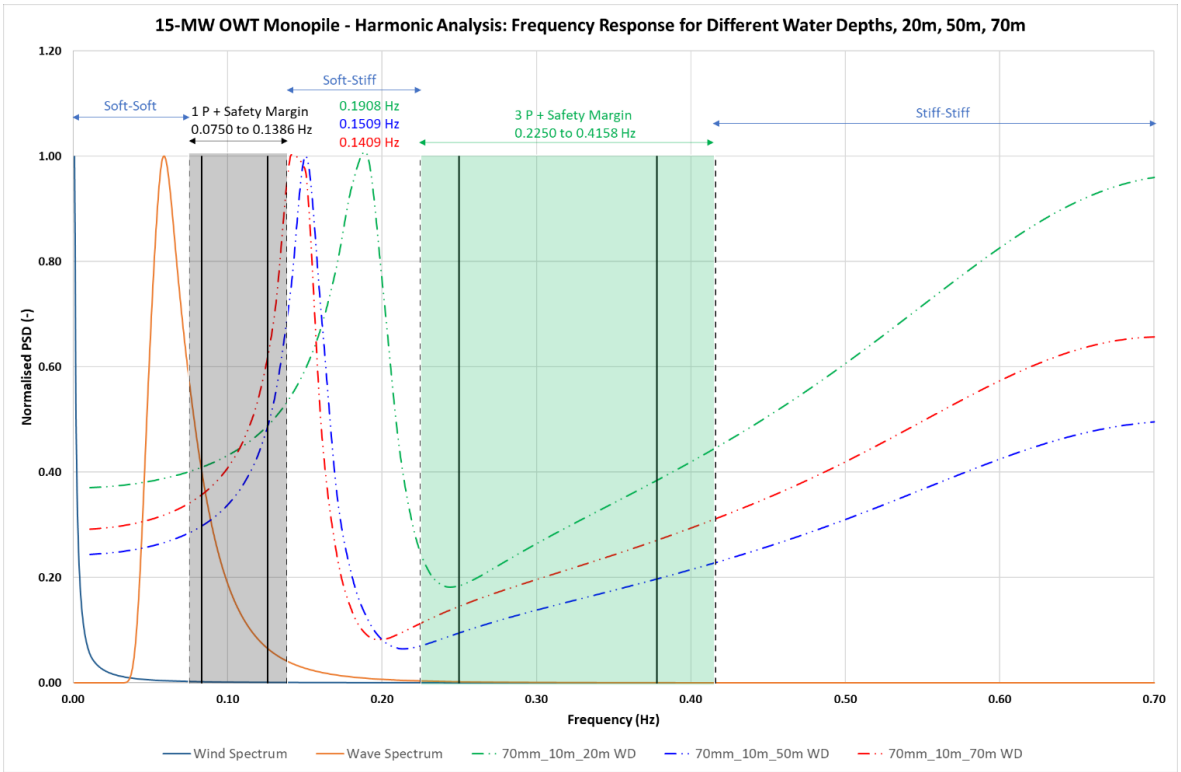

Figure 5.18 – 15-MW OWT Monopile Harmonic Response Analysis

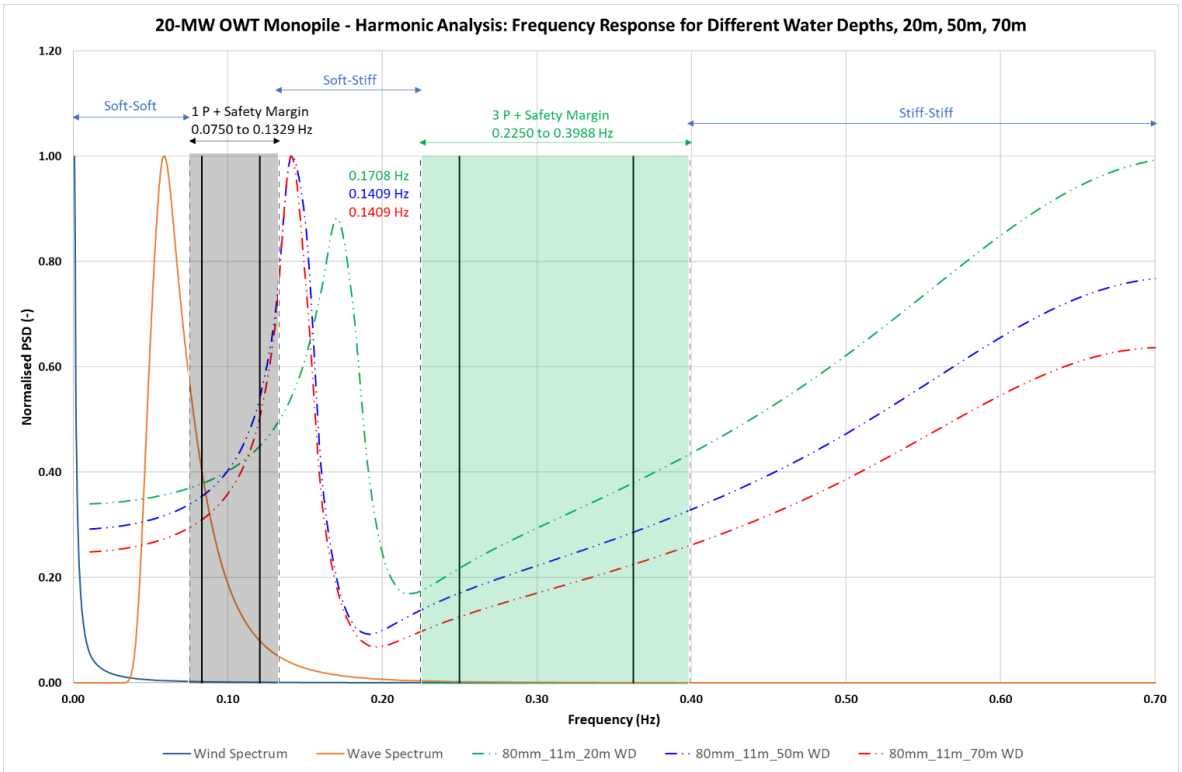

Figure 5.19 – 20-MW OWT Monopile Harmonic Response Analysis

5.12 Conclusions and Research Contribution

The research investigated the structural response of existing generation 5-MW and 10-MW offshore wind turbines (OWT) and new generation 15-MW and 20-MW OWT monopile structures. The structural response was examined in relation to the systems' natural modal frequency, harmonic response, first buckling mode, stresses, and deflections. The turbines were subjected to a 50-year return environmental (primarily wind and wave) and turbine machine loading conditions (thrust, 1P rotor frequency, and 3P blade frequency). The outcome of the research was presented as the "back-bone" structural design envelope for different turbine capacities, water depths, and configurations to enhance OWT monopile engineering feasibility design, including current and future research developments.

The following conclusions can be drawn:

A. The offshore wind turbine monopile structure is dynamically sensitive to soil properties, modelling techniques, and environmental loading conditions. This leads to a complex non-linear structural response, as presented in the design envelopes for the different configurations (turbine capacity, water depth, and section properties). Therefore, design improvement does not necessarily equate to simply increasing the structure size and section properties. An informed and justifiable design selection from the design envelope along with further verification is required to achieve a suitable and cost-effective safe design.

B. Structural design envelopes are aimed at simplifying the complex engineering behaviour and feasibility stage design. The envelope defines and provides an understanding of how large and how deep/far these new generation OWT structures can be installed and safely operated.

C. The governing design criterion was observed to shift between the natural structure frequency and the first buckling mode, subject to the selected configurations and installation conditions. Stresses are of less concern and, as such, it is assumed that fatigue due to stress accumulation is not a limiting factor provided that external resonance initiation loads/frequencies are avoided, as demonstrated in the harmonic response analysis.

D. The susceptibility of the offshore wind turbine monopile to buckling caused by installation loads and fatigue damage was not investigated in this study. Nevertheless, these factors are significant and may be useful additional inputs in the design envelope. As such, they may be considered in future research aimed at continuous improvements of the structural design envelope tool.

E. The results and interpretation presented in this article assume that the structure is defect-free, and so do not account for any fabrication, transportation, installation, and operational related flaws. Structural

defects/flaws should be assessed, where necessary, in addition to the structural response and configuration selected from the design envelope.

F. Due to the dynamic and sensitive nature of the OWT structure outlined in sub-section A, and although the responses and design envelope presented in this article are generally applicable, it is necessary that site-specific assessment is performed on the selected configurations from the design envelopes.

G. Further research is required to improve our understanding of the application and determination of appropriate total damping for new generations of larger and heavier OWT monopiles.

The unique knowledge contribution of this stage of the research are presented in Table 5.18.

Section	Unique Contribution	Contribution to Understanding
Offshore wind monopile structural design envelope	Developed offshore wind monopile structural design envelope as a tool for engineering feasibility and indicative section sizing and design.	Useful design tool for early stage and feasibility design, leading to detailed design. The design envelope can be used by both experienced and graduate structural engineers. This tool will also help in generating useful and timely design information for tendering and investment purposes.
	Developed new methodology that will enable cost-effective structural design of offshore wind monopiles. The design envelope provides new approaches on how to visualise and assess offshore wind monopiles.	Helps structural designers by providing a new way of completing structural engineering design and analysis of offshore wind monopiles.
	Provides a new technique to consider a complex array of potential failure mechanisms in a clear manner that identifies the trade-offs in the design parameters.	Enables offshore wind monopile structural designers to cleverly see the trade-offs in the design that links to efficient solution and failure modes.
	Demonstrated the structural dynamic response of existing concepts 5-MW and 10-MW and future generation 15-MW and 20-MW offshore wind monopiles.	Simplified and clarified the complex structural response of existing and future generations of offshore wind monopiles. This information will be useful to both experienced and graduate structural designers.
	Provides knowledge on the impact of installation water depths of up to 70m on the structural response and design of offshore wind monopiles.	This information will support and provide confidence to stakeholders in exploring deeper waters and provide direction on how to address challenging design concerns.
	Provides knowledge on the influence of the tower and monopile section sizes (diameters and thicknesses) on the structural response and design.	This information will be useful in achieving cost-effective design, reducing material waste and analytical run-time. Provides insight on how heavy and large the future generations of offshore wind monopiles can become, including the benefits of increasing or reducing the section sizes.
	Outlines the governing structural design criteria for 5-MW to 20-MW offshore wind monopiles.	Provides an important platform for both existing and future concepts, how far and how deep the structures can be installed and the limiting criteria for offshore wind monopiles of up to 20-MW. The information presented in the envelopes can be cautiously extrapolated for greater than 20-MW capacities.

Table 5.18 – Unique Knowledge Contribution

6 OVERALL RESEARCH CONCLUSIONS AND UNIQUE CONTRIBUTION

A comprehensive literature review and gap analysis was performed as part of this research to understand the structural design challenges faced by the offshore wind monopile industry and to identify the improvements made to date. The review and gap analysis were centred on previous academic research, industry case studies and development, and the offshore wind turbine design codes, from the first release/revision in 2004 to the latest 2018 revision. Although this research is primarily based on the DNVGL design guidelines, other industry design codes and standards have been considered. The comprehensive literature review and gap analysis is stage one of this research and is fundamental to the research scope and objective of contributing to the efficient and cost-effective structural design of offshore wind monopiles.

Stage one identified the important questions and areas of interests in the structural design of offshore wind monopiles. These findings formed the basis for the next phase (or stage two) of this research which was to investigate and provide understanding and direction on the influence of modelling techniques on offshore wind monopiles. The NREL 5-MW reference turbine was used as the case study for generating the required offshore wind monopile model in stage two, with particular focus on the influence of soil-structure modelling and its interaction on structural response. The findings and improved approach from the research on the influence of the modelling techniques were implemented in stage three of this research study. Stage three involves investigating and providing understanding of offshore wind monopile structural response under 50-year return conditions, using 10-MW offshore wind monopile as the reference model and case study. The findings and knowledge gained from studying the offshore wind monopile response under 50-year return conditions forms the background and application for the next and final stage of this research which is the development and definition of the offshore wind monopile structural design envelope. The structural design envelope is generated and defined for the existing concepts 5-MW and 10-MW offshore wind monopiles and future generation 15-MW and 20-MW offshore wind monopiles.

The important research conclusions and contributions are as follows:

A. Structural design envelopes are aimed at simplifying the complex engineering behaviour and feasibility design phase that will feed into the Front-End Engineering Design (FEED) detailed design phase. The envelope defines and provides an understanding of how large and how deep/far the existing and new generation OWT structures can be installed and safely operated.

B. The offshore wind turbine monopile structure is dynamically sensitive to soil properties, modelling techniques, and environmental loading conditions. This leads to a complex non-linear structural response, as presented in the design envelopes for the different configurations (turbine capacity, water depth, and section properties). Therefore, design improvement does not necessarily equate to simply increasing the structure size and section properties. An

informed and justifiable design selection from the design envelope along with further site-specific verification is required to achieve a suitable and cost-effective safe design.

C. The governing design criterion was observed to shift between the natural structure frequency and the first buckling mode, subject to the installation conditions and selected configurations from the design envelope. The buckling response is improved by increasing the monopile wall thickness to a constant diameter. However, this may not satisfy other design criteria, leading to a requirement to increase the diameter which may impact the global structural response.

D. Stresses are of less concern and, as such, it is assumed that fatigue due to stress accumulation is not a limiting factor provided that external resonance initiation loads/frequencies are avoided, as demonstrated in the harmonic response analysis. This study and the interpretation of the results assume that the OWT structure is defect-free; hence, defects that may exacerbate and accelerate fatigue damage such as manufacturing flaws, installation flaws, flaws initiated and progressed during operations, and corrosion must be assessed on a site-basis.

E. Investigation on the influence of modelling techniques was conducted on the 3D mass moil, the API-RP, and the JeanJean springs-supported monopile models. Despite several modelling techniques refinements and improvement on the API-RP and Jean-Jean modelling approaches, the findings show that the total deflections for the refined API-RP and JeanJean springs-supported models were observed to be 27% and 12% more than the 3D mass soil model, respectively.

F. The investigation further reveals the influence and significance of modelling techniques on the buckling capacity and response of the monopile structure when subjected to external loads. The 3D mass soil model monopile structure utilisation due to buckling is 74%. This compares with 148% and 140% for the API-RP and JeanJean springs-supported models, respectively, for the same design and loading conditions. The poor buckling capacity and response of the springs-supported models are exacerbated by the local punching of the springs on the monopile shell.

G. Although, the springs-supported models may currently be suitable in other industries and applications, such as for smaller pipe application in the Oil and Gas sector, this investigative study on the influence of modelling techniques shows that the springs-supported models would benefit from extensive refinements and calibration for offshore wind turbine monopile applications with larger and heavier structure sections.

The salient unique knowledge contribution of the overall research is presented in Table 6.1.

Section	Unique Contribution	Contribution to Understanding
Overall research conclusions and contribution	Developed offshore wind monopile structural design envelope as a tool for engineering feasibility and indicative section sizing and design.	Useful design tool for early stage and feasibility design, leading to detailed design. The design envelope can be used by both experienced and graduate structural engineers. This tool will also help in generating useful and timely design information for tendering and investment purposes.
	Developed new methodology that will enable cost-effective structural design of offshore wind monopiles. The design envelope provides new approaches on how to visualise and assess offshore wind monopiles.	Contribution that provides and helps structural designers with a new way of completing structural engineering design and analysis of offshore wind monopiles.
	Outlines the governing structural design criteria for 5-MW to 20-MW offshore wind monopiles. New technique for considering a complex array of potential failure mechanisms in a clear manner that identifies the trade-offs in the design parameters.	Provides important platform for both existing and future concepts, how far and how deep the structures can be installed and the limiting criteria for offshore wind monopiles of up to 20-MW. Enables offshore wind monopile structural designers to cleverly see the trade-offs in the design that links to efficient solution and failure modes.
	Demonstrated the structural dynamic response of existing concepts 5-MW and 10-MW and future generation 15-MW and 20-MW offshore wind monopiles.	Simplified and clarified the complex structural response of existing concepts and future generations of offshore wind monopiles. This information will be useful to both experienced and graduate structural designers.
	Modelled and compared three notable industry structural design and analytical approaches using 5-MW offshore wind monopile as case study: API p-y springs, JeanJean springs supported monopile, and 3D mass soil-monopile model.	Provides understanding and quantitative information on the modelling approaches and recommendations for offshore wind monopiles application. Improvement techniques for springs supported monopiles such as the effective positioning of the springs around the circumference of the monopile foundation that would lead to a relatively improved structural response and results.
	Established that the springs supported models in their current form are unsuitable for heavier and larger offshore wind turbine monopile structures, demonstrated using stress, deflection, buckling, and harmonic response outputs.	Saves valuable engineering manhours in avoiding unsuitable modelling techniques. Provides recommendation on how the springs supported models may be improved, where necessary, for providing quick indicative feasibility checks.

Table 6.1 – Overall Unique Knowledge Contribution

7 RECOMMENDATIONS FOR FUTURE RESEARCH

Recommendations for future research work are presented in this section. Important assumptions and modelling simplifications made in this research are also outlined, including possible steps for addressing and improving on the engineering design of offshore wind monopiles.

A. Although current industry codes and standards provide guidelines for best practice, they do not fully cover new transport and installation activities and assessments required for the future concept of OWT structure installations. Hence, the current industry design codes and standards require updating in-line with new technologies, concerning transportation and installation analysis and operations of the new generation larger and heavier offshore wind monopile structures.

B. The Mohr-Coulomb constitutive model is used in this research for the soil foundation modelling and interaction. This Mohr-Coulomb constitutive model is an elastic-perfectly plastic model which serves as a good first-order model covered in this research. This research can be repeated in future work by considering a non-linear elastic-plastic strain hardening model such as the Modified Cam-Clay model, or Plaxis Hardening Soil model which is a second order model for soils in general, including softs soils as well as harder types of soils.

C. Future research work can be extended to include detailed geotechnical design checks using both the Standard Method based on the Beam on Winkler foundation and the Advanced Method based on finite element analysis. Additional loading conditions and combinations can be considered to expand the range of in-service and operational scenarios.

D. The impact of cyclic loading and foundation scour on the new generation larger and heavier offshore wind monopiles structural dynamic response is currently unknown. This is another area of interest that is yet to be fully investigated, hence, the need for future research work to capture the influence of cyclic loading and scour on larger and heavier structures with increased turbine capacity loads.

E. The soil springs-supported structure models may currently be suitable in other industries and applications, such as for the smaller pipes used in the Oil and Gas sector, however this research has revealed that the springs-supported models would benefit from extensive refinements and calibration for offshore wind turbine monopile applications with larger and heavier structure sections. The PISA project for soil-structure modelling and interaction is an example of research progress aimed at addressing some of the modelling issues in the offshore wind turbine industry, including the influence on the structure's fatigue life. However, more research work, including testing and monitoring, is required to improve the use and

application of springs-supported models for the design and analysis of the new generation of larger and heavier offshore wind monopiles.

F. The findings from this research indicate that fatigue design will not be a challenging design criterion provided resonance due to external loads is avoided or properly designed. The coupled structural response due to fatigue design is not investigated as part of this research and in the generation of the structural design envelope; hence, the investigation of the influence of fatigue in the structural design envelope is recommended in future research work to provide clarity and detailed design assurance.

G. The assessment and control of construction peak noise for the new generation concepts of offshore wind monopiles is an area of interest that requires investigation, including the noise exposure level, excessive pile inclination, and plastic deformation of the thin-shell pile head associated with driving larger and heavier OWT monopiles into the designed embedment depth.

H. The offshore wind monopile buckling response and interpretation investigated in this research assumes that the OWT structure is designed to resist pile driving and installation related buckling. The turbine pile drivability and susceptibility to buckling due to pile hammer and associated installation challenges of the larger and heavier offshore wind monopiles are not investigated within this study. Therefore, it is recommended that these design challenges be considered in future research projects to provide a better understanding leading to design improvements.

I. This research and the interpretation of the results assumes that the offshore wind monopile structure is defect-free; hence, defects that may exacerbate and accelerate fatigue damage such as manufacturing flaws, installation flaws, flaws initiated and progressed during operations, and corrosion must be assessed on a site-basis and be considered in future research projects.

J. Total damping of 10% was used in this research. This comprised the tower oscillation damping, steel material damping, aerodynamic damping, hydrodynamic damping, and soil damping. It was influenced by the character of the individual loads, and can be determined from structural analytical investigations, sensitive checks, full-scale tests, and where necessary, assumptions are made. The findings from this study (including earlier research contributions) imply that the impact of total damping significantly decreased for new generation larger and heavier wind turbines of 15-MW to 20-MW OWT monopiles. In some instances, total damping contributed to the non-convergence of the analytical solution. Although sensitivities were performed, the application of total damping and the extent of its influence in assessing new generation larger and heavier OWT monopiles are a subject for future detailed research.

8 REFERENCES

[1] Lin CY, Huang CC, Wu TY. A Comparative Study of the API and NORSOK Standards Apply to Design Analysis for an Offshore Wind Turbine with Jacket Support Structure. International Society of Offshore and Polar Engineers; 2015.

[2] Page AM, Løkke A, Skau KS, De Vaal JB. A family of practical foundation models for dynamic analyses of offshore wind turbines. Offshore Technology Conference; 2019.

[3] 61400-3 E. 61400-3 (2009) Wind Turbines—Part 3: Design Requirements for Offshore Wind Turbines. British Standards Institution; 2009.

[4] 61400-1 E. IEC 61400-1:2019 Wind energy generation systems - Part 1: Design requirements. British Standards Institution; 2019.

[5] DNV-GL. Certification of lifetime extension of wind turbines. Service Specification DNVGL-SE-0263. 2016.

[6] DNV-GL. AS: DNVGL-ST-0262–Lifetime extension of wind turbines. Tech. rep; 2016.

[7] DNV-GL. DNV-OS-J103 standard for floating wind turbines. DET NORSKE VERITAS AS; 2013. p. V001T01A20.

[8] Byrne BW, Burd HJ, Zdravkovic L, Abadie CN, Houlsby GT, Jardine RJ, et al. PISA design methods for offshore wind turbine monopiles. Offshore Technology Conference; 2019.

[9] Burd HJ, Abadie CN, Byrne BW, Houlsby GT, Martin CM, McAdam RA, et al. Application of the PISA design model to monopiles embedded in layered soils. Géotechnique. 2020;70:1067-82.

[10] Byrne BW, Burd HJ, Zdravković L, McAdam RA, Taborda DMG, Houlsby GT, et al. PISA: new design methods for offshore wind turbine monopiles. Revue Française de Géotechnique. 2019:3.

[11] Arany L, Bhattacharya S, Macdonald JHG, Hogan SJ. A critical review of serviceability limit state requirements for monopile foundations of offshore wind turbines. Offshore Technology Conference; 2015.

[12] Sunday K, Brennan F. A review of offshore wind monopiles structural design achievements and challenges. Ocean Engineering. 2021;235:109409.

[13] Sunday K, Brennan F. Influence of soil–structure modelling techniques on offshore wind turbine monopile structural response. Wind Energy. 2022.

[14] DNVGL. DNVGL-ST-0126: Support structures for wind turbines. Oslo, Norwary: DNV2018.

[15] Veritas DN. DNV-OS-J101-Design of offshore wind turbine structures. 2004.

[16] Veritas DN. DNV-OS-J101–Design of Offshore Wind Turbine Structures. 2007.

[17] Veritas DN. DNV-OS-J101-Design of offshore wind turbine structures. 2009.

[18] Veritas DN. DNV-OS-J101 offshore standard. Design of offshore wind turbine structures. 2010.

[19] Veritas DN. Offshore Standard DNV-OS-J101 Design of Offshore Wind Turbine Structures. 2011.

[20] Veritas DN. DNV-OS-J101 Design of offshore wind turbine structures. 2013.

[21] Veritas DN. Design of Offshore Wind Turbine Structures (DNV-OS-J101). Oslo, Norway, May. 2014.

[22] DNVGL. DNVGL-ST-0126: Support structures for wind turbines. Oslo, Norway: DNV. 2016.

[23] Lichtenstein L. DNV GL Standard Harmonization Recommended Practice on Corrosion Protection of Offshore Wind Farms. International Society of Offshore and Polar Engineers; 2015.

[24] Bs BS. Guidance on methods for assessing the acceptability of flaws in metallic structures. British Standards Institution. 2000.

[25] Fajuyigbe A, Brennan F. Fitness-for-purpose assessment of cracked offshore wind turbine monopile. Marine Structures. 2021;77:102965.

[26] Stutzmann J, Ziegler L, Muskulus M. Fatigue crack detection for lifetime extension of monopile-based offshore wind turbines. Energy Procedia. 2017;137:143-51.

[27] Veritas DN. Buckling strength of shells. Recommended practice DNV-RPC202 Høvik, Norway. 2002.

[28] de Normalisation CE. EN 1993-1-6: 2007 Eurocode 3-Design of steel structures, Part 1.6: General rules–Strength and stability of shell structures. London: British Standards Institute; 2007.

[29] DNV-GL. DNVGL-RP-0416: Corrosion protection for wind turbines. DNV GL, Oslo, Norway. 2016.

[30] Colone L, Natarajan A, Dimitrov N. Impact of turbulence induced loads and wave kinematic models on fatigue reliability estimates of offshore wind turbine monopiles. Ocean Engineering. 2018;155:295-309.

[31] Marino E, Giusti A, Manuel L. Offshore wind turbine fatigue loads: The influence of alternative wave modeling for different turbulent and mean winds. Renewable Energy. 2017;102:157-69.

[32] DNVGL. DNVGL-ST-0437: Loads and Site Conditions for Wind Turbines. 2016.

[33] Vis IFA, Ursavas E. Assessment approaches to logistics for offshore wind energy installation. Sustainable energy technologies and assessments. 2016;14:80-91.

[34] Damiani RR. Design of offshore wind turbine towers. Offshore Wind Farms: Elsevier; 2016. p. 263-357.

[35] Veritas DN. DNV-OS-C401 Fabrication and Testing of Offshore Structures. 2014.

[36] Matha D, Brons-Illig C, Mitzlaff A, Scheffler R. Fabrication and installation constraints for floating wind and implications on current infrastructure and design. Energy Procedia. 2017;137:299-306.

[37] Sarker BR, Faiz TI. Minimizing transportation and installation costs for turbines in offshore wind farms. Renewable Energy. 2017;101:667-79.

[38] Lu JY, Mony SK, Carlsen H, Sixtensson C. Solution to Design Challenges and Selections of Wind Turbine Installation Vessels. Offshore Technology Conference; 2011.

[39] Hu H-T, Yang C, Yeh D-S, Liaw S-R, Lin C-K, Liu Y-M. Finite element frequency analysis of offshore wind turbine structure under soil and structure interaction. International Society of Offshore and Polar Engineers; 2016.

[40] Api RP. 2A-WSD (2014). Recommended Practice for Planning Designing and Constructing Fixed Offshore Platforms–Working Stress Design. 2014.

[41] Api RP. 2GEO (2011). Recommended practice for geotechnical foundation design consideration. 2011.

[42] Jeanjean P, Watson PG, Kolk HJ, Lacasse S. The new API Recommended Practice for Geotechnical Engineering: RP 2GEO. Frontiers in Offshore Geotechnics II: CRC Press; 2010. p. 921-6.

[43] O'Neill MW, Murchinson JM. Fan evaluation of py relationships in sands. A report to the American Petroleum Institute. 1983.

[44] Dunnavant TW, O'Neill MW. Experimental p-y model for submerged, stiff clay. Journal of Geotechnical Engineering. 1989;115:95-114.

[45] Api RP. 2A-WSD (2000). Recommended practice for planning, designing and constructing fixed offshore platforms-working stress design. 2000;21.

[46] Dubois J, Thieken K, Terceros M, Schaumann P, Achmus M. Advanced incorporation of soil-structure interaction into integrated load simulation. International Society of Offshore and Polar Engineers; 2016.

[47] Huang Y, Guo Z, Hong Y, Tong J, Tang L, Wang L. Investigations on Dynamic Reponses of Offshore Wind Turbine Supported by Monopile in Sand. International Society of Offshore and Polar Engineers; 2016.

[48] Veldkamp HF, Van Der Tempel J. Influence of wave modelling on the prediction of fatigue for offshore wind turbines. Wind Energy: An International Journal for Progress and Applications in Wind Power Conversion Technology. 2005;8:49-65.

[49] Nicolai G, Ibsen LB. Investigation on Monopiles Behavior under Cyclic Lateral Loads in Dense Sand. International Society of Offshore and Polar Engineers; 2015.

[50] Lombardi D, Bhattacharya S, Wood DM. Dynamic soil–structure interaction of monopile supported wind turbines in cohesive soil. Soil dynamics and earthquake engineering. 2013;49:165-80.

[51] Zachert H, Wichtmann T, Triantafyllidis T. Soil structure interaction of foundations for offshore wind turbines. International Society of Offshore and Polar Engineers; 2016.

[52] Matlock H. Correlations for design of laterally loaded piles in soft clay. Offshore technology in civil engineering's hall of fame papers from the early years. 1970:77-94.

[53] Reese LC, Cox WR, Koop FD. Field testing and analysis of laterally loaded piles om stiff clay. Offshore technology conference; 1975.

[54] Jeanjean P. Re-assessment of py curves for soft clays from centrifuge testing and finite element modeling. Offshore Technology Conference; 2009.

[55] Zhang Y, Andersen KH, Jeanjean P. Verification of a framework for cyclic py curves in clay by hindcast of Sabine River, SOLCYP and centrifuge laterally loaded pile tests. Applied Ocean Research. 2020;97:102085.

[56] Zhang Y, Andersen KH, Jeanjean P, Karlsrud K, Haugen T. Validation of monotonic and cyclic py framework by lateral pile load tests in stiff, overconsolidated clay at the haga site. J Geotech Geoenviron Eng. 2020;146:04020080.

[57] Jeanjean P, Zhang Y, Zakeri A, Andersen KH, Gilbert R, Senanayake A. A framework for monotonic py curves in clays. 141 ed: Society for Underwater Technology; 2017. p. 108-41.

[58] Senanayake A, Gilbert RB, Manuel L. Estimating natural frequencies of monopile supported offshore wind turbines using alternative PY models. Offshore Technology Conference; 2017.

[59] Zakeri A, Clukey E, Kebadze B, Jeanjean P, Walker D, Piercey G, et al. Recent advances in soil response modeling for well conductor fatigue analysis and development of new approaches. Offshore Technology Conference; 2015.

[60] Haiderali AE, Madabhushi GSP. Evaluation of the py Method in the Design of Monopiles for Offshore Wind Turbines. 2013. p. 1824-44.

[61] Bhattacharya S. Design of foundations for offshore wind turbines: John Wiley & Sons; 2019.

[62] Osman AS, Bolton MD. Simple plasticity-based prediction of the undrained settlement of shallow circular foundations on clay. Géotechnique. 2005;55:435-47.

[63] Morrow MM, Shastri A, Delos-Reyes MA. Scouring and Mitigating Efforts for the M3 Wave APEX Device. Offshore Technology Conference; 2019.

[64] Arany L, Bhattacharya S, Adhikari S, Hogan SJ, Macdonald JHG. An analytical model to predict the natural frequency of offshore wind turbines on three-spring flexible foundations using two different beam models. Soil Dynamics and Earthquake Engineering. 2015;74:40-5.

[65] Zaayer MB, Vugts JH. Sensitivity of dynamics of fixed offshore support structures to foundation and soil properties. Duwind; 2001. p. 69-72.

[66] Zaaijer MB. Foundation models for the dynamic response of offshore wind turbines. 2002. p. 1.

[67] Nam W, Oh K-Y, Epureanu BI. Evolution of the dynamic response and its effects on the serviceability of offshore wind turbines with stochastic loads and soil degradation. Reliability Engineering & System Safety. 2019;184:151-63.

[68] Devriendt C, Jordaens PJ, De Sitter G, Guillaume P. Damping estimation of an offshore wind turbine on a monopile foundation. IET Renewable Power Generation. 2013;7:401-12.

[69] Petersen B, Pollack M, Connell B, Greeley D, Davis D, Slavik C, et al. Evaluate the effect of turbine period of vibration requirements on structural design parameters: technical report of findings. Applied Physical Sciences: Report Number M10PC00066. 2010;8.

[70] James GH, Carne TG, Veers PS. Damping measurements using operational data. 1996.

[71] Li L, Liu Y, Yuan Z, Gao Y. Dynamic and structural performances of offshore floating wind turbines in turbulent wind flow. Ocean Engineering. 2019;179:92-103.

[72] Jiang Z, Karimirad M, Moan T. Response analysis of parked spar-type wind turbine considering blade-pitch mechanism fault. International Journal of Offshore and Polar Engineering. 2013;23.

[73] Malekjafarian A, Jalilvand S, Doherty P, Igoe D. Foundation damping for monopile supported offshore wind turbines: A review. Marine Structures. 2021;77:102937.

[74] Valamanesh V, Myers AT. Aerodynamic damping and seismic response of horizontal axis wind turbine towers. Journal of Structural Engineering. 2014;140:04014090.

[75] Tarp-Johansen NJ, Andersen L, Christensen ED, Mørch C, Frandsen S, Kallesøe B. Comparing sources of damping of cross-wind motion. The European Wind Energy Association; 2009.

[76] Rezaei R, Fromme P, Duffour P. Fatigue life sensitivity of monopile-supported offshore wind turbines to damping. Renewable Energy. 2018;123:450-9.

[77] Lackner MA, Rotea MA. Passive structural control of offshore wind turbines. Wind energy. 2011;14:373-88.

[78] Windenergie GL. Overall damping for piled offshore support structures'. Guideline for the Certification of Offshore Wind Turbines,(Edn). 2005.

[79] Hansen MH, Thomsen K, Fuglsang P, Knudsen T. Two methods for estimating aeroelastic damping of operational wind turbine modes from experiments. Wind Energy: An International Journal for Progress and Applications in Wind Power Conversion Technology. 2006;9:179-91.

[80] Shirzadeh R, Devriendt C, Bidakhvidi MA, Guillaume P. Experimental and computational damping estimation of an offshore wind turbine on a monopile foundation. Journal of Wind Engineering and Industrial Aerodynamics. 2013;120:96-106.

[81] Zaaijer MB, Van der Tempel J. Scour protection: a necessity or a waste of money. 2004. p. 43-51.

[82] Damgaard M, Andersen JKF. Natural frequency and damping estimation of an offshore wind turbine structure. International Society of Offshore and Polar Engineers; 2012.

[83] Damgaard M, Ibsen LB, Andersen LV, Andersen JKF. Cross-wind modal properties of offshore wind turbines identified by full scale testing. Journal of Wind Engineering and Industrial Aerodynamics. 2013;116:94-108.

[84] 2005 E--. EN 1991-1-4: 2005 : Actions on structures. EN 1991-1-4: 20052005.

[85] Carswell W, Johansson J, Løvholt F, Arwade SR, Madshus C, DeGroot DJ, et al. Foundation damping and the dynamics of offshore wind turbine monopiles. Renewable energy. 2015;80:724-36.

[86] Salzmann DJC, Van der Tempel J. Aerodynamic damping in the design of support structures for offshore wind turbines. Paper of the Copenhagen offshore conference; 2005.

[87] Hovde GO. Fatigue and overload reliability of offshore structural systems, considering the effect of inspection and repair. 1997.

[88] Sørensen JD, Faber MH, Rackwitz R, Thoft-Christensen PT. Modeling in optimal inspection and repair. 1991. p. 281-8.

[89] Jensen BB. Corrosion protection of offshore wind farms, protecting internal sides of foundations. NACE International; 2015.

[90] Black AR, Mathiesen T, Hilbert LR. Corrosion protection of offshore wind foundations. NACE International: Houston, TX, USA. 2015.

[91] Moan T. Reliability-based management of inspection, maintenance and repair of offshore structures. Structure and Infrastructure Engineering. 2005;1:33-62.

[92] Lomholt TN, Egelund S, Mathiesen T, Bangsgaard DB. Unification of Corrosion Protection for Offshore Wind Farms-Collaboration in Partnerships. NACE International, CORROSION; 2018.

[93] Weinell CE, Black AR, Mathiesen T, Nielsen PK. New developments in coatings for extended lifetime for offshore wind structures. NACE International, CORROSION; 2017.

[94] Jensen BB. Specifying corrosion protection for the offshore wind turbine industry. NACE International, CORROSION 2017; 2017.

[95] Bouty C, Schafhirt S, Ziegler L, Muskulus M. Lifetime extension for large offshore wind farms: Is it enough to reassess fatigue for selected design positions? Energy Procedia. 2017;137:523-30.

[96] Herion S, Hrabowski J, Faber T. Extension of Service Life and Considerations on Corrosion Problems of Offshore Wind Energy Converters. International Society of Offshore and Polar Engineers; 2009.

[97] Aeran A, Siriwardane SC, Mikkelsen O. Life extension of ageing offshore structures: time dependent corrosion degradation and health monitoring. International Society of Offshore and Polar Engineers; 2016.

[98] Ricles JM, Bruin WM, Sooi TK, Hebor MF, Schonwetter PC. Residual strength assessment and repair of damaged offshore tubulars. Offshore Technology Conference; 1995.

[99] Grolvlen M, Bardal E, Berge S, Eide O, Engesvik K, Haagensen PJ, et al. Localized Corrosion on Offshore Tubular· Structures: Inspection and Repair Criteria. Offshore Technology Conference; 1989.

[100] Mathiesen T, Black A, Gronvold F. Monitoring and inspection options for evaluating corrosion in offshore wind foundations. NACE Corrosion-2016, paper no C-2016. 2016;7702.

[101] Schaumann P, Lochte-Holtgreven S, Bechtel A. Grouted joints in monopiles-analyses and discussion of earlier design approaches for connections without shear keys. International Society of Offshore and Polar Engineers; 2014.

[102] Schaumann P, Bechtel A, Lochte-Holtgreven S. Grouted joints for offshore wind turbine jackets under full reversal axially loading conditions. International Society of Offshore and Polar Engineers; 2013.

[103] Schaumann P, Bechtel A, Lochte-Holtgreven S. Fatigue performance of grouted joints for offshore wind energy converters in deeper waters. The Twentieth International Offshore and Polar Engineering Conference; 2010.

[104] Müller N, Kraemer P, Leduc D, Schoefs F. FBG Sensors and Signal-Based Detection Method for Failure Detection of an Offshore Wind Turbine Grouted Connection. International Journal of Offshore and Polar Engineering. 2019;29:1-7.

[105] Müller N, Kraemer P, Leduc D, Schoefs F. Fiber Bragg Grating sensors and signal based detection method for failure detection of an offshore wind turbine grouted connection. The 27th International Ocean and Polar Engineering Conference; 2019.

[106] Schaumann P, Lochte-Holtgreven S, Eichstädt R, Camp T, McCann G. Numerical Investigations on Local Degradation and Vertical Misalignments of Grouted Joints in Monopile Foundations. International Society of Offshore and Polar Engineers; 2013.

[107] Shamsuddoha M, Hüsken G, Pirskawetz S, Baeßler M, Kühne H-C, Thiele M. Remediation of Cracks Formed in Grouted Connections of Offshore Energy Structures Under Static Loads. The 28th International Ocean and Polar Engineering Conference; 2018.

[108] Dallyn P, El-Hamalawi A, Palmeri A, Knight R. Prediction of wear in grouted connections for offshore wind turbine generators. Structures; 2017. p. 117-29.

[109] Klose M, Mittelstaedt M, Mulve A. Grouted connections-offshore standards driven by the wind industry. International Society of Offshore and Polar Engineers; 2012.

[110] Theotokoglou EE, Papaefthimiou G. Computational Analysis of Grouted Connections. The 27th International Ocean and Polar Engineering Conference; 2017.

[111] Alwan A-A, Boswell LF. Behaviour and Analysis of Grouted Connections in Offshore Monopile Wind Turbine Structures subject to Bending Moment Loading. International Society of Offshore and Polar Engineers; 2014.

[112] Schaumann P, Wilke F. Design of large diameter hybrid connections grouted with high performance concrete. International Society of Offshore and Polar Engineers; 2007.

[113] Gjersøe NF, Hansen N-EO, Iversen P. Long term behaviour of lateral dynamically loaded steel grout joints. The Twenty-first International Offshore and Polar Engineering Conference; 2011.

[114] Tebbett IE. Recent developments in the design of grouted connections. SPE Production Engineering. 1987;2:223-32.

[115] Cotardo D, Lohaus L, Werner M. Practical performance of OPC-grout for offshore wind turbines in large-scale execution tests. The 27th International Ocean and Polar Engineering Conference; 2017.

[116] Alwis NC, Dier AF. Guidance for Grouted Sleeves in Repair of Offshore Installations. Offshore Technology Conference; 2016.

[117] Luo MYH, Zhang B, Harwood M, Maher J. Spar Topsides-to-Hull Connection–Welded Vs. Grouted. The Fourteenth International Offshore and Polar Engineering Conference; 2004.

[118] Lohaus L, Cotardo D, Werner M. A Test System to Simulate the Influence of Early Age Cycling on the Properties of Grout Material. International Society of Offshore and Polar Engineers; 2014.

[119] Cotardo D, Haist M, Lohaus L. Early-Age Movement in Grouted Joints for Offshore Applications-Determination of the Development of Grout-Stiffness. International Society of Offshore and Polar Engineers; 2019.

[120] MacLeay AJ, Hodgson T. Beatrice Offshore Wind Project, Wind Turbine Generator Foundation Design. Offshore Technology Conference; 2019.

[121] Igwemezie V, Mehmanparast A, Kolios A. Materials selection for XL wind turbine support structures: A corrosion-fatigue perspective. Marine Structures. 2018;61:381-97.

[122] Igwemezie V, Mehmanparast A, Kolios A. Current trend in offshore wind energy sector and material requirements for fatigue resistance improvement in large wind turbine support structures–A review. Renewable and Sustainable Energy Reviews. 2019;101:181-96.

[123] Zhang M, Wu Q, Wu Y, Du J, Xu Y, Xu X. Fatigue Damage Analysis for Offshore Wind Turbine Considering Coupled Loads Effects. International Society of Offshore and Polar Engineers; 2018.

[124] Zhang L, Zhao J, Zhang X, Ma QW. Integrated Fatigue Load Analysis of Wave and Wind for Offshore Wind Turbine Foundation. International Society of Offshore and Polar Engineers; 2010.

[125] Miner MA. Cumulative damage in fatigue. 1945.

[126] Kauzlarich JJ. The Palmgren-Miner rule derived. Tribology Series: Elsevier; 1989. p. 175-9.

[127] Dong W, Moan T, Gao Z. Long-term fatigue analysis of multi-planar tubular joints for jacket-type offshore wind turbine in time domain. Engineering structures. 2011;33:2002-14.

[128] Dong W, Moan T, Gao Z. Fatigue reliability analysis of the jacket support structure for offshore wind turbine considering the effect of corrosion and inspection. Reliability Engineering & System Safety. 2012;106:11-27.

[129] Schaumann P, Raba A, Lochte-Holtgreven S. Load Sequence Effects in the Fatigue Design of Welded Spatial Tubular Joints in Jackets. The Twenty-second International Offshore and Polar Engineering Conference; 2012.

[130] Iso N. Petroleum and natural gas industries—Fixed steel offshore structures. International Organization for Standardization. 2007.

[131] Lo T-W, Yu Q, Kim K. Verification of Fatigue Analysis Methods for Bottom Founded Offshore Wind Turbine Support Structures. Offshore Technology Conference; 2015.

[132] Manzocchi M, Wang L, Wilson M. Online Structural Integrity Monitoring of Fixed Offshore Structures. Offshore Technology Conference; 2012.

[133] Rahim A, Sparrevik P, Mirdamadi A. Structural Health Monitoring for Offshore Wind Turbine Towers and Foundations. Offshore Technology Conference; 2018.

[134] Rytter A. Vibrational based inspection of civil engineering structures. 1993.

[135] Vestli H, Lemu HG, Svendsen BT, Gabrielsen O, Siriwardane SC. Case Studies on Structural Health Monitoring of Offshore Bottom-Fixed Steel Structures. International Society of Offshore and Polar Engineers; 2017.

[136] DNV-GL. Probabilistic methods for planning of inspection for fatigue cracks in offshore structures. DNV GL, Oslo, Norway, Standard No DNVGL-RP-C210. 2015.

[137] May P, Sanderson D, Sharp JV, Stacey A. Structural integrity monitoring: Review and appraisal of current technologies for offshore applications. 2008. p. 247-63.

[138] Velarde J, Kramhøft C, Sørensen JD. Uncertainty Modeling and Fatigue Reliability Assessment of Concrete Gravity Based Foundation for Offshore Wind Turbines. International Society of Offshore and Polar Engineers; 2018.

[139] Søensen JD, Tarp-Johansen NJ. Reliability-based optimization and optimal reliability level of offshore wind turbines. International Journal of Offshore and Polar Engineering. 2005;15.

[140] Sørensen JD, Frandsen S, Tarp-Johansen NJ. Fatigue reliability and effective turbulence models in wind farms. Marcel Dekker; 2007.

[141] Madsen HO, Skjong RK, Tallin AG. Probabilistic fatigue crack growth analysis of offshore structures, with reliability updating through inspection. 1987.

[142] Melchers RE, Beck AT. Structural reliability analysis and prediction: John wiley & sons; 2018.

[143] Moan T. Reliability and risk analysis for design and operations planning of offshore structures. ICOSSAR'93 (Innsbruck) Balkema. 1994:21-43.

[144] Faber MH. On the treatment of uncertainties and probabilities in engineering decision analysis. 2005.

[145] Paté-Cornell ME. Uncertainties in risk analysis: Six levels of treatment. Reliability Engineering & System Safety. 1996;54:95-111.

[146] Horn J-T, Krokstad JR, Leira BJ. Impact of model uncertainties on the fatigue reliability of offshore wind turbines. Marine Structures. 2019;64:174-85.

[147] Gaertner E, Rinker J, Sethuraman L, Zahle F, Anderson B, Barter GE, et al. IEA wind TCP task 37: Definition of the IEA 15-megawatt offshore reference wind turbine. National Renewable Energy Lab.(NREL), Golden, CO (United States); 2020.

[148] Bouzid DA, Bhattacharya S, Otsmane L. Assessment of natural frequency of installed offshore wind turbines using nonlinear finite element model considering soil-monopile interaction. Journal of Rock Mechanics and Geotechnical Engineering. 2018;10:333-46.

[149] Randolph MF. The response of flexible piles to lateral loading. Geotechnique. 1981;31:247-59.

[150] Api Rp 2A-Wsd A. Recommended practice for planning, designing and constructing fixed offshore platforms—working stress design. American Petroleum Institute Washington, DC; 2000.

[151] Sahasakkul W, Nguyen H, Sari A. An improved methodology on design and analysis of offshore wind turbines supported by monopiles. Offshore technology conference; 2016.

[152] Ti KS, Huat BBK, Noorzaei J, Jaafar MS, Sew GS. A review of basic soil constitutive models for geotechnical application. Electronic Journal of Geotechnical Engineering. 2009;14:1-18.

[153] Jonkman J, Butterfield S, Musial W, Scott G. Definition of a 5-MW reference wind turbine for offshore system development. National Renewable Energy Lab.(NREL), Golden, CO (United States); 2009.

[154] COM624P L. SOIL PROPERTIES. 2023 ed: The Missouri Department of Transportation 2023.

[155] Veritas DN. Recommended practice DNV-RP-C205: environmental conditions and environmental loads. DNV, Norway. 2010.

[156] Manceau S, McLean R, Sia A, Soares M. Application of the Findings of the PISA Joint Industry Project in the Design of Monopile Foundations for a North Sea Wind Farm. Offshore Technology Conference; 2019.

[157] Ma Y, Martinez-Vazquez P, Baniotopoulos C. Buckling Analysis for Wind Turbine Tower Design: Thrust Load versus Compression Load Based on Energy Method. Energies. 2020;13:5302.

[158] Kühn M. Soft or stiff-a fundamental question in the design of offshore wind energy converters. BOOKSHOP FOR SCIENTIFIC PUBLICATIONS; 1997. p. 575-8.

[159] Wang S, Larsen TJ, Bredmose H. Ultimate load analysis of a 10 MW offshore monopile wind turbine incorporating fully nonlinear irregular wave kinematics. Marine Structures. 2021;76:102922.

[160] Bak C, Zahle F, Bitsche R, Kim T, Yde A, Henriksen LC, et al. The DTU 10-MW reference wind turbine. 2013.

[161] Leimeister M. Rational Upscaling and Modelling of a Semi-Submersible Floating Offshore Wind Turbine: Norwegian University of Science and Technology and Delft University of Technology; 1st June, 2016.

[162] Ramirez L, Fraile D, Brindley G. Offshore wind in Europe: Key trends and statistics 2019. 2020.

[163] Ashuri T, Martins JRRA, Zaaijer MB, van Kuik GAM, van Bussel GJW. Aeroservoelastic design definition of a 20 MW common research wind turbine model. Wind energy. 2016;19:2071-87.

[164] Sartori L, Bellini F, Croce A, Bottasso CL. Preliminary design and optimization of a 20MW reference wind turbine. 4 ed: IOP Publishing; 2018. p. 042003.

[165] de Souza CES, Bachynski-Polić EE. Design, structural modeling, control, and performance of 20 MW spar floating wind turbines. Marine Structures. 2022;84:103182.

[166] Jiang Z. Installation of offshore wind turbines: A technical review. Renewable and Sustainable Energy Reviews. 2021;139:110576.

[167] Sergiienko NY, da Silva LSP, Bachynski-Polić EE, Cazzolato BS, Arjomandi M, Ding B. Review of scaling laws applied to floating offshore wind turbines. Renewable and Sustainable Energy Reviews. 2022;162:112477.

[168] Aleem M, Bhattacharya S, Cui L, Amani S, Salem AR, Jalbi S. Load utilisation (LU) ratio of monopiles supporting offshore wind turbines: Formulation and examples from European Wind Farms. Ocean Engineering. 2022;248:110798.

[169] Broms BB. Lateral resistance of piles in cohesionless soils. Journal of the soil mechanics and foundations division. 1964;90:123-56.